Epidemiological Compartment Modelling of Malaria and Analyses of *P. falciparum* Prevalence Data in India

Inayat

Roll No: MS15022

A dissertation submitted for the partial fulfilment

of BS-MS dual degree in Science

June 2020

Indian Institute of Science Education and Research Mohali

Sector - 81, SAS Nagar, Mohali 140306, Punjab, India

Certificate of Examination

This is to certify that the dissertation titled "Epidemiological Compartment Modelling of Malaria and Analyses of *P. falciparum* Prevalence Data in India" submitted by Ms. Inayat (Reg. No. MS15022) for the partial fulfillment of BS-MS dual degree programme of the Institute, has been examined by the thesis committee duly appointed by the Institute. The committee finds the work done by the candidate satisfactory and recommends that the report is accepted.

Prof Somdatta Sinha Dr Sharvan Sehrawat Dr Arunika Mukhopadhaya

(Co-Supervisor) (Supervisor)

Dated: 13 June 2020

Declaration

The work presented in this dissertation has been carried out by me under the guidance of Prof Somdatta Sinha and Dr. Arunika Mukhopadhaya at the Indian Institute of Science Education and Research, Mohali. This work has not been submitted in part or in full for a degree, a diploma, or a fellowship to any other university or institute. Whenever contributions of others are involved, every effort is made to indicate this clearly, with due acknowledgment of collaborative research and discussions. This thesis is a bonafide record of original work done by me and all sources listed within have been detailed in the bibliography.

Inayat

(Candidate)

Dated: 13 June 2020

In my capacity as the supervisor of the candidate's project work, I certify that the above statements by the candidate are true to the best of my knowledge.

Prof Somdatta Sinha

(Co-Supervisor)

Dr Arunika Mukhopadhaya

(Supervisor)

Acknowledgement

First of all, I wish to record a deep sense of gratitude to Prof Somdatta Sinha, my supervisor for her valuable guidance and constant support. Her dedication towards scientific research is infectious and I hope to inculcate the same qualities someday. I am indebted to her critical insights and patient guidance during the entire process of this thesis. I thank Dr. Arunika Mukhopadhaya and Dr. Sharvan Sehrawat sincerely for guiding me throughout the year, and taking care of all the requirements towards the completion of this work.

I must also thank Himanshu Aggarwal for troubleshooting my codes and never missing out on silly errors. I'd like to extend my gratitude towards Saurabh Bedi, Sveekruth Pai and Hayman Gosain-for keeping the work environment light and filled with discussions on all topics under the sun. Coffee and tea breaks with Sinhalab will never be forgotten.

My journey at IISER will be incomplete if I do not thank the friends who have kept me sane and smiling for the past five years. Since two years, I have had health issues that could have taken a great toll on me, if I did not have them for support. From all-night study sessions to all-night movies, Srishti has been much more than a roommate and particularly in the past year, Ojaswi and Jaskaran have motivated me to push my self get healthier- both physically and mentally, and I cannot thank them enough. I'd also like to thank my family for being my ultimate cheerleaders, and for their eternal optimism that keeps me motivated. The countless hardships that they have gone through to raise me only keeps me grounded and I hope to be able to live up to their expectations. Finally, I would like to thank DBS, IISER Mohali and INSPIRE-DST for facilities and financial support.

List of Figures

List of Tables

Contents

Abstract

Malaria is an endemic infectious disease in India and continues to be a significant public health concern. Mathematical and statistical methods have been used to study the complex behaviour of infectious diseases, through different modelling and data analysis techniques. This thesis embodies work in both the aspects and presents results in epidemiological compartment modeling, and analysis of a historical data set of *Plasmodium falciparum* induced malaria in India. Usually in epidemiological compartment models, the population in each compartment is considered to be homogeneous in many biological and environmental factors. I have focused on an existing mathematical model to explore and investigate the behavior of hypothetical immunological responses, owing to heterogeneity in immunity in host population, and studied temporal equilibrium properties and disease prevalence patterns. I have analysed the emergence and establishment of *P. falciparum* as the dominant malarial parasite in India, through visualization and descriptive statistical analysis such as, spatial time series, temporal correlation heat maps, and principal component analysis, of a historical data-set (1965-1995). The results clearly demonstrate the spatio-temporal patterns of its evolution and, the hot-spots of *falciparum* malaria prevalent states. These approaches can be used for the analysis of any other infectious disease data.

Chapter 1

Introduction

1.1 The Empress of All Maladies: Malaria and its Types

Malaria is an age-old infectious disease caused by the protozoan parasites of genus *Plasmodium* that is transmitted by the bite of infected female *Anopheles* vectors to humans. The infection continues to plague the poorest regions of the world including Sub-Saharan Africa and southeast Asia. In the twentieth century , it was estimated that malaria alone was responsible for 150 million to 300 million deaths worldwide, which accounted for 2-5 percent of all deaths [13].

In the past few decades, malaria has been geographically restricted to tropical and subtropical regions, thriving in conditions that are suitable for the propagation and development of the parasite. The current distribution of the parasite is gov-

erned by factors that transcend beyond the basic biology of the diseases, malaria is now known to be affected by climatic changes, migration and heterogeneity in immune responses due to disparity in socio-economic factors. Four different types of malaria parasites predominantly affect humans- *P. falciparum, P. vivax, P. malariae* and *P. ovale* [17].

Plasmodium falciparum is associated with high mortality, as *falciparum* -infected erythrocytes, particularly those with mature trophozoites, adhere to the vascular endothelium of venular blood vessel walls and do not freely circulate in the blood [79]. When this sequestration of infected erythrocytes occurs in the vessels of the brain it is believed to be a factor in causing cerebral malaria, which is often associated with fatality [27].

1.1.1 Georaphical Distribution of the Parasite Species

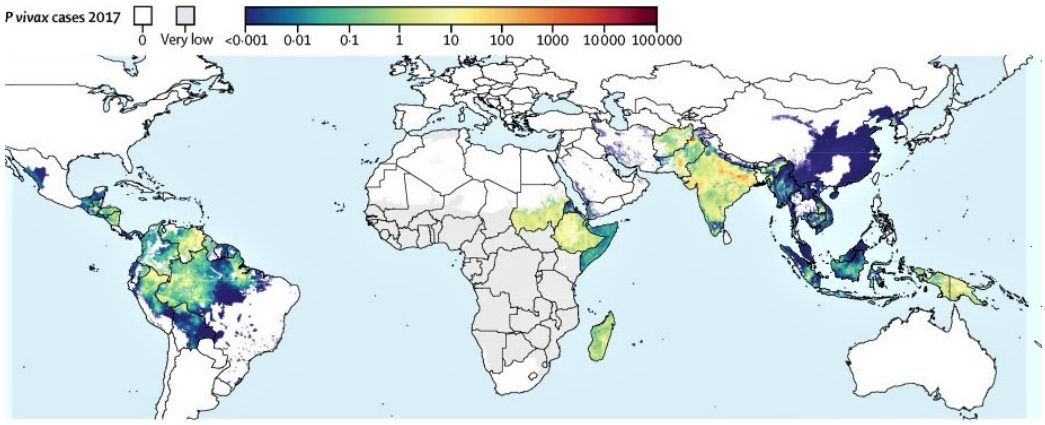

Figure 1.1: Endemicity of *P. vivax* in 2017 [9]

P. vivax is historically thought to be endemic in the south-eastern regions (Figure 1.1); with India alone contributing to more than 47% diagnosed *P. vivax* infections [83]. Evolutionarily, *P. falciparum* and *P. vivax* evolved from parasites in-

fecting wild-living African apes until the spread of the protective Duffy-negative mutation eliminated *P. vivax* from human populations. Despite the declines in

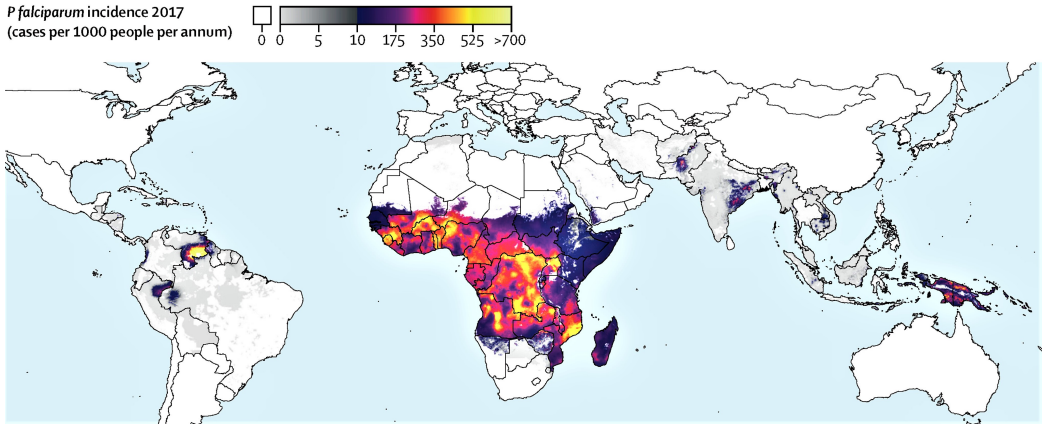

Figure 1.2: Endemicity of *P. falciparum* in 2017 [82]

burden, approximately 90% of people within sub-Saharan Africa continue to reside in endemic areas (Figure 1.2) and this region accounted for 93% of the total malaria cases in 2018 [83]).

1.1.2 The Dual Host-parasite Life Cycle: Weapon of Mass Destruction

One of the major hurdles in combating malaria parasite is the current gap in understanding the host–parasite interactions within the human host. The ability of the parasite to evade the human immune system has ensured its successful establishment and propagation for centuries. It has now become evident that the parasite infection of the human liver, erythrocytes and the mosquito mid-gut are all crucial to the survival of the parasite within the host and are backed by intensive molecular interactions between the host and the parasite [2]. A schematic diagram depicting the various stages of the life cycle of the malaria parasite is

given in Figure 1.3.

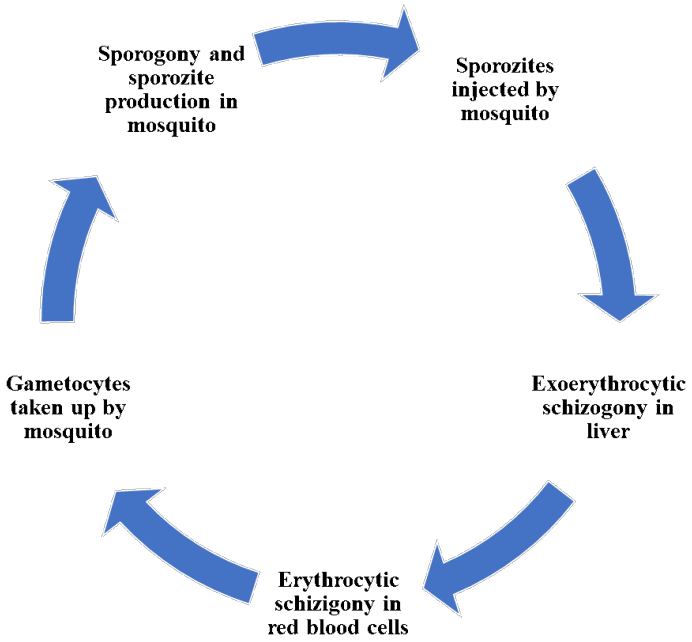

Figure 1.3: Schematic of dual host transmission cycle of malaria parasite [17]

1.2 Epidemiological Compartmental Modelling

Mathematical modelling is an important part of investigating and understanding infectious diseases spread and underlying epidemiology. Mathematical models enhance our understanding of realistic determinants of disease spread, its dynamics in susceptible populations, and to uncover its dynamics to address disease-control policies and test scientific hypotheses restrained by laboratory and field methods due to ethical constraints. Compartmental infectious disease methods are an amalgamation of our scientific understanding of the disease biology, and its links to transmission which might be unclear and complex through experimental

methods. It gives a critical understanding of the impact of the infectious disease on the population, its realistic public health burden and aids policy makers to critique measures taken to reduce transmission and burden in affected regions.

The processes that govern infectious diseases transcend multiple scales- the epidemiology of an infectious disease is linked to intra-cellular dynamics of the host, the interaction of the hosts immune system with the infectious agent and the organismal level impacts of disease spread – the susceptibility of a population, the environment and socio-economical structure of a geographical region which affects the transmission strength and preparedness against an infectious disease outbreak. In recent times, it makes even more sense to investigate realistic infectious disease models- to predict and control outbreaks to minimize disease burden due to epidemics. For this purpose, mathematical models of infectious diseases focus on both – within host dynamics that has revelations significant to our understanding of biology of the disease, and between-host models that have profound impacts on our understanding of epidemiology of infectious diseases at population level [32, 11, 71].

Ideally, the host population in which the infection spreads, is divided into several compartments, with an underlying assumption that each individual in the is a representative of the respective compartment and has identical characteristics [32]. The compartmental models often follow standard notations for compartments. For example, an SEIR model will have: **S** indicates the proportion of *Susceptible* individuals in a population, who have either not contracted the infection, or have become susceptible again after recovery. **E** compartment stands for the individuals that have been *Exposed* to the infectious agent, which has not manifested into an

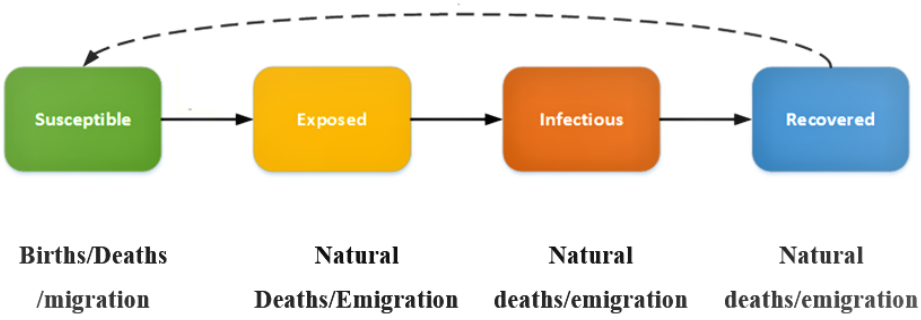

Figure 1.4: Schematic for SEIR Compartmental Model

infection. The individuals in an *Infected* compartment, **I** represent the proportion of human class which have become infected by the parasite. Such individuals may manifest clinical symptoms or remain asymptomatic. Finally, a *Recovered* class, **R** represents the individuals that have recovered from the infection- naturally or due to treatment. Individuals in the *R* compartment may go back to the *S* class if they do not develop immunity on recovery. Many variations of this formalism is known depending on the disease types: Schematically, one such compartmental model is represented in Figure 1.4. Below each compartment, biological and demographic factors (e.g. births/deaths, migration etc.) affecting the proportion of the class have also been depicted.

1.3 Compartmental Modelling of Malaria

A compartmental model for malaria was first proposed by Ronald Ross. As discussed in section 1, there are two hosts required - human and mosquito - for the malaria parasite life cycle to continue. The Ross model followed an simple **SI** structure as shown in Figure 1.5. Here both Susceptible humans (S_h) and

mosquitoes (S_m) get infected through mosquito-bites as shown by the red dotted lines in the figure. After infection, humans I_h recover and go back to the S compartment making it an **SIS** compartment model, whereas it is a SI model for mosquito since the infected mosquito I_m eventually dies. Ross, through his

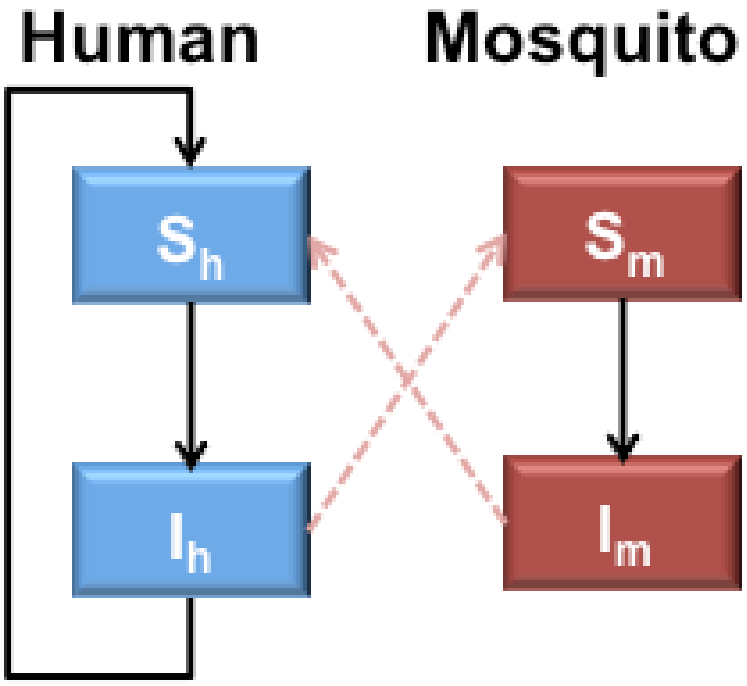

Figure 1.5: Schematic of the Ross model compartments and the interactions for disease evolution [56]. The red lettered compartment indicates the new compartment introduced in that model.

model, proved that reduction of mosquito proportion, beyond a certain "threshold" was potent enough to control disease spread. It was almost four decades later that George Macdonald [54, 53], re-emphasized on the importance of mathematical epidemiology, through twenty years of field research. Macdonald improvised Ross's model by characteristically incorporating the weakest link in the disease transmission cycle- the latency period of the exposed female mosquito and its reduced survival chance owing to infection and introduced the effect of

super-infection and re-infection in the host population [75, 10]. This drove the World Health Organization (WHO) to co-ordinate a large-scale elimination program which selectively focused on using the insecticide dichlorodiphenyltrichloroethane (DDT) that dramatically controlled the vector population to aid the elimination of malaria transmission among susceptible populations throughout the world [62]. Since the first model published by Ross, epidemiologists have modi-

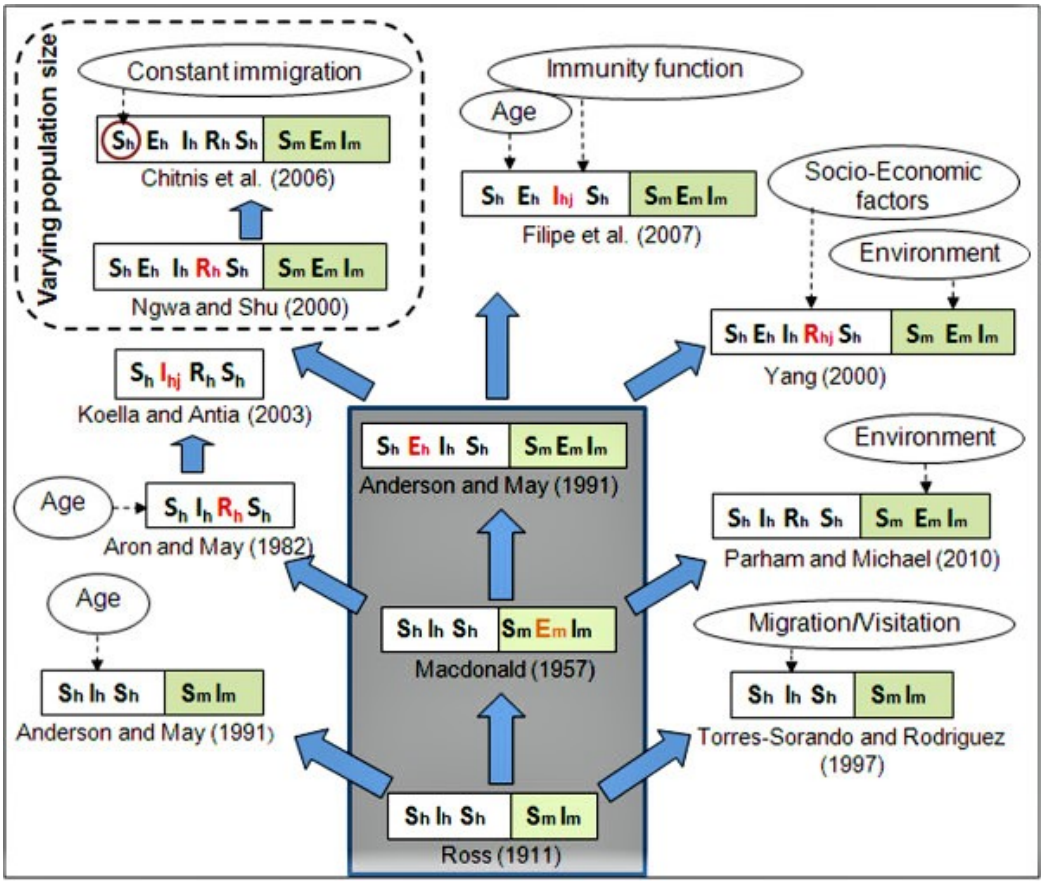

Figure 1.6: Evolution of Epidemiological Models of Malaria [56].The red lettered compartment indicates the new compartment introduced in that model.

fied the structure of the mathematical compartmental models for over a century to incorporate parameters that have been discovered to be associated with the infectious disease (Figure 1.6), but the battle against the parasite is yet to be won.

1.4 Malaria and its Control in India

Several states in India inhabited by ethnic tribes are entrenched with malaria; owing to heterogeneity in healthcare access; failed intervention strategies, and underestimation of disease prevalence. The two major human malaria species in India are *Plasmodium vivax* and *Plasmodium falciparum* ; India contributes to approximately half of all vivax malaria cases worldwide. Entrenched with higher infectious-diseases burden, it is these regions that are at a higher risk due to inadequate facilities and growing resistance against *P. falciparum*, that has established itself as the dominant malarial parasite in India over the past few decades (Figure 1.7).

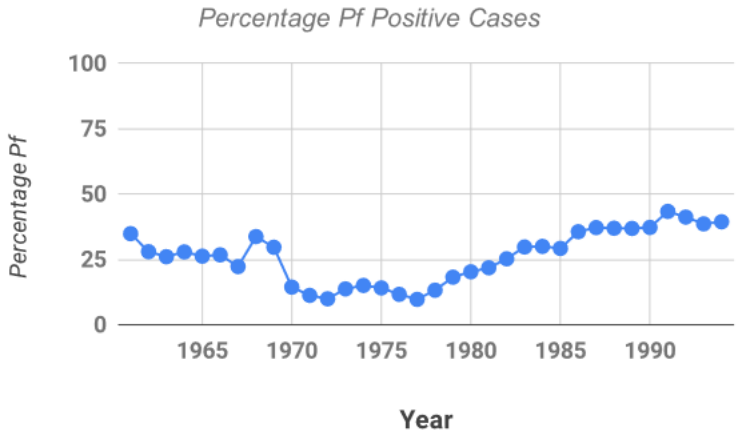

Figure 1.7: Relative contribution of *P. falciparum* to clinical malaria in India between 1961-95 [33].

India also contributes to about 75% of malaria cases in southeast Asia [83]. In addition to the biological and ecological variation in the infectious disease endemicity [1], disparity in socio-economic conditions- areas with high population

density and poor living conditions, unavailability of protection against infectious bites, absence of public health-care centers and low testing rates act as breeding grounds for infectious diseases. Upon diagnosis, poor prognosis or mortality owing to low nutritional status contributes to the enhanced malaria burden in the country. All these factors also underlie a wide variation and reduction in the immunity status of individuals in different populations in India - making it a serious impediment to improving public health against any infectious disease in India.

1.4.1 History of Malaria in India and Current Epidemiological Situation

India has had a long and chequered history of malaria, characterized by small to large scale epidemics over centuries. Historically, the highest incidence of malaria in India occurred in the 1950s, with an estimated 75 million cases and 0.8 million deaths per year [18]. The launch of the National Malaria Control Program (NMCP) in 1953 resulted in a significant decline in the number of reported cases to less than 50,000 and no reported mortality, by 1961. This was achieved by widespread DDT spraying as the primary strategy following the WHO guidelines as described in section 1.3, However malaria resurged to 6.45 million cases in 1976 due to failure in transmission control methods [49] making it the biggest epidemic in the 20th century.

1.5 Strategies for Malaria Control in India

Interventions against malaria effectively began in India post-independence. In 1953, the Government of India had launched the National Malaria Control Programme (NMCP) with an aggressive focus on indoor residual spraying of DDT. Within half-a-decade, the intervention strategies helped to substantially reduce the annual incidence of malaria. The National Malaria Eradication Programme (NMEP) was launched in 1958, to achieve further control against the infectious disease, which initially prove to be successful, but post 1967, the failure of control methods, combined with the mosquito's resistance to insecticides and the parasite's growing resistance to antimalarial drugs, India witnessed a growing epidemic from mid-1970s to mid-1980s, with most recorded impact in the late 1970s [64]. Post epidemic, the *falciparum* malaria cases have continued to rise. Currently, India's first-line treatments for *P. falciparum* are artemether-lumefantrine and artesunate-amodiaquine, with some north eastern regions presenting a failure rate of more than 10 percent [70, 42], pushing the need for improvisation in control and treatment policies.

1.6 Thesis outline

The work presented in this thesis involves two different theoretical approaches to study development and spread of malaria in a population - mathematical modeling and prevalence data analysis. Mathematical models are framed based on the biological facts of the infection process during host-pathogen interactions. Disease prevalence data analysis use descriptive methods and statistical techniques to find

patterns based on which future predictions can be made. The results are presented in the following five chapters:

1. Chapter-1 gives an overview of Malaria in India and the modelling methods applied to Malaria.

2. Chapter-2 elucidates the model and important parameters of a compartmental model of malaria. The mathematical and statistical methods that are used to study the epidemiological dataset of malaria prevalence in India are also included in this chapter.

3. Chapter 3 describes all the immunity related parameters and functional forms incorporated in the compartmental model in separate subsections. The detailed description about the model and its numerical and analytical analyses are also discussed in detail.

4. Chapter-4 reports the detailed analysis of a historical epidemiological dataset (1965-1995) of malaria prevalence in India. Both visual descriptions and statistical analysis of the dataset are presented in separate sections.

5. Chapter-5 highlights the major findings of the complete study and discusses future work in each area of study.

Chapter 2

Model and Methods

2.1 A Compartmental Model for Malaria

A detailed epidemiological model for malaria was developed considering SEIS compartments for the human host and SEI for the mosquito population as shown in Figure 2.1 [57]. The compartments on the upper left of Figure 2.1 represent the four epidemiological classes for humans, and the compartments on the right represent the epidemiological classes for mosquito populations. The transmission of the parasite from mosquito to human is represented using a *red dotted* line and the transmission from human to mosquitoes is depicted using a *black dotted* line. The arrows are indicative of transition from one epidemiological class to the other (described in the model).

The assumption of the model is a human population with a continuous age structure, in which individuals can be Susceptible $(S_h(a,t))$, $Exposed(E_h(a,t))$, Infected with symptomatic (severe and clinical disease) $(I_{hS}(a,t))$, or with asymp-

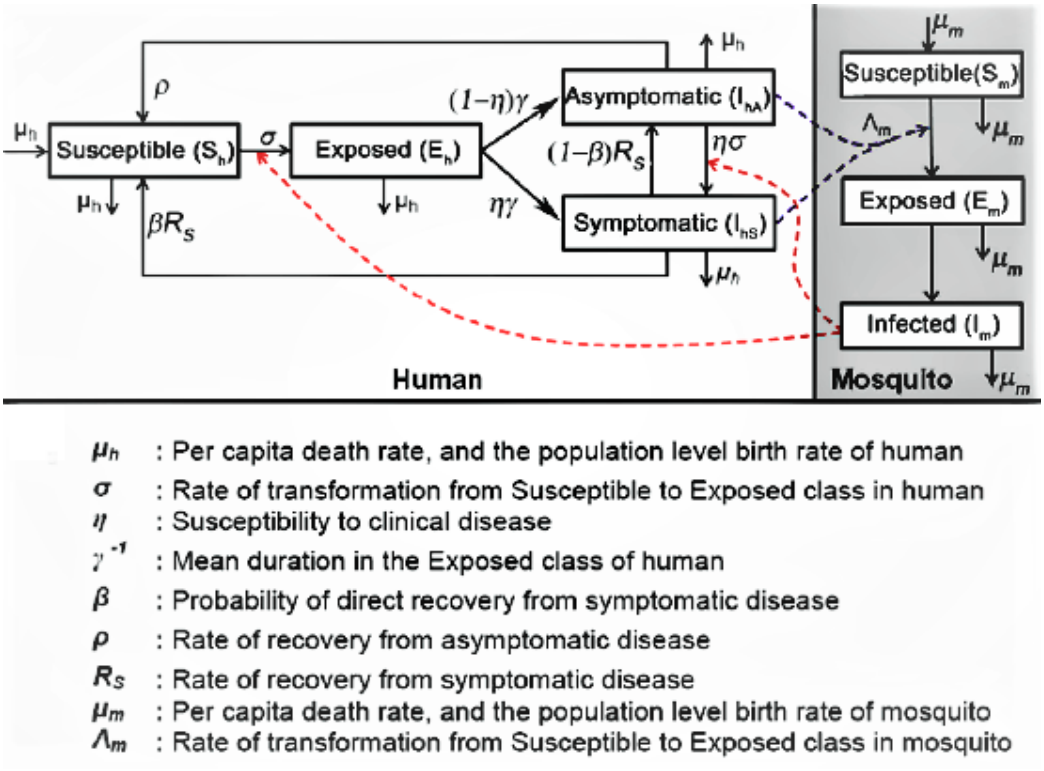

Figure 2.1: Schematic diagram for the Compartmental model of Malaria with parameters.

tomatic disease $(I_{hA}(a,t))$. A parallel mosquito population can either be Susceptible $(S_m(t))$, Exposed $(E_m(t))$ or Infected $(I_m(t))$. However, explicit age dependence has been excluded to analyse the model better and parameters with age-dependence are discretely independently calculated.

The model thus then transforms into a system of seven-coupled ordinary time dependent differential equations; which can be solved with or without incorporating delay (tau = 0.019 yr) i.e. the latent period in the mosquito population. Basic assumptions of the model include the following:

The mosquito and human populations are both normalized to one, under the as-

sumption that the total population overall remains constant. At any given instant:

$$S_h + E_h + I_{hS} + I_{hA} = 1 \tag{2.1.1}$$

$$S_m + E_m + I_m = 1 \tag{2.1.2}$$

The force of infection, σ is the rate at which the susceptible class of human population moves to the exposed human compartment, and depends on the number of infectious bites; and is age-dependent, and peaks in childhood [12]. Given that m is density of mosquitoes, α, the biting rate, and b is the probability of inoculation upon being bitten by an infectious mosquito; the force of infection can be defined as:

$$\sigma_m(a) = m\alpha b(1 - e^{-\frac{a}{a_0}}) \tag{2.1.3}$$

Where a is the age of the human host; and a_0 is the age at which half of the total exposure is achieved.

Susceptible individuals, upon being inoculated remain in the exposed class for a mean duration of 1-2 weeks $1/\gamma$, while they are still infectious. It is the immunity of the individual human host that determines whether the exposed individual will manifest symptomatic clinical infection (proportion equivalent to η) or move to asymptomatic class. Asymptomatic individuals still run the risk of getting re-infected at rate equal to $\eta\gamma$.

Asymptomatic individuals can become susceptible again, via clearance of parasites at a rate ρ. β, defined as the probability of recovery from clinical infection; and a fraction f of the clinically infected individuals get recovered post treatment at a rate ρ_t and the rest recover under the effects of immunity at a rate ρ_s.

Hence, the rate at which symptomatic individuals move to the susceptible compartment can be formulated as a cumulative effect of ρ_s and ρ_t, given as:

$$R_S = f\rho_t + (1-f)\rho_s \tag{2.1.4}$$

Mosquitoes that are susceptible become infected upon biting individuals that are symptomatic and asymptomatic, thus propagating the dual host-vector cycle of the malarial parasite. This facilitation is incorporated in the model through probabilities C_{IS} and C_{IA}, that denote the chance of infection upon biting an infected human individual. Overall, mosquitoes get infected at a rate given as:

$$\lambda_m = \alpha(C_{IS}I_{hS} + C_{IA}I_{hA}) \tag{2.1.5}$$

The model also incorporates the reduced survivability of the mosquito upon infection; an infected mosquito only passes the disease to human population if it survives a period of latency, here considered to be as approximately seven days. This reduced probability is considered using the function $\psi = e^{-\tau\mu_m}$. The comparative lifespan of the mosquito with respect to human population is negligible, hence the model assumes no disease induced mortality.

The model equations for human compartments are:

$$\frac{dS_h}{dt} = \mu_h + \beta R_S I_{hS} + \rho I_{hA} - \sigma I_m S_h - u_h S_h \tag{2.1.6}$$

$$\frac{dE_h}{dt} = \sigma I_m S_h - \eta\gamma E_h - (1-n)\gamma E_h - \mu_h E_h \tag{2.1.7}$$

$$\frac{dI_{hS}}{dt} = \eta\gamma E_h + \eta\sigma I_m I_{hA} - \beta R_s I_{hS} - (1-\beta) R_S I_{hS} - \mu_h I_{hS} \tag{2.1.8}$$

$$\frac{dI_{hA}}{dt} = (1-\eta)\gamma E_h + (1-\beta) R_s I_{hS} - \eta\sigma I_m I_{hA} - \rho\ I_{hA} - \mu_h I_{hA} \tag{2.1.9}$$

For mosquitoes:

$$\frac{dS_m}{dt} = \mu_m - \lambda_m S_m - \mu_m S_m \tag{2.1.10}$$

$$\frac{dE_m}{dt} = \lambda_m S_m - \psi\lambda_m(t-\tau) S_m(t-\tau) - \mu_m E_m \tag{2.1.11}$$

$$\frac{dI_m}{dt} = \psi\lambda_m(t-\tau) S_m - \mu_m I_m \tag{2.1.12}$$

These equations are studied in detail in Chapter 3 along with a comprehensive study of the host immunity functions.

2.2 METHODS

2.2.1 Numerical Methods

The Numerical integrations of the differential equations in were carried and plotted using the ode45 and dde23 solvers in MATLAB R2106b [58].

2.3 Malaria Data of *P. falciparum* in India: Origin & Acquisition

The data for this thesis project to investigate *falciparum* malaria prevalence was acquired through three volumes published by the Ministry of Health and Family Welfare, Govt. of India between 1986-1996. The volumes titled “National

Malaria Eradication Programme (Two Volumes- 1986)" and "Epidemiology and Control of Malaria in India (1996)" contain key information regarding the infectious disease and its determinants (Figure 2.2). The epidemiological parameters from the dataset are described in Table 2.1. The volumes with data were scanned and the historical dataset was extracted using OCR. This was done using an online OCR software that recognizes the entire character and matches it to the matrix of characters stored in the software [81].

Figure 2.2: Schematic for dataset acquisition and analysis.

Parameter	Description	Formula, if applicable
Pf%; *P. falciparum* percentage	The percentage contribution of *P. falciparum* to total malaria positive cases	$\frac{Total\ no.\ of\ positive\ falciparum\ cases}{Total\ no.\ of\ positive\ cases} * 100$
S*f*R; Slide *falciparum* positivity rate	An estimate of the monthly/yearly *falciparum* load in the population	$\frac{Total\ no.\ of\ positive\ falciparum\ cases}{Total\ no.\ of\ blood\ smears\ examined} * 100$
AFI; Annual *falciparum* parasite incidence	Parameter for estimating malaria endemicity in an area and impact of control interventions	$\frac{Total\ no.\ of\ positive\ falciparum\ cases}{Total\ populatio\ under\ surveillance} * 100$

Table 2.1: Summary of the epidemiological dataset parameters.

2.4 Statistical Methods for Data Analysis

2.4.1 Spatial Time Series

Time series analysis is used to identify the fluctuation in time-dependent data and helps in the evaluation of present situation and helps in pattern recognition and future predictions. The analysis of a historical dataset of *falciparum* malaria prevalence in India theoretically enables us to probe further into the parameters that might have aided in its manifestation as the dominant malarial parasite in India. The spatio-temporal time series for all Indian States with respect to *falciparum* prevalence has been evaluated using the software QGIS (Version 3.10.6) [78].

2.4.2 Principle Component Analysis

Principal Component analysis helps in extracting features to reveal the internal structure of the data in a way that best explains its variance. If a multivariate dataset is visualized as a set of coordinates in a high-dimensional data space, PCA helps in obtaining a lower-dimensional picture of the dataset to understand its composition [46]. In the case of the historical dataset of malaria prevalence, we extract features from the geographic and temporal data to cluster geographic regions and years based on the groupings obtained as the output. The Principal components are a series of linear least square fits to a sample, each orthogonal to all the previous.

Mathematically, Given a sample of n observations on a vector of p variables

$$X = (x_1, x_2, x_3, \ldots, x_p)$$

where X is the matrix with column-wise zero-empirical mean, where the n rows represent a different repetition of the experiment, and each of the p columns gives a particular kind of feature.

The first principal component of the sample is defined by the linear transformation:

$$z_1 = a_1^T X = \sum_{i=1}^{p} a_{i1} x_i \tag{2.4.1}$$

where the vector $a_1 = (a_{11}, a_{21}, a_{31}, \ldots, a_{p1})$ is chosen such that,

$$var[z_1] \textit{ is maximised}$$

Similarly, the kth Principal component of the sample by the linear transformation is given as:

$$z_k = a_k^T X, \;\; k = 1, \ldots, p$$

where the vector $a_k = (a_{1k}, a_{2k}, a_{31}, ..., a_{pk})$ is chosen such that the

$$var[z_k] \textit{ is maximised}$$

$$\text{subject to } cov[z_k, z_l] = 0 \;\; for \;\; k > l \geq 1 \text{ and } a_k^T a_k = 1$$

Note: All Statistical Analyses for the historical dataset of malaria were performed using the Python's packages for data science [80].

Chapter 3

Analysis of a Compartmental Model of Malaria

Severe malaria can manifest into coma and subsequent death if not treated and is almost exclusively caused by *P. falciparum* infections. To combat the complicated effects of repeated infections, hosts can mount a level of protective immunity which shields them against subsequent infections facilitated by a wide range of molecular mechanisms. A few of the presumed mechanisms of adaptive immunity to malaria can be given as [77]:

- Antibody mediated blocked invasion of sporozoites into liver cells.
- Interferon-γ (IFN-γ) and $CD8^+$ T cells mediated inhibition parasite development in hepatocytes.
- IFN-γ and $CD4^+$ T cells dependent activation of macrophages to phagocytose intra-erythrocytic parasites and free merozoites. Antibodies mediated

complement-dependent lysis of extracellular gametes, and preventon of fertilization of gametes and the development of zygotes.

Different types of immune responses act together to enhance protection against the malaria parasite in endemic regions. In the compartmental model discussed in this chapter, immunity has been classified as:

1. Maternal immunity: immunity passed on at birth to infants (Section 3.5).
2. Anti-disease or clinical immunity: acquired immunity against clinical symptoms of malaria (Section 3.6).
3. Anti-parasite immunity: acquired immunity against the parasite to eliminate parasite load in the human-host in endemic regions (Section 3.7).

In this chapter, first an in-depth mathematical and numerical analysis of the detailed epidemiological model [57] for malaria (see section 2.1 in Chapter 2) is reported, and then some new analysis done on the host immunity related functions with an aim to study how variation in host immunity may affect the steady state levels of infection.

3.1 Steady-State Solutions of the Compartmental Model

For constant age, it is seen that if $S_h > 0$, then $dS_h/dt \geq 0$ for $I_{hS} \geq 0$, $I_{hA} \geq 0$, $I_m \geq 0$. Therefore, we are able to analyze two positive fixed points for the model- disease free and endemic equilibrium point.

3.1.1 Disease-free Equilibrium

Disease-free equilibrium points for the compartmental model are steady-state solutions where there is no disease present in both the host and vector populations. For the given system, the disease-free equilibrium is exactly one unique point which is given as:

$$E_0^* = (S_h^*, E_h^*, I_{hS}^*, I_{hA}^*; S_m^*, E_m^*, I_m^*) = (1,0,0,0;1,0,0). \tag{3.1.1}$$

3.1.2 Endemic Equilibrium

Endemic equilibrium points are the steady-state solutions of the model for which the disease persists (all state variables are non-zero). From the model, the steady-state solutions can be calculated in terms of S_m^* [57].

$$S_h^* = \left[\frac{(\gamma+\mu_h)\mu_m(\mu_h \quad K_1 + \ R_S K_2)}{\sigma\psi\alpha\gamma\{\eta C_{1S}K_3 + (1-\eta)C_{1A}K_4\}S_m^*}\right] \tag{3.1.2}$$

$$E_h^* = \left[\frac{\mu_m(\mu_h K_1 + \ R_S \quad K_2)\,(1-S_m^*)}{\alpha\gamma\{\eta C_{1S}K_3 + (1-\eta)C_{1A}K_4\}S_m^*}\right] \tag{3.1.3}$$

$$I_{hS}^* = \left[\frac{\eta K_3\mu_m\,(1-S_m^*)}{\alpha\{\eta C_{1S}K_3 + (1-\eta)C_{1A}K_4\}S_m^*}\right] \tag{3.1.4}$$

$$I_{hA}^* = \left[\frac{(1-\eta)K_4\mu_m\,(1-S_m^*)}{\alpha\{\eta C_{1S}K_3 + (1-\eta)C_{1A}K_4\}S_m^*}\right] \tag{3.1.5}$$

$$E_m^* = (1-\psi)\,(1-S_m^*) \tag{3.1.6}$$

$$I_m^* = \psi\,(1-S_m^*) \tag{3.1.7}$$

Where, $K_1 = \sigma\eta\psi\,(1-S_m^*) + \rho + \mu$

$_h$, $\qquad K_2 = \sigma\eta^2\psi(1-S_m^*)+\rho+\mu_h$

$K_3 = \sigma\psi(1-S_m^*)+\rho+\mu$

$_h$ $\qquad K_4 = (1+\eta)(R_S+\mu_h)$

S_m^* can be computed by solving the equation:

$$AS_m^{*^2} + BS_m^* + C = 0 \tag{3.1.8}$$

Where:

$A = -\sigma^2\eta\psi^2\mu_h\{\alpha\gamma C_{IS} + (\gamma+\eta R_S+\mu_h)\mu_m\}$

$B = \sigma\psi\mu_h[\alpha\gamma\eta C_{IS}(\sigma\psi+\rho+\mu_h)+\alpha\gamma(1-\eta)C_{IA}\{(1+\eta)R_S+\mu_h\}]+\sigma\psi\mu_h\mu_m[\rho(\gamma\eta+R_S+\mu_h)+(\gamma+\mu_h)\{2\sigma\eta\psi+(1+\eta)\mu_h\}+R_S\{\gamma+2\sigma\eta^2\psi+(1+\eta^2)\mu_h\}]$

$C = -\mu_h\mu_m[(\sigma\psi+\mu_h)\{(\gamma+\mu_h)(\sigma\eta\psi+\mu_h)+R_S(\gamma+\sigma\eta^2\psi+\mu_h)\}+\rho\{\gamma\sigma\eta\psi+(\gamma+\sigma\psi+\mu_h)(R_S+\mu_h)\}]$

3.2 Basic Reproduction Number

The basic reproduction number, R_0, is defined as the expected number of secondary cases produced by a single infected individual in a susceptible population over the course of the infectious period. The R_0 is a theoretical value that is generally calculated from a mathematical model of the respective epidemic. Often used to access the severity of an infectious disease epidemic, it is extremely crucial for

determining the strength of interventions necessary to contain the infection [24].

If $R_0 < 1$, the epidemic is considered to have been eliminated from the population. For $R_0 > 1$, the outbreak is classified to have transformed into an epidemic; which happens to be a case with seasonal malaria in endemic regions where small-to-large scale epidemics occur consistently. For this particular model, the reproduction number is calculated using the mathematical theory of epidemics [25].

Let us assume that there are n compartments of which m are infected. We define the vector $\bar{x} = x_i,\ i = 1, \ldots,\ n$, where x_i denotes the number or proportion of individuals in the ith compartment.

Let $F_i(\bar{x})$ be the rate of appearance of new infections in compartment i and let where V_i^+ is the rate of transfer of individuals into compartment i by all other means and V_i is the rate of transfer of individuals out of the ith compartment. The difference $F_i(\bar{x})V_i(\bar{x})$, gives the rate of change of x_i.

Assuming that the criterion for F_i and V_i as described by [28] is met, the matrix operator matrix operator FV^{-1} can be calculated using the partial derivatives of F_i and V_i, where $i,\ j = 1, \ldots, m$ and x_0 is the disease-free equilibrium, where

$$F_i = \left[\frac{dF_i}{dx_j}\right] \,\&\, V_i = \left[\frac{dV_i}{dx_j}\right] \tag{3.2.1}$$

$$R_0 = r\left(FV^{-1}\right) \tag{3.2.2}$$

$$R_0 = \frac{\alpha^2 \gamma m b \left(1 - e^{-\frac{a}{a_0}}\right) \psi \left[\eta C_{IS}(\rho + \mu_h) + C_{IA}\left\{1 - \eta^2\right\} R_S + (1-\eta)\mu_h\right]}{(\gamma + \mu_h)(\rho + \mu_h)(R_S + \mu_h)\mu_m} \tag{3.2.3}$$

On rearranging the terms,

$$R_0 = \frac{\alpha\gamma\sigma\psi[\eta C_{IS}(\rho+\mu_h)+C_{IA}\left\{\left(1-\eta^2\right\}R_S+(1-\eta)\mu_h\right]}{(\gamma+\mu_h)(\rho+\mu_h)(R_S+\mu_h)\mu_m} \tag{3.2.4}$$

Depending on the age specific parameters; as discussed above the sensitivity of R_0 can be calculated numerically and compared at different ages with respect to N-fold change in mosquito related parameters [8]. From the above results, it is

Parameter values			Basic Reproduction Number (R_0)		
mosquito density, m	τ (in days)	μ_m (1/day)	age = 3 years	age = 20 years	age = 40 years
0.5	5	0.05	4.97	5.79	5.02
0.5	5	0.5	0.05	0.06	0.05
0.5	15	0.05	3.02	3.52	3.05
0.5	15	0.5	0.000029	0.00004	0.0003
10	5	0.05	99.50	115.88	100.42
10	5	0.5	1.05	1.22	1.05
10	15	0.05	60.43	70.41	61.62
10	15	0.5	0.0072	0.0084	0.0072

Table 3.1: Variation in R_0 due to vector related parameters (m, I_m, τ, μ_m) and *age* of the human host.

imperative to consider that mosquito mortality rate is a critical factor while investigating realistic disease transmission between the host-vector. From the calculations of R0 it is evident that even when the mosquito density is decreased significantly, it is the mosquito mortality that produces the most pronounced effects in disease propagation.

Another interesting feature that the calculation highlights is the high reproduction number at the age 20 years, in comparison to younger and older ages of the hu-

man host. It is indeed the outcome of acquired immunity due to exposure that enables people in higher age groups to sustain the infection better, hence decreasing the overall reproduction number in older age group. It might appear intuitive or trivial even, but mosquito mortality is the driver of prevalence pattern of the clinical infection in humans. Hence, strengthening intervention strategies that focus on mosquito density reduction through accelerated mortality are imperative in malarial transmission control [57, 8].

3.3 Numerical Solutions of the Compartment Model

At a constant age, the compartmental model for host-vector transmission is a system of seven ordinary differential equation for which the time series can be numerically derived. All parameters and their numerical values used for simulations are given in Table 3.2. The numerical results for the model in subsequent sections have been obtained assuming no extrinsic delay in the latent period for the mosquito population. S_h; E_h; I_{hS} and I_{hA} are $Susceptible$, $Exposed$, $Symptomatic$ and $Asymptomatic$ proportions of the host population.

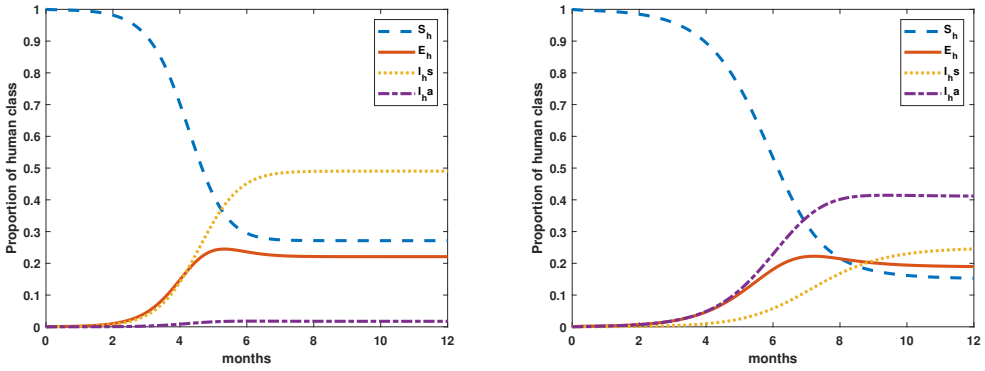

(a) Time series at age = 2 years

(b) Time series for human population compartments at age= 20 years

Figure 3.1: Time evolution of human compartments at age = 2 and 20 years

From the numerical simulation results, it can be seen that the human host compartments reach their equillibrium levels few months post onset of the infection. Figure 3.1 represents the time series for age = 2 & 20 years, where at age = 2 years, the equilibrium of asymptomatic infection is a negligible proportion of the human population, because of poorly developed immunity against the infectious disease (Figure 3.1a). Symptomatic prevalence peaks at age = 3 years; hence at 2 years of age, the symptomatic class is the largest contributor to the population. At age = 20 years; the human population acquires immunity against the parasite, hence there is a drop in the proportion of the symptomatic class. With the development of anti-parasite immunity, a significant proportion of the human class has a tendency to tolerate a higher parasite load, while remaining asymptomatic as shown in the time-series for the human compartments.

Parameter	Description	Value	Units	References
$\sigma_m(1 - e^{-a/a_0})$	Force of infection which is age-dependent	–	ibppy	assumes exposure is a monotonic increasing function of body size
a_0	Age at which half the total increase in exposure occurs	3	Yr	setting dependent; typical range between 3-5 years [34]
b	Probability of successful inoculation upon an infectious bite by an infected mosquito	0.2		Realistic values are setting and potency dependent, maximal value is $\sim$0.5
ρ_t	Rate of recovery from clinical malaria upon chemotherapy	1/21	day^{-1}	varies with line of the chosen drug; [27]
ρ_s	Mean rate of natural recovery from clinical malaria;	1/180	day	baseline value1; [34]
ρ_0	Mean rate of recovery from asymptomatic to sub-patent	1/180	day^{-1}	baseline value1; immunity function
ϕ	Probability of becoming a symptomatic case upon infection (susceptibility)	0.5		baseline value; immunity function described
$1/\gamma$	Mean incubation period in humans	7	days	(Estimated in [57]); Range 7-14 days
C_{IS}, C_{IA}	Probability of mosquito infection upon biting a human in state Ihs, Iha respectively	0.35, 0.03	–	[3]
τ	Latent period in mosquito	21	day	varies with drug taken
f	Proportion of symptomatic cases treated effectively	0.5	–	setting dependent; assumed to be 0.5
μ_h	Human natural mortality rate (assumed to be constant with age)	0.0125	yr^{-1}	Setting dependent; [57]
a_{max}	Maximum age in the human community	60	Yr	Age distribution dependent; [57]
α	Biting rate by a female mosquito	0.67	day^{-1}	[39]

Table 3.2: Summary table for the compartmental model parameters and their numerical values

3.3.1 Age Prevalence Patterns

For fixed parameters provided in the summary table 3.2; the age prevalence of the symptomatic individuals can be computed numerically as the equilibrium of the symptomatic compartment at each age. In settings with high endemicity;

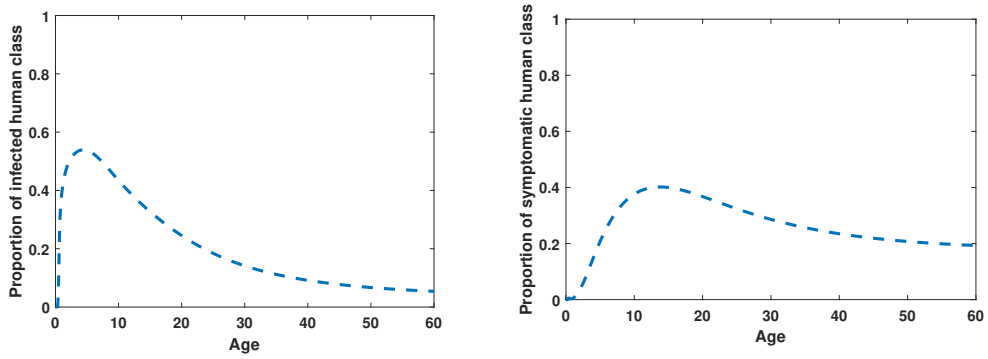

(a) symptomatic human class vs age

(b) Asymptomatic human class vs age

Figure 3.2: Age prevalence pattern of (a) symptomatic human class and (b) asymptoatic human class at EIR=100 (Table 3.2).

acquisition of clinical immunity with age and exposure contributes to significant reduction in incidence over subsequent years, and adults develop lower number of symptomatic episodes per year eventually. Similarly, due to immunity development in adults, the overall prevalence of asymptomatic individuals peaks in youth; due to partial development of acquired immunity to parasitemia and then gradually declines with age. Since asymptomatic individuals are still capable of being infectious, the disease remains endemic in the population (Figure 3.2b).

3.3.2 Prevalence Pattern Dependence on Exposure

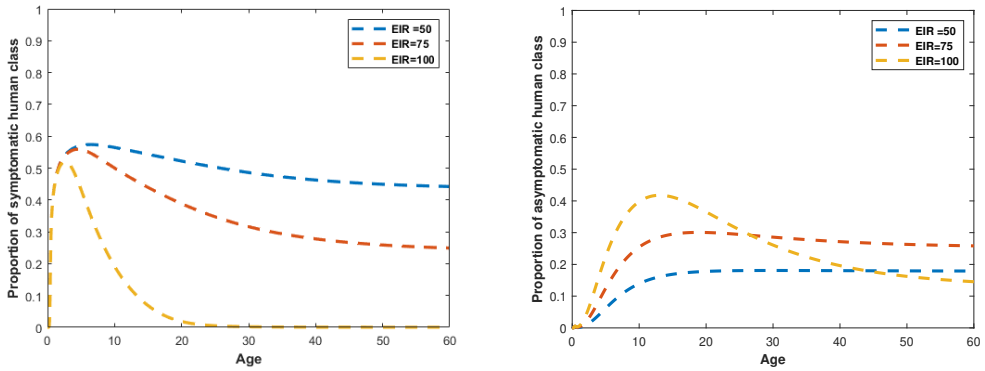

(a) Symptomatic proportion at EIR =50, 75, 100 ibppy

(b) Asymptomatic proportion at EIR =50, 75, 100 ibppy

Figure 3.3: Age related disease prevalence dependence on exposure

Prevalence of symptomatic individuals from the numerical studies is highest at certain age, and continues to decline after a certain threshold. However, the patterns of reduction are heavily dependent on the transmission intensity. At higher transmission intensities, repeated exposure to the parasite propagates the development of stronger immunological responses, hence at higher transmission rates, the curve for disease prevalence falls more steeply with age as compared to settings with lower and intermediate transmission intensities (Figure 3.3a).

Asymptomatic individual proportion in the model is sensitive to the parameters that govern host-vector interactions. Numerically, the disease peaks between the ages 10-20 (years) of the host, but the maxima at higher inoculation rates is high- which is expected. However, eventually the asymptomatic prevalence equilibria

become significantly lower at older ages as the inoculation rate is increased as seen in Figure 3.3b.

This is possibly due to the dependence of anti-parasite immunity on entomological interaction rate, i.e. as individuals are exposed to a higher parasite load through transmission, the immune system development becomes rapid to prevent disease transmission in the population. Intermediate level of inoculation yields a rather conflicting output of the asymptomatic class prevalence. The final equilibrium level of asymptomatic individuals exposed to intermediate EIR is higher as compared to low and high transmission settings [67].

Plausibly, the prevalence pattern could be such because although population in intermediate settings develop immunity; it is not long lasting enough to shield for extended periods as compared to populations with high-transmission settings and people in low transmission settings do not experience as pronounced levels of infection to experience prevalence levels as pronounced in areas with higher endemicity.

3.3.3 Disease Prevalence Variation due to intrinsic host parameters

As expected, the asymptomatic class in the human population increases if the parasite immunity duration is shortened; the prevalence curve for asymptomatic individuals decline steeply when the parasite immunity last longer and reaches a lower population-level equilibrium. Similarly, if the clinical immunity duration is shortened due to extrinsic or intrinsic factors including exposure, nutrition or health status, the symptomatic prevalence equilibrium levels are much higher.

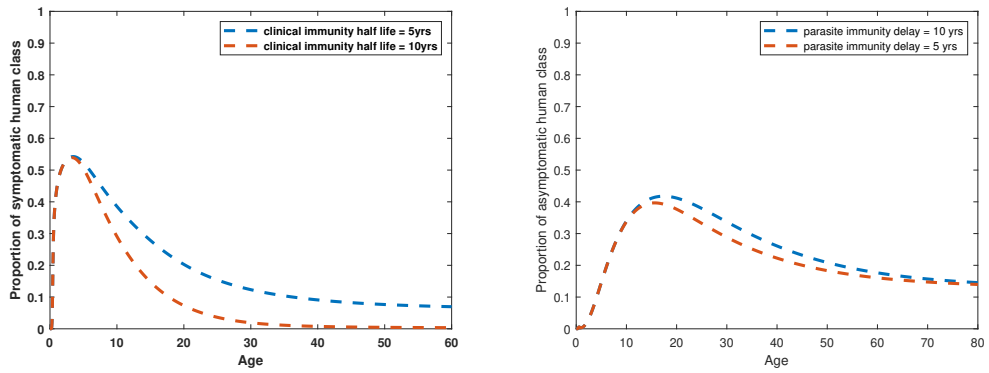

(a) Symptomatic class variation with immunity (b) Asymptomatic class variation with immunity

Figure 3.4: Variation in age Prevalence patterns of infected human class due to host immunity

In the subsequent sections; the effects of different types of immunity have been visualised by incorporating mathematical functions and are discussed in detail using the parameters described in Table 3.3

3.4 Modelling of Immunity to Malaria

The last few decades have indeed witnessed a substantial decline in malaria transmission in Sub-Saharan Africa and South-east Asia, but due to gaps in our understanding of anti-malarial immunity, endemic regions still possess a significant challenge towards control and eradication [15]. In most regions with high transmission rates, small-to-large scale epidemics continue to pose a significant disease burden on native populations and it is not only the biology of the infectious disease, but also the socio-economic heterogeneity of the disease that contributes to

malaria burden in under-developed and developing endemic regions.

The interaction between the human immune system and the parasite is complex, and poorly studied even in present times. The experimental obstacles to the understanding these interactions are pronounced, because field results are often variable and unreproducible in laboratories- owing to the heterogeneity in the host, as well ethical constraints of epidemiological research. One of the early models of mathematical modelling of immunity to malaria, proposed by [7] incorporated the maintenance of acquired immunity in response to repeated exposure as the rate of reversion, γ, which is defined as the average duration for which immunity lasts, assuming that immunity can last up to a period τ years if repeated exposure does not occur, in a completely susceptible population experiencing a rate of h infections per year. Mathematically, the rate of reversion is a monotonically-decreasing function defined as:

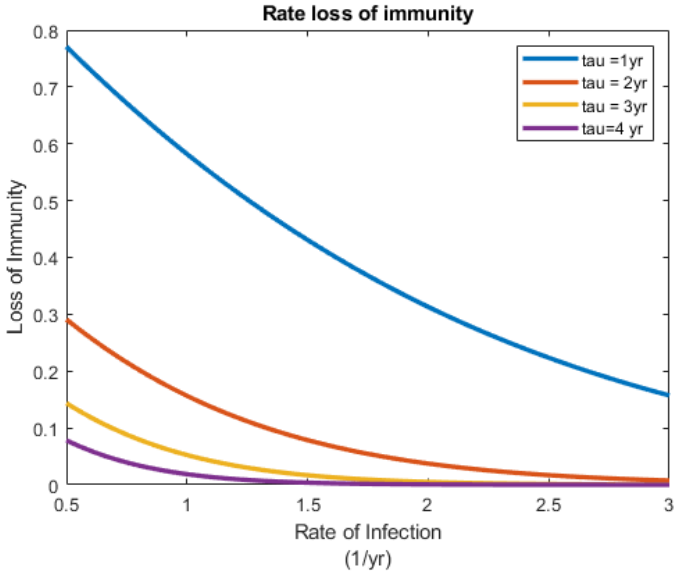

Figure 3.5: Rate of loss of immunity, γ [6].

$$\gamma(h) = \frac{he^{-h\tau}}{1-e^{-h\tau}} \tag{3.4.1}$$

The rate of loss of immunity, as proposed by Aron, decays faster as exposure is loss, and the acquisition of immunity and its maintenance are outcomes of continuous exposure. More advanced models, such as the compartmental model with heterogeneity in host and vector parameters [57] incorporate the age, exposure, host-vector interactions in the modelling of immunity functions.

The model described in Figure 2.1 incorporates maternal, clinical and anti-parasite immunity by formulating the results of the immunity variables as parameters that affect susceptibility and recovery from clinical and asymptomatic disease in endemic regions. Details of all immunity related parameters used in the model are given in Table 3.3.

3.5 Maternal Immunity Against Malaria

Analytically; the maternal immunity is simply a decaying function of the immunity attained at birth from the mother and decays with age as:

$$\frac{dC_m}{da} = -\frac{C_m}{d_m}, \tag{3.5.1}$$

Where a is the age of the human host; and C_{m0} is the initial maternal immunity passed on at birth [45]. The immunity declines with a half-life of d_m, estimated to be about three months in endemic settings [60].

Parameter	Description (Immunity Functions)	Value	Unit	Range; if applicable
d_m	Half-life of maternal immunity protection	0.25	Yr	0.1-0.5; the results are not sensitive within this range
p_m	Proportion of level of maternal immunity conferred	0.5		Assumed parameter
ρ_0	Baseline rate of recovery	1/180	day^{-1}	
d_S	Half-life of anti-disease immunity	5	Yr	
d_l	Delay phase in the development of anti-parasite immunity	10	Yr	Function of the age-dependent host-immune system; independent of exposure
d_A	Half-life of anti -parasite immunity	20	Yr	Estimated [34]
d_U	Baseline average duration of subpatent infections	180	Yr	
w_A	Maximal realistic amplification of the recovery rate	30	–	
H_S	Half-saturation level of anti-disease immunity	40	–	Variable; dependent on exposure and immunity related parameters
H_A	Half-saturation level of anti-parasite immunity	800	–	Variable; dependent on exposure and immunity related parameters
k_S	Determines the steepness of immunity function for anti-disease immunity	2	–	
k_A	Determines the steepness of immunity function for parasite immunity	2	–	

Table 3.3: Summary of immunity-related parameters and their numerical values for simulations

Upon solving, the functional form of the maternal immunity can be expressed as:

$$C_m(a) = C_m(0)e^{-a/d_m} \tag{3.5.2}$$

The maternal immunity duration in infants is dependent on the average entomological inoculation rate they are subjected to; i.e. infants that are subjected to higher levels of transmission have higher relative residual immunity that they derive maternally which is possibly an evolutionary immunological response. From the numerical simulation results,it is seen immunity might last up to 24 months

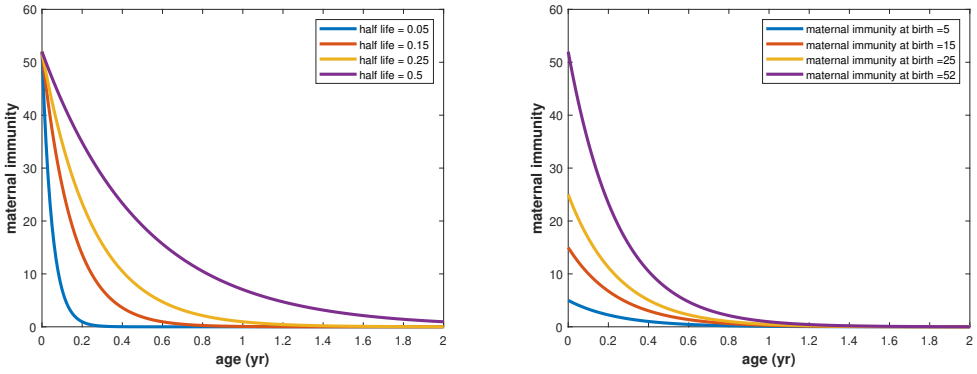

(a) maternal immunity dependence on d_m

(b) maternal immunity dependence on initial value, C_{m0}

Figure 3.6: Maternal immunity dependence on intrinsic parameters.

(2 years) in infants in whom the half-life of the maternal immunity is greater (Figure 3.6a). Realistically, this could be crucial for preventing first infections in infants in areas of high endemicity [21, 20].

However; it is not the mere presence, but the value of initial maternal immunity that dictates the interaction between the derived passive immunity and malaria exposure (Figure 3.6b). Children from areas of high transmission might inherit higher levels of maternal antibodies, and this might lead to significant protection early in life. Once this passive immunity is exhausted, immunity against the clinical malaria infection remains a function of exposure and individual host immune system, incorporated by the anti-disease immunity [67].

The clinical immunity against the infection stems from a cumulative effect of proportion of immunity that is passed on to an individual at birth in endemic settings, and then develops due to exposure once the maternal immunity is weaned.

Upon analysing the maternal immunity minimas at different mosquito densities,

Mosquito Density, m	Immunity Minima value	Time taken to attain minima (in yrs)
3	0.0011	0.9610
6	0.0018	0.7880
9	0.0025	0.6850

Table 3.4: Maternal immunity minima dependence on mosquito densities (m=3,6,9)

it is seen that the minima are extrinsically dependent on mosquito density of the settings. At higher mosquito density, the residual maternal immunity is higher than at low and intermediate densities, and the minima occurs rather earlier and is hence forth taken over by the clinical immunity, which is greater than the passive maternal immunity (Table 3.4).

3.6 Clinical Immunity

As the maternal immunity weans off, children in endemic settings begin developing immunity against the symptoms of clinical malaria [26] boosted by immunological responses to exposure.Mathematically, assuming that time dependent interventions are absent; the age dependence of clinical immunity can be expressed by solving exposure and age dependent differential equations given as:

$$\frac{dC_f}{d_a} = \sigma I_m - \frac{C_f}{d_s} \tag{3.6.1}$$

Where σI_m is the force of infection acting upon an individual and d_s is the half-life with which clinical immunity is lost in absence of exposure to parasite.

Analytically, the final expression for clinical immunity at any given age can be

expressed as:

$$C_f(a) = \frac{\sigma(a_{max})d_s(1+a_0e^{-a/a_0} - d_se^{-a/a_0})}{(d_s - a_0) + C_m(0)e^{-a/d_m}} \tag{3.6.2}$$

The clinical immunity is a saturating function with respect to age; and the initial maternal immunity is hypothesized to be half of the immunity attained at the age of saturation (setting dependent, [27].

3.6.1 Residual Maternal Immunity

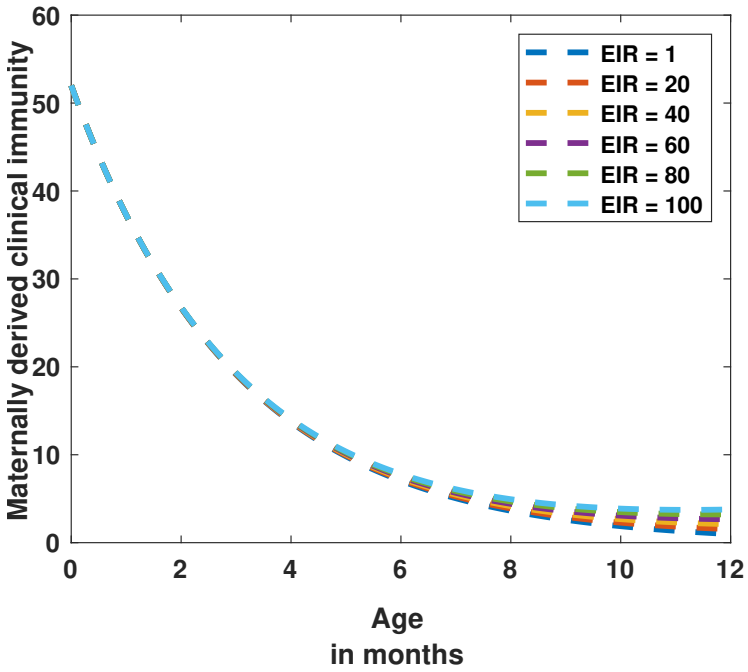

Figure 3.7: Dependence of maternally derived clinical immunity on transmission intensity.

During the first few months of an infant's life, immunity against the malaria infection is a consequence of maternal anti-bodies against the disease acquired at the time of birth. Depending on the transmission rates, infants might acquire anti-

disease immunity due to exposure disproportionately- i.e. in areas with higher endemicity, infants might have higher residual immunity due to additional effects of immunity boosted by consistent exposure to the parasite (Figure 3.7).

3.6.2 Clinical Immunity Dependence on Exposure

The maxima of clinical immunity are calculated as $\sigma(a_{max})d_s$ where $\sigma(a_{max})$ is the force of infection acting on the highest individuals in the population. For numerical results, the force of infection is expressed in the form of fixed Entomological Inoculation Rate, EIR:

$$\sigma(a) = EIRb(1 - e^{-a/a_0}) \tag{3.6.3}$$

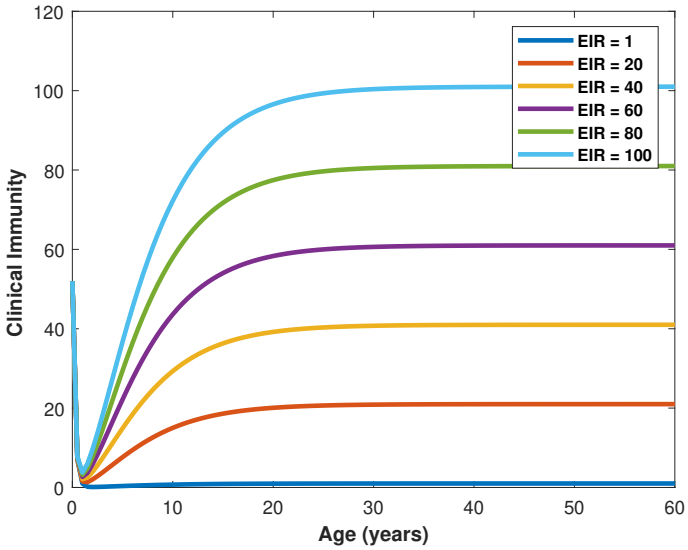

Figure 3.8: Variation in clinical immunity to due to heterogeneity in exposure

Since EIR is a function of mosquito dependent parameters; exploring the clinical

immunity development with respect to age reveals that in high transmission areas, the clinical immunity is always higher at any given age. The development curve of the immunity at the highest EIR is also the steepest, i.e. clinical immunity develops fast enough to shield against consistent exposure.

To singularly explore the effects of mosquito related parameters on final maturation levels of clinical immunity, simulations to compare different parameter combinations reveal to us that even though the effect of singular parameters appears to linearly change the equilibrium level of immunity, the cumulative effect is a non-linear curve that depends on exposure parameters. On assigning theoretical values

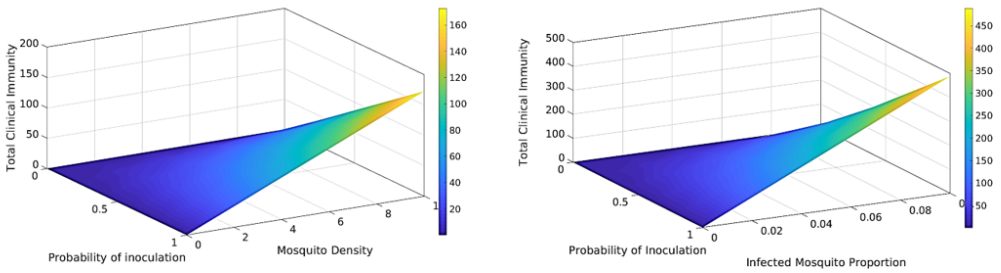

(a) Total Clinical Immunity vs m & b

(b) Total Clinical Immunity vs I_m & b

Figure 3.9: Clinical Immunity dependence on cumulative effect of vector related parameters - m, I_m and b. All other parameter values taken from Table 3.2.

to the probability of successful inoculation one observes that it is not the mosquito density alone, but the probability of inoculation and infected mosquito proportion that drive the acquisition of immunity. Bites by mosquitoes unviable of transmitting the disease would not drive immune responses against the infection; exposure

to the parasite is what develops the immunity against clinical symptoms [48].

3.6.3 Susceptibility to Malaria

The clinical immunity is incorporated through the susceptibility function; which defines the probability of being susceptible to clinical symptomatic disease. The dependence of Susceptibility function [34] on clinical immunity can be given as follows:

$$\eta = \frac{1}{1 + (\frac{C(a,t)}{C_{m0}})^{k_S}} \tag{3.6.4}$$

The susceptibility to malaria as a function of age under the effects of parasite ex-

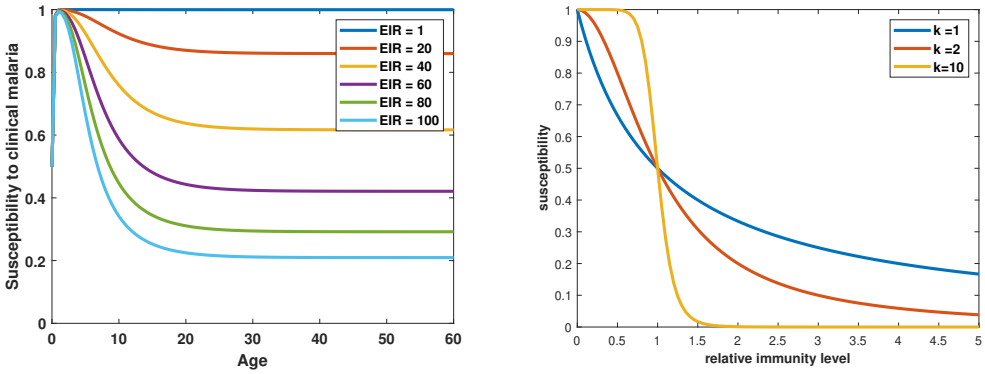

(a) Susceptibility vs Age (EIR =50, 75, 100) (b) Susceptibility vs relative immunity (k=1,2,10)

Figure 3.10: Variation in Susceptibility based on (a) extrinsic (Age at different transmission intensities) and (b) intrinsic parameters (relative immunity level at different amplification rates).

posure is a decreasing saturating function as seen in Figure 3.10a, and stabilizes in

older aged individuals, which is why children are worst affected by manifestation of the clinical disease and mortality due to severe infection.

Susceptibility can also be expressed as a function of relative immunity level with respect to the immunity possessed at birth (Figure 3.10b; and can be analyzed for different degrees of the steepness function. The highest assumed value for steepness leads to rapid fall in susceptibility theoretically; but is not the realistic depiction of susceptibility behavior in populations. For this model; steepness degree of both the susceptibility function and recovery rates has been fixed to two, which is most realistically replicable in human susceptible populations.

3.7 Anti-Parasite Immunity

Parasite immunity is associated with the recovery from asymptomatic infection; and with a latent immunity level accumulating through age dependent exposure and no surviving innate immunity. The anti-parasite immunity is the acquired immunity of the host; that is responsible for clearance of parasite and matures later in life due to maturation of the host immune system with age, and due to repeated exposure to the parasite. The immunity accumulates through a delay phase L_A (age-dependent maturity) function and the force of infection; and then decays when exposure is lost [76].

Cytokines induced during natural response malaria infections during clinical paroxysms in human *Plasmodium vivax* infections, mediate killing of intra-erythrocytic blood stage malaria parasites [59]. Mathematically, age-dependent anti-parasite

immunity [57] is modelled by the equations:

$$\frac{dL_A}{da} = \sigma I_m - \frac{L_A}{d_l} \tag{3.7.1}$$

$$\frac{dP}{da} = \frac{L_A}{d_l} - \frac{P}{d_A} \tag{3.7.2}$$

Since the anti-parasite immunity function models acquired immunity, at the time of birth, $L_A(0) = P(0) = 0$.

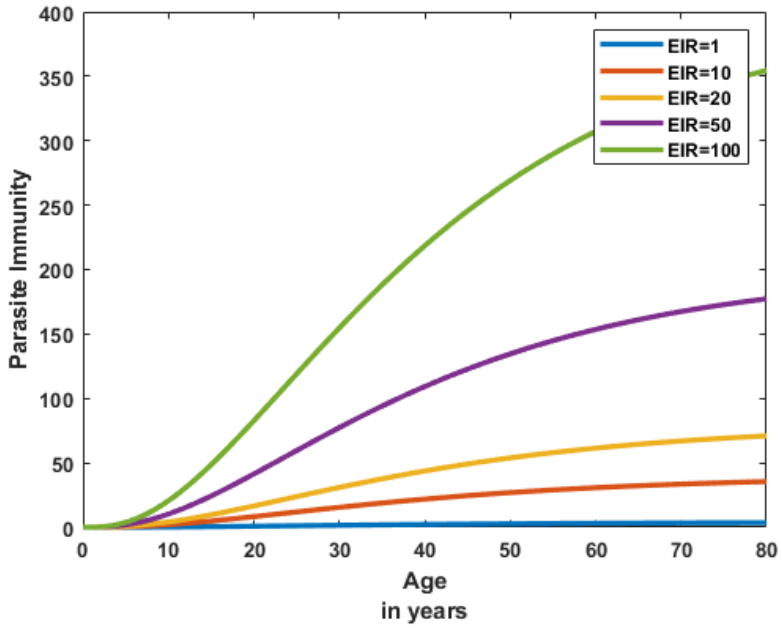

Figure 3.11: Dependence of maternally derived clinical immunity on transmission intensity.

Parasite immunity depends majorly on the host's age and immune system development; but in endemic settings, high transmission rates promote the rapid development of immunity to clear parasites from the host and increase tolerance for high parasitic loads to prevent clinical symptoms. In the first years of an individual's

life this shielding effect is generally poor; but with the age associated development of immune system and exposure, most adults develop acquired immunity against malaria, which is dictated by the individual immune system capabilities, not so much by exposure. This acquired immunity is also known to have a genetic basis in endemic areas [36, 40].

3.7.1 Comparison of Clinical and Parasite Immunity Development

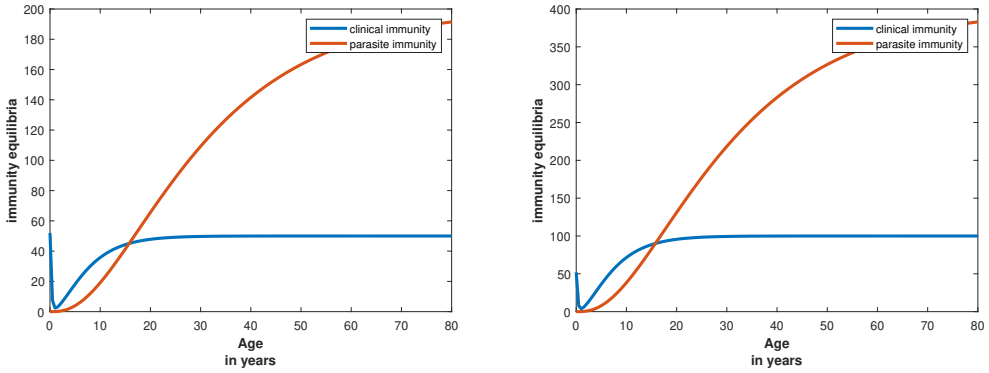

(a) Immunity Equilibria vs Age at EIR = 50 ibbpy(b) Immunity Equilibria vs Age at EIR = 100 ibbpy

Figure 3.12: Comparison of Clinical and Parasite Immunity in different transmission settings.

The behavior of anti-disease immunity and anti-parasite immunity is not dictated only by exposure, the curves for both types of immunity show explicit dependence on age. However, the immunity equilibrium value is a function of the force of infection acting on the human population. In areas of high endemicity, both

clinical immunity and parsite immunity are stronger, to reduce clinical symptoms, and clear parasite reservoirs (Figure 3.12).

As already known, the clinical immunity in the first few years of life shields against the infection and the parasite immunity develops slower during childhood. But once established through the age-related delay, the parasite immunity is what dominates the acquired immunity against malaria which leads to stronger immune responses and lower rates of detected parasitaemia upon reinfection, and this results in lower parasite densities in the adult human population [29, 30].

3.7.2 Recovery Rate Estimates

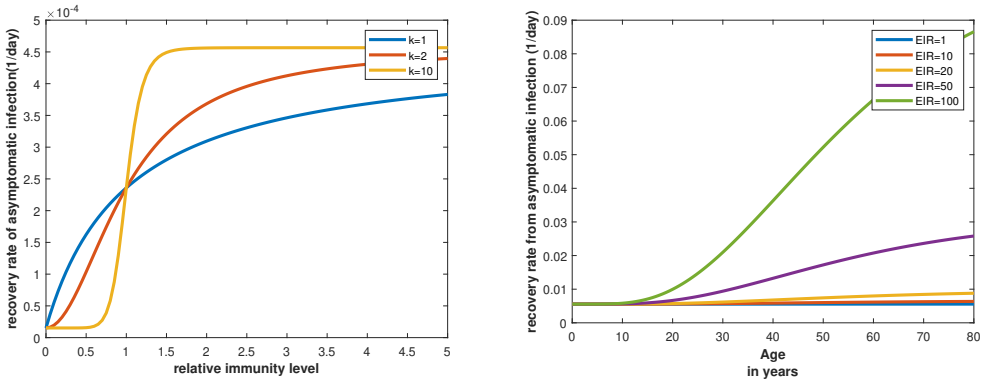

(a) Recovery rate vs relative immunity level (b) Recovery rate dependence on exposure

Figure 3.13: Dependence of recovery rates on (a) intrinsic and (b) extrinsic parameters.

The anti-parasite immunity function has been used to model the recovery rates against the disease and clearance of parasites. The mathematical expression of the recovery rate, is formulated as:

$$\rho = \rho_0 \left[1 + (w_A - 1) \frac{P_a / {H_A}^{k_A}}{1 + P_a / {H_A}^{k_A}} \right] \tag{3.7.3}$$

where ρ_0 is the baseline recovery rate, without treatment and w_A is the maximum amplification of the baseline rate.

The recovery rate estimate is most-realistic with respect to the discussed compartmental model when and $k_A = 2$, which is visualized through the numerical solutions of the recovery rate function given in Figure 3.13. The recovery rate depends on the age and host-vector interaction both; hence for higher levels of independent EIR, the recovery rate curve grows rapidly as compared to lower transmission rates.

Hence, adults in endemic settings become well adapted to clear non-complicated infections without treatment. In the results give in this section, the k_a parameter has been used to model the steepness of the recovery function and is setting dependent and individual-host dependent.

3.7.3 Sub-patent Infections

The asymptomatic class in human population also includes a portion of individuals that are immune-protected and this state is achieved not directly due to age; but due to continued re-exposure. A host reaching such a state would have to go through an extended period of exposure; this is incorporated through the "*super-infection*" recovery form or the recovery without any treatment.

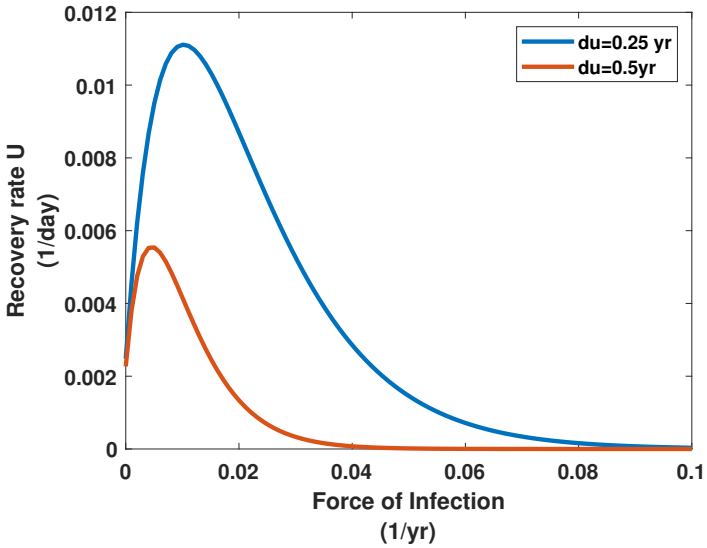

Figure 3.14: Sub-patent infection recovery rate vs age

Mathematically,

$$r_U(\sigma(\alpha)) = \frac{(\sigma(\alpha)}{e^{\sigma(\alpha)d_U} - 1} \tag{3.7.4}$$

where $\sigma(\alpha)$ is the exposure at age a; which increases with body size and the mean rate of clearance of sub-patent infections is d_U . This class of humans has not been incorporated in the model, but its existence in known [34].

It has now been proven that the acquisition of immunity that is partially protective is a domineering feature of the malarial epidemiology in endemic regions [48]. In highly endemic settings, interventions that can reduce but do not eliminate the transmission of the parasite can have drastic consequences (malaria epidemic in India (1976-77)). Short-term decline in malaria incidence due to intervention is not successful, due to loss of acquired anti-malarial immunity due to lowered ex-

posure to parasites [15, 34, 6]. Anti-parasite and clinical immunity develop in parallel, reducing the probability of developing clinical malaria upon each infection due to *Plasmodium* [73].

Since immunity depends on a range of parameters, association of anti-malarial immunity with protection from malaria can be contradictory if the studies fail to take into account differences in the transmission rates geographically. This conflict arises because high malaria exposure is possibly a driver of high anti-malarial immunological response [41], which might lead to an apparent positive association between the immune response and rate of infection.

Chapter 4

Analyses of *Plasmodium falciparum* Malaria Prevalence in India (1961-95)

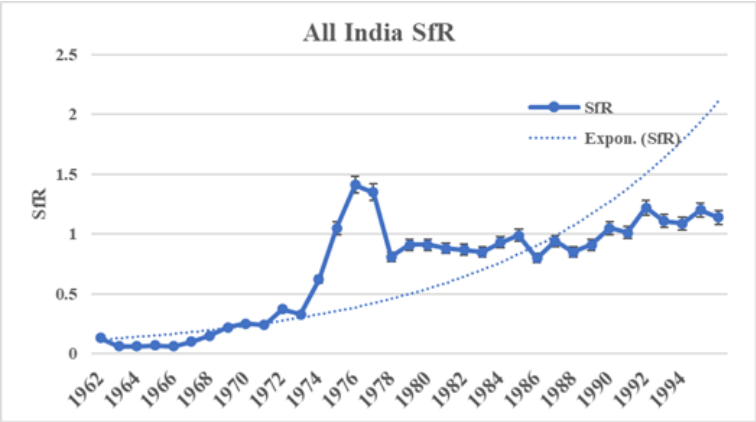

Figure 4.1: **S*f*R** in India between 1961-95.

Even though the majority of malaria cases in India are caused by the parasite *Plasmodium vivax*, the past few decades have seen an exponential rise in the con-

tribution of the parasite *Plasmodium falcliparum* as the causative agent of malaria in India (shown in Figure 4.1), which is also more lethal. The highest recorded cases of *falciparum* malaria have been reported in the state of Orissa, and approximately 46 million inhabitants are at the risk of this infection. The interplay of various factors like favourable climate, geo types, large forest coverage, difficulty in accessing remote and hilly villages and prevalence of efficient *Anopheles* mosquito vectors, along with wide-spread low economic status, have resulted in persistent malaria transmission in different parts of the state [66].

During 1961-95, the mean S*f*R in India rose from approximately zero to 1.14, peaking at 1.5 during the epidemic in mid 1970s. Since then, the *falciparum* malaria has only gone up and accounts for approximately 60% of all malaria cases in India [83].

In this chapter, different descriptive statistical methods have been applied to a historical dataset of India between 1961-95 to highligt the spatio-temporal properties of *falciparum* emergence in the country.

4.1 Time Series of S*f*R in States between 1961-95

The scatter plot depicting the S*f*R time-series in states and at the all India level reinforces the features we have derived with other statistical methods in subsequent sections- owing to geographical, ecological and socio-economic diversity, S*f*R across the nation are not homogenously distributed. However, the continuous structure of the time series data, is in synchrony with the overall malaria prevalence in India; i.e. the low prevalence 1960s due to extreme transmission control strategies, the building up of an epidemic in mid 1970s which only declined grad-

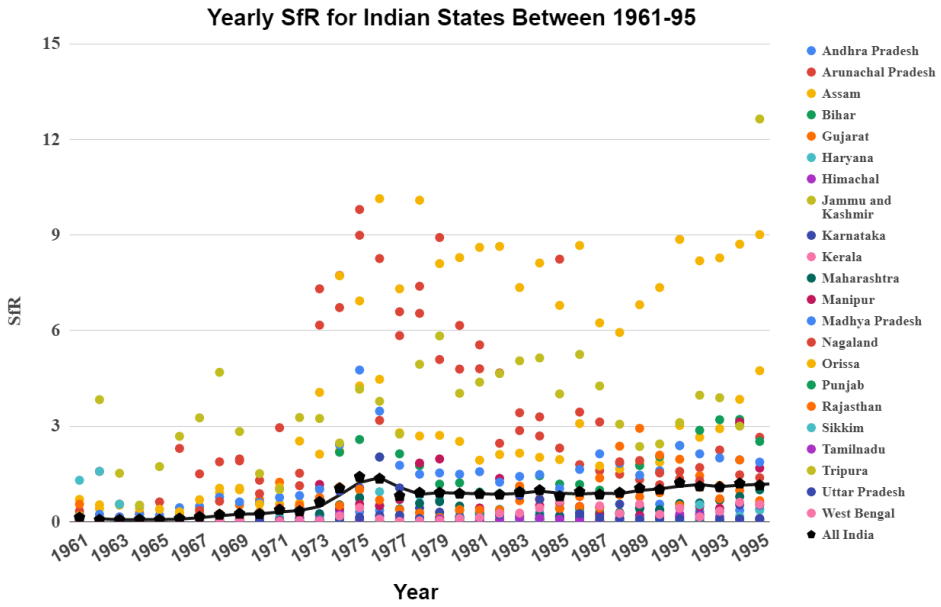

Figure 4.2: S*f*R cases in India between 1961-95

ually by mid 1980s- only to propagate the emergence of *P. falciparum* induced malaria in the country.

The frequency of outliers in the Figure 4.2 is significant enough for us to conclude that the all India S*f*R is undermined by the nullifiers- the states experiencing close to no contribution of *falciparum* parasite to malaria prevalence. Such states could be shielded ecologically or could have different testing and control strategies to contain the infectious disease.

4.2 Spatial-Temporal Analysis of S*f*R in India

Analyses of spatial data in India is complex- and data collection techniques and methodologies vary across different regions. Changes in administrative bound-

aries across timelines make it difficult to analyse spatial data accurately. During 1961-95, 10 new states were formed and the administrative and political plans for these states were revised seven times [50]. To incorporate this variability, the state boundaries for all regions in India have been adjusted accordingly in Table 4.1.

No. of States in India	No. of Union Territories	Year	State Added	Former Status	U.T. Added	Former Status
15	10	1961				
16	9	1963	Nagaland	Union Territory		
17	10	1966	Haryana	Part of Punjab	Chandigarh	Part of Punjab
18	9	1971	Himachal Pradesh	Union Territory		
21	11	1972	Meghalaya	Part of Assam		
21	11	1972	Manipur, Tripura	Union Territories	Mizoram, Arunachal	Part of Assam
22	11	1975	Sikkim	Independent Dynasty		
25	9	1987	Mizoram, Arunachal, Goa	Union Territories		

Table 4.1: State administrative changes between 1961-95 in India

4.2.1 Spatial time series of S*f*R data in India

In this sub-section, the spatial time series of S*f*R prevalence has been depicted using maps of India between 1961-95 by incorporating changes made in state boundaries over the time period (Table 4.1). Please note that the colour intensity scale is different for some plots to highlight the high-low among the states.

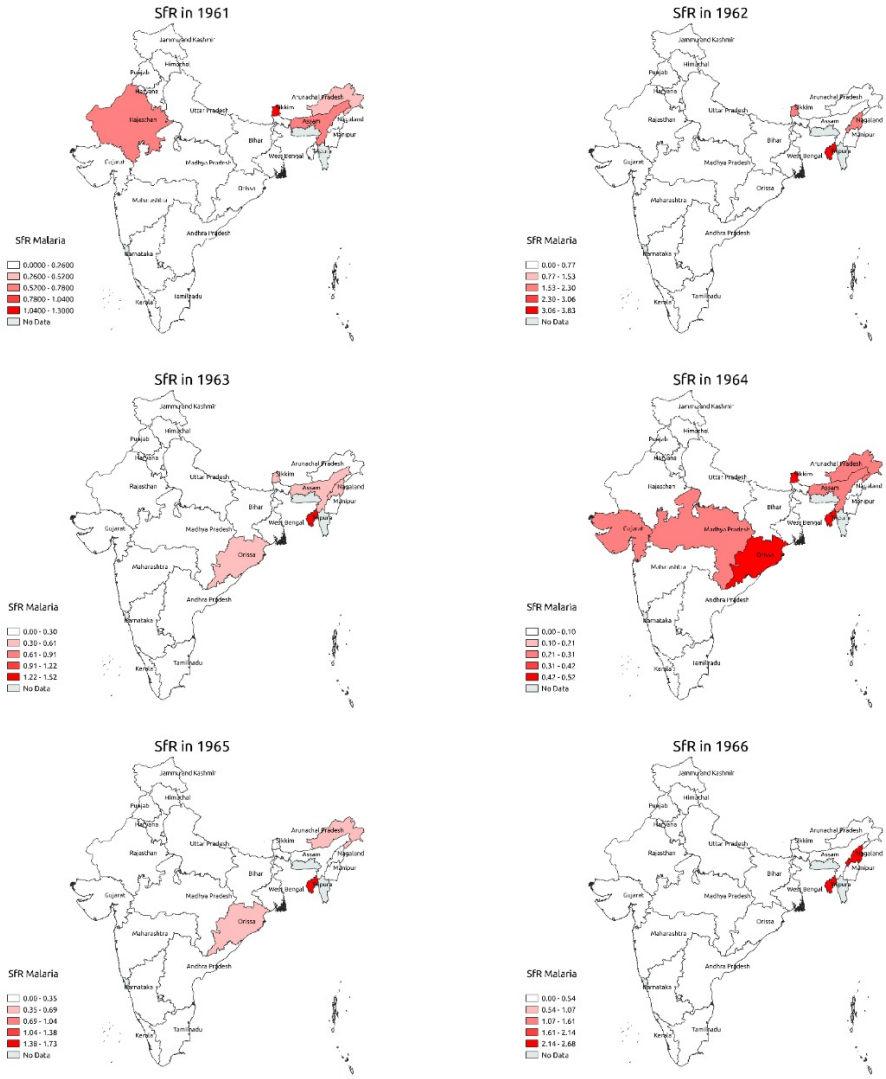

Figure 4.3: S*f*R in India between 1961-66.

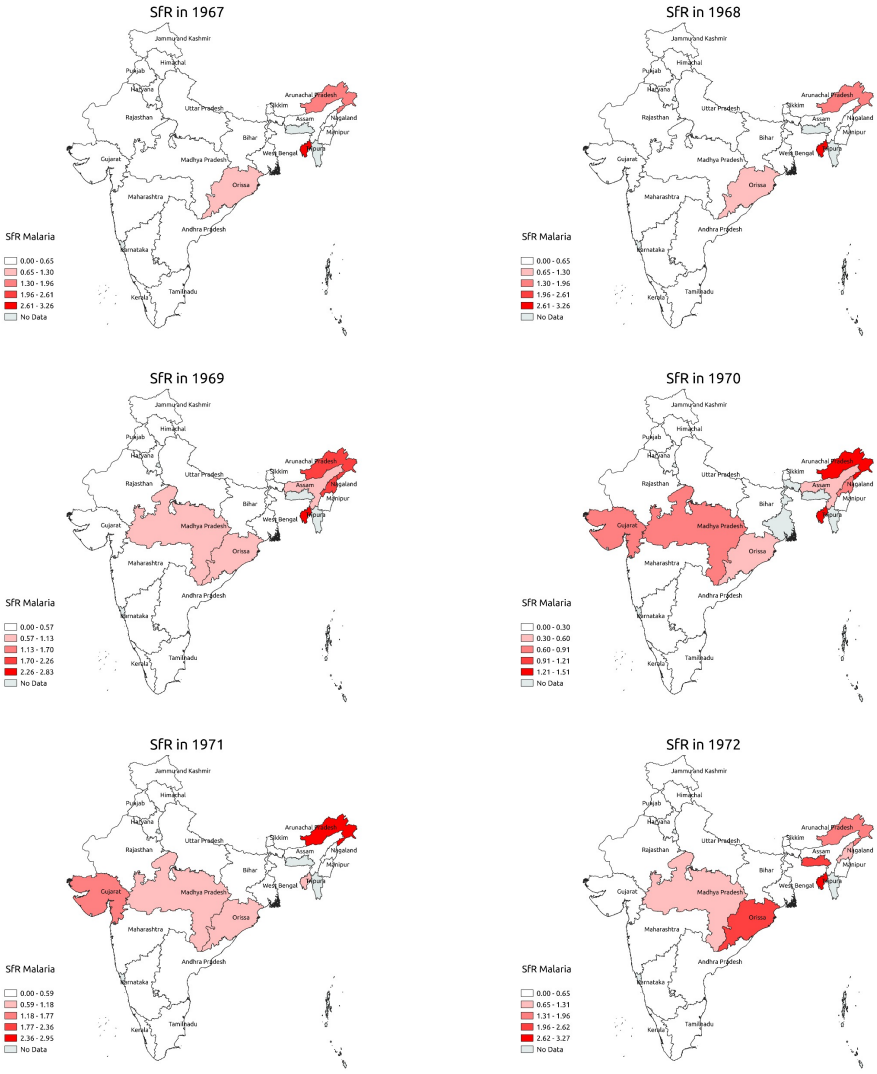

Figure 4.4: S*f*R in India between 1967-72.

On analysing S*f*R prevalence of all states spatially, the hot-spots that emerge through the time series are mostly restricted to north-eastern states of India between 1961-72 (Figure 4.3 and Figure 4.4). *P. falciparum* parasite is believed to have propagated in the country through the north-eastern states. The borders to south east Asian countries which are high in *P.f* could be responsible for S*f*R in

these states. Gujarat and Orissa also show elevated levels in some years, however, the overall S*f*R prevalence is abysmally low during this period.

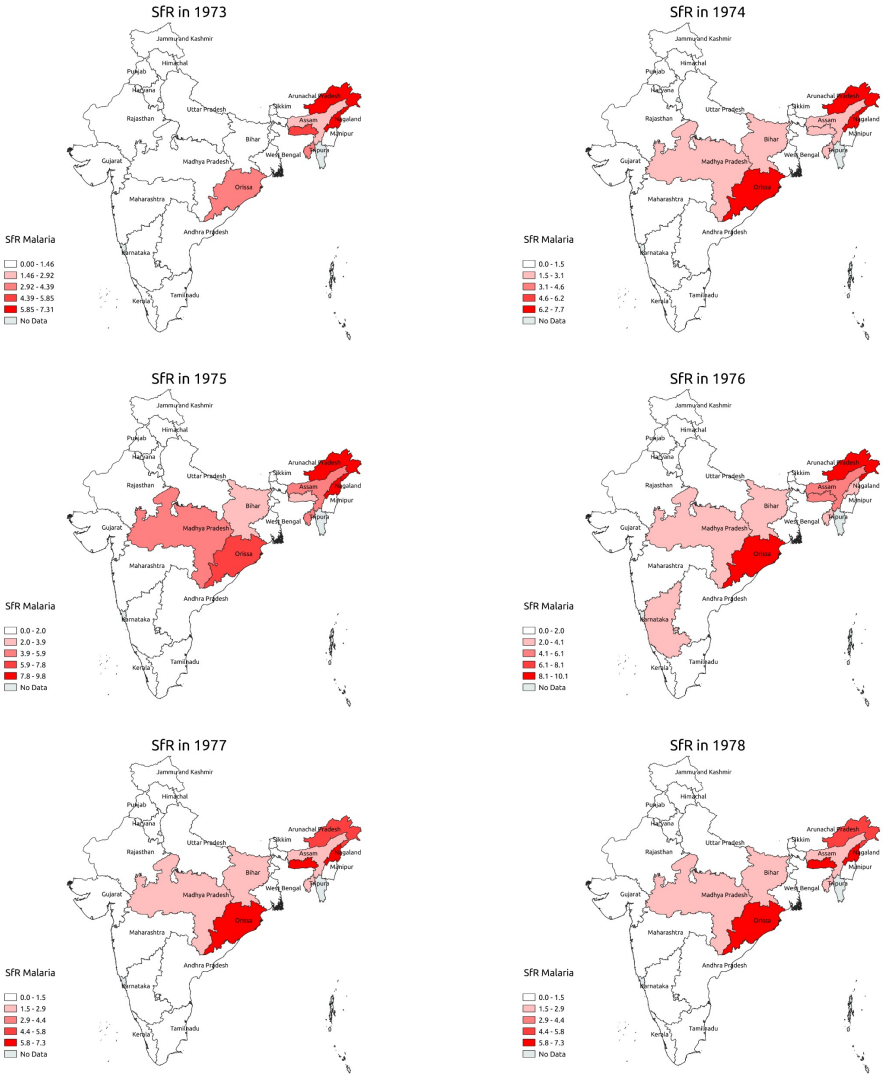

Figure 4.5: S*f*R in India between 1973-78.

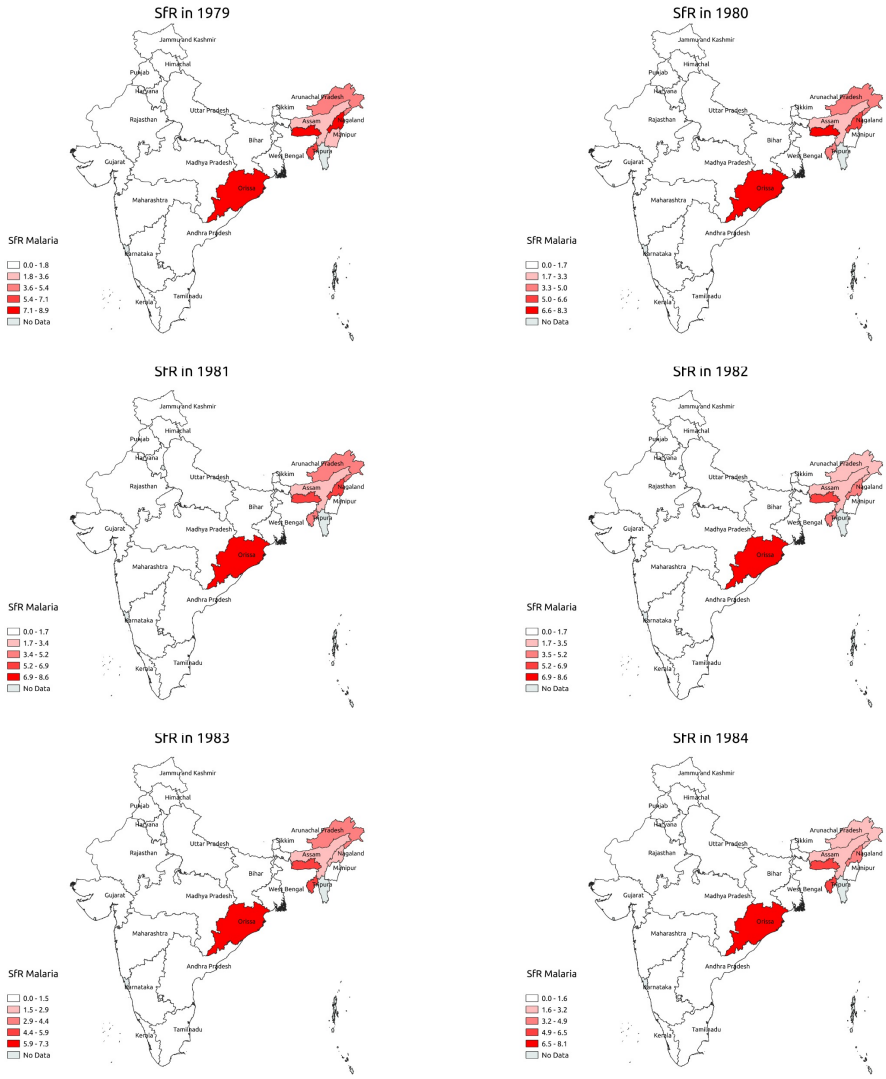

Figure 4.6: S*f*R in India between 1977-83.

Post 1970, an interesting pattern in the spatial prevalence seems to emerge in areas that are not even similar geographically or environmentally- i.e. the regions of existing hot-spots-Orissa and north-eastern states are joined by regions of central and western parts of the country, appearing as if a linear slice cutting through the country. These regions including the states of Gujarat, Madhya Pradesh, Ra-

jasthan and Maharashtra, show oscillating behaviour between 1970-1985- in some years, the prevalence goes up and then comes down.

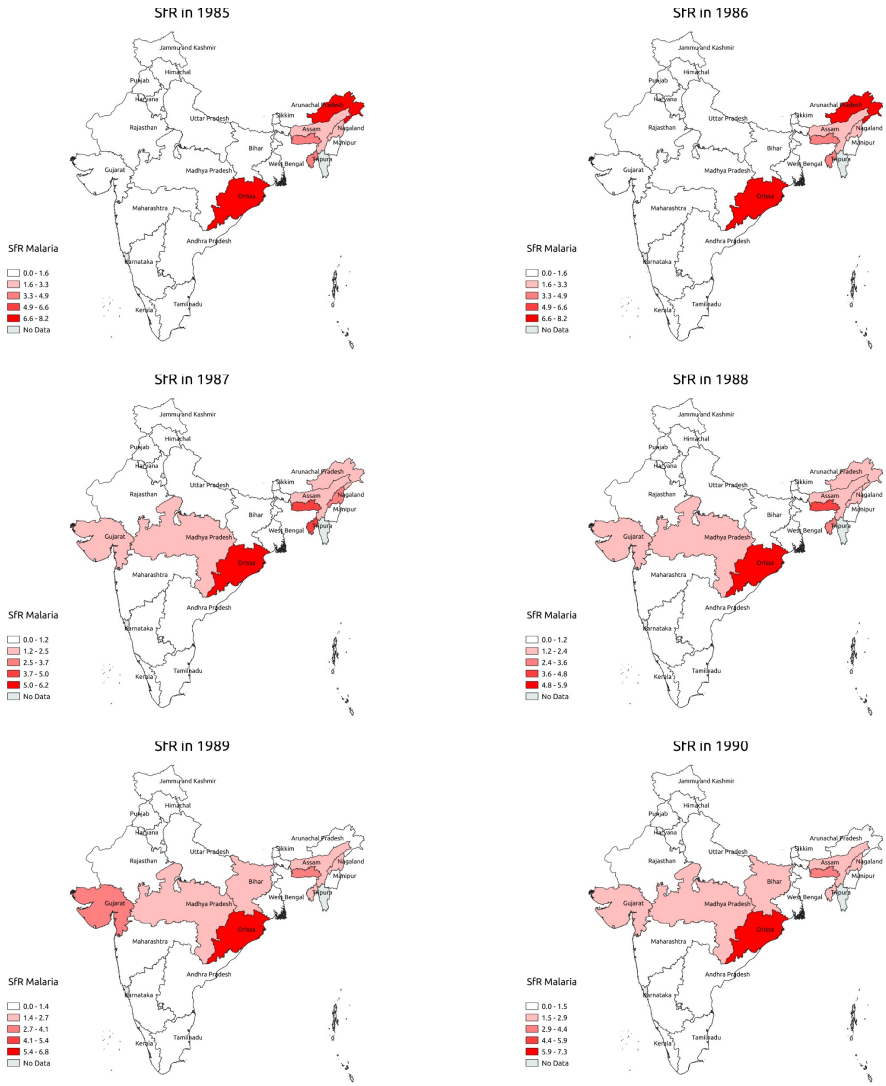

Figure 4.7: SfR in India between 1984-89.

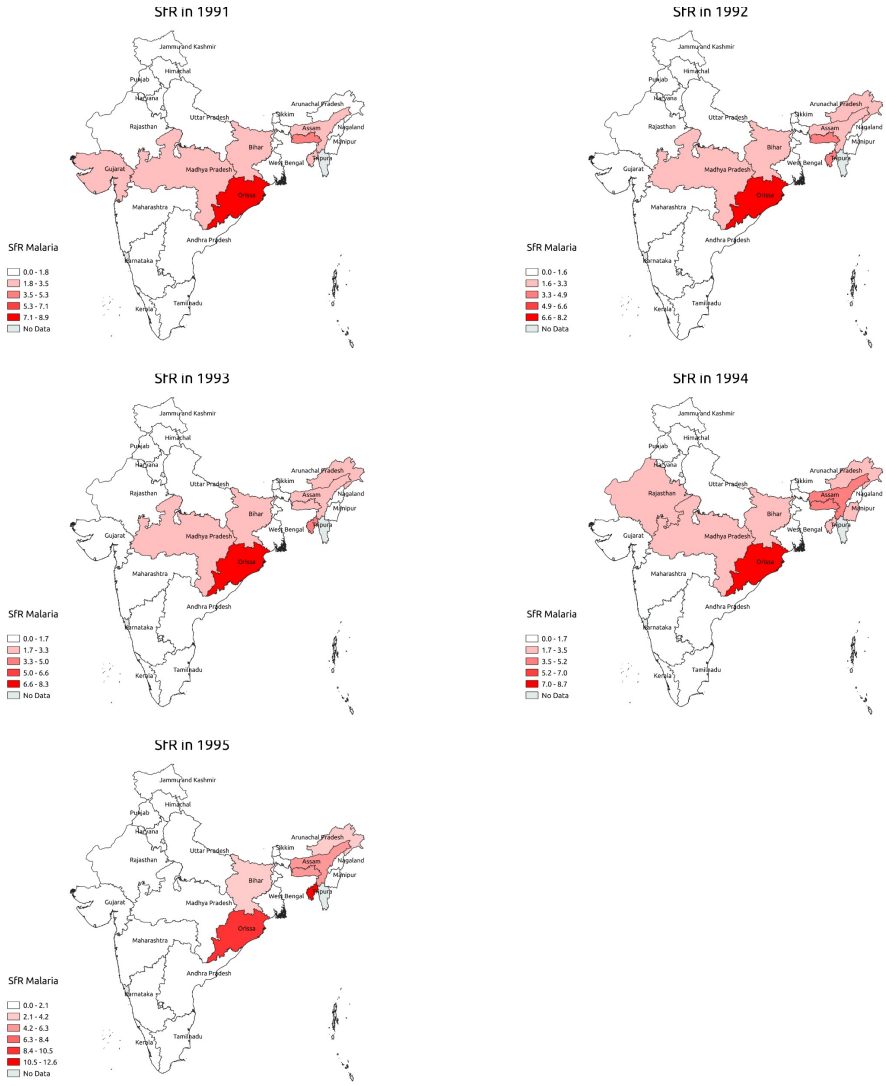

Figure 4.8: S*f*R in India between 1989-95.

Post 1985, the S*f*R hubs that have been established so far- the north-eastern regions with the states of Arunachal Pradesh, Assam and Tripura, along with Orissa- are established as focal-points, with Gujarat, Bihar, Rajasthan and Madhya Pradesh occasionally significantly contributing to the prevalence.

4.3 Classification of Indian states based on *falciparum* prevalence between 1961-95

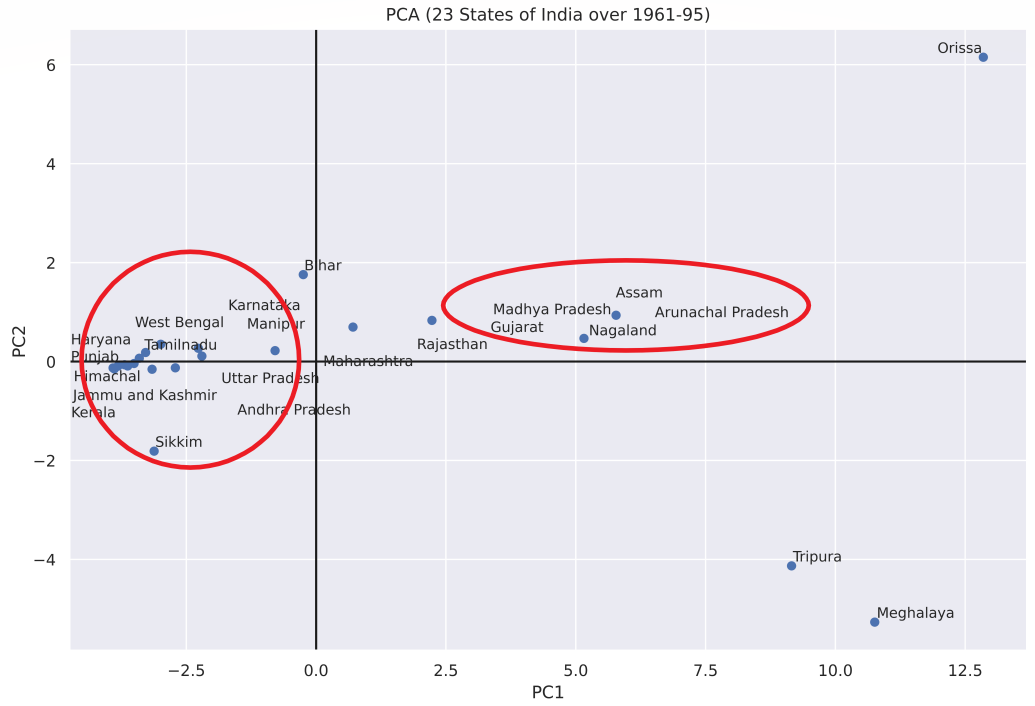

Figure 4.9: Classification of *falciparum* malaria affected states between 1961-95 using PCA. The first two components are plotted.

PCA analysis (see section 2.4.2 in Chapter 2) shown in Figure 4.9 reveals how the states are clustered based on S*f*R malaria for all years and all states. The variance plot in Figure 4.10 shows that two components can explain about 80% of the variance in the data for the clustering of states presented by the independent variables in 35 dimensions. Hence, we are able to effectively visualize the states of low, high and intermediate prevalence with their distinctive characteristics in the PC1-PC2 plot in Figure 4.9. The consistent high prevalence states from our time series

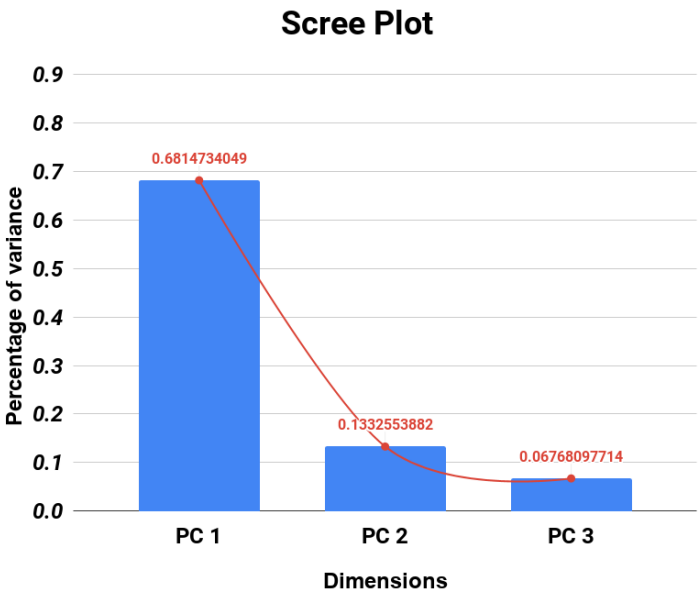

Figure 4.10: Variance plot of state-wise PCA analysis

- Meghalaya and Tripura and Orissa - are distinctively apart from the consistently low prevalence states through out the time-series. States with lower overall S*f*R cluster together. The states that show variable intermediate-high prevalence are also distinguished from the rest - as is the case with Rajasthan, Madhya Pradesh, Arunachal Pradesh, Nagaland and Assam. Orissa- the established hub is furthest apart from all clusters.

4.4 Temporal Classification of S*f*R in India

To identify the underlying temporal pattern of all states in various years, principal component analysis is done on all states contribution in each year for 35 years (Figure 4.11). The PC1-PC2 plot shows the years towards the beginning of the time series cluster together- years with extremely low *falciparum* malaria.

In similar fashion, the years that witnessed the highest impact of the epidemic – 1975-76, are positioned together. Interestingly, the manifestation of *P. falciparum*

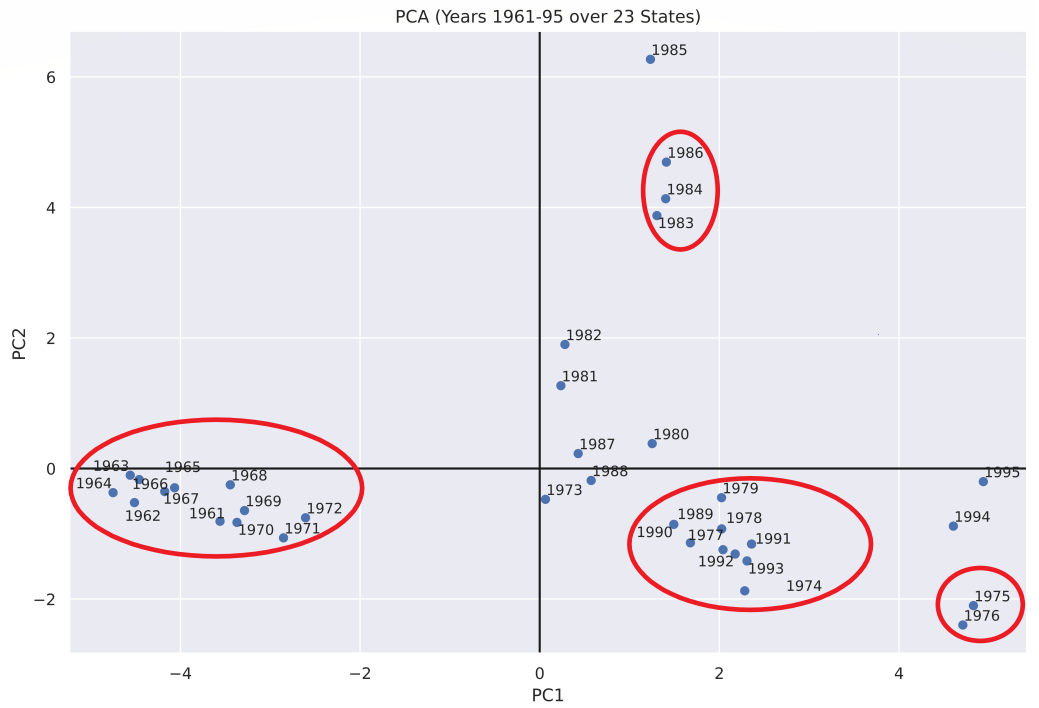

Figure 4.11: Year-wise clustering based on PC1-PC2 state S*f*R in India

as the dominant malaria parasite is reinforced, as the last years contributing to the time series are at shortest distance from the years that experienced the epidemic in full force- depicting that the infection load due to *P. falciparum* is sustained.

The variance plot in Figure 4.12 for the PCA reveals that the two components only represent 56% of the variance in the independent variables. Hence, the year-wise clusters are not as distinct as state-wise clusters. This could probably have stemmed from the huge variation in prevalence among states in the early years and variability in data collection procedures across the years and states.

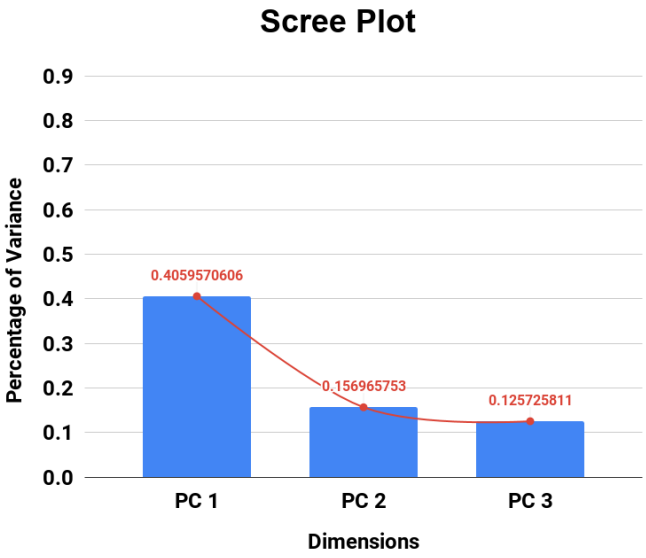

Figure 4.12: Variance plot of yearwise PCA analysis

4.5 Temporal Correlation Heatmaps

Figure 4.13 shows the temporal correlation of SfR time series between pairs of states in India during 1961-95. The 35 year period is divided in three stages - pre-epidemic (1961-74), during epidemic (1975-1985), and post epidemic (1986-95). The pairwise correlation coefficients are plotted to to identify the geographical areas that behave similarly across the time.

Before the epidemic, most states seem correlated, since the overall prevalence is low throughout the country, except for a few – the outliers that begin to surface early on, most of them being states in the north-eastern region of the country. It shows that when the epidemic is building up, correlations between states are high (1961-74). During the epidemic years and its dying down, the correlation between the states disintegrates as the states use differential control measures to stop the

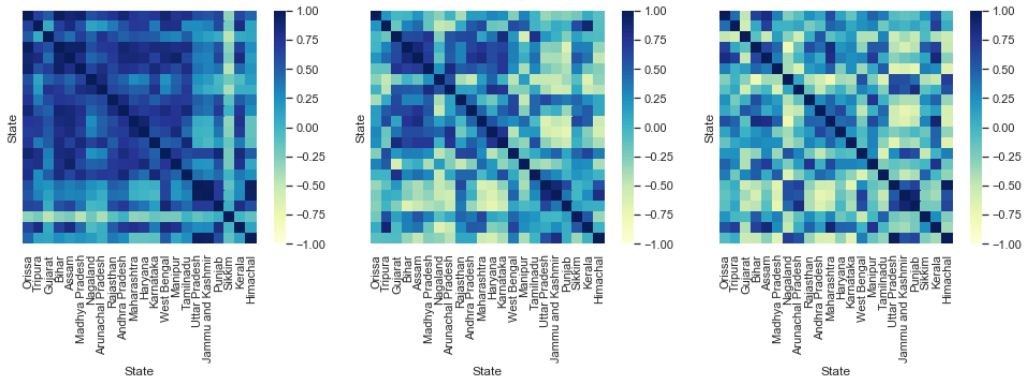

(a) pre-epidemic (1961-974) (b) during epidemic (1975-85) (c) post-epidemic (1986-95)

Figure 4.13: S*f*R temporal correlation heatmaps for states in India between 1961-95

epidemic and progress differently throughout the epidemic owing to geographic, ecological, en- vironmental and demographic factors.

This trend continues post epidemic also, most states follow completely different trajectories and do not seem correlated, partly because of disproportion in incidence, even if there is an overall increase in S*f*R throughout the country.

4.6 Relative contribution of states to *falciparum* malaria in India between 1961-95.

The relative contribution of each state of *falciparum* malaria in India can be visualised by descriptive pie charts, to identify the trends with respect to the disease prevalence. From the pie-chart distributions given below, it is evident that only a few states concentrated in the north eastern parts of the country initially contribute to *falciparum* malaria in India. Even within the states that contribute, S*f*R

prevalence is extremely low. As the epidemic builds up, the contribution of other states, along with the initial hot-spots also go up, even though the quantitative contribution is lower than the established hot-spots. Towards 1995, more states contribute in smaller proportions to the overall *falciparum* malarial prevalence, as the parasite gradually manifests itself as the dominant malarial parasite in India.

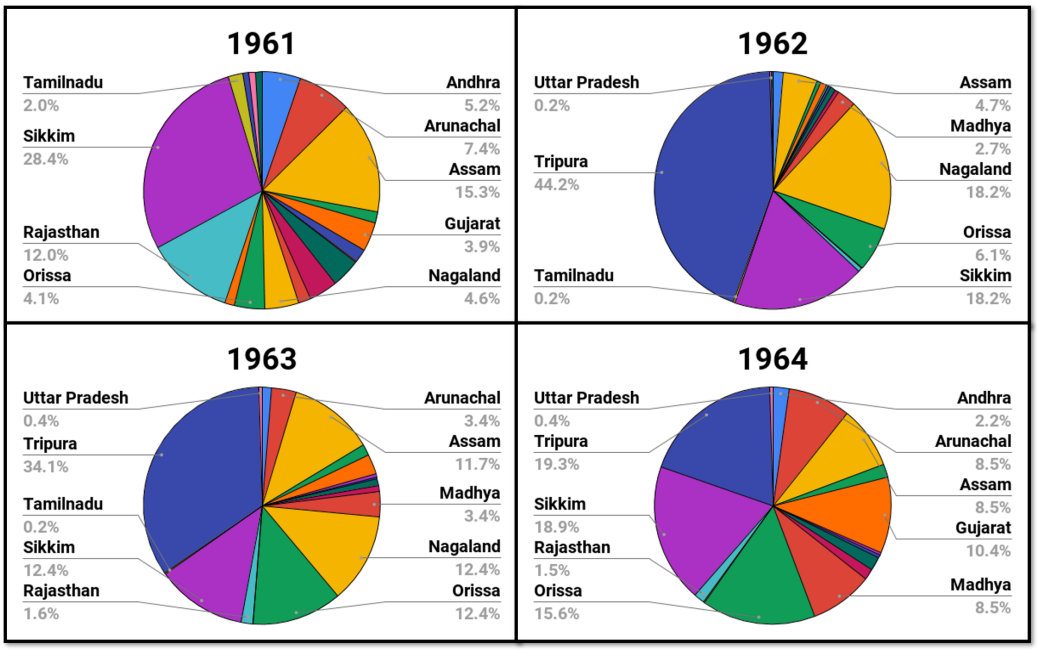

Figure 4.14: Relative contribution of high-prevalence states to S*f*R between 1961-64.

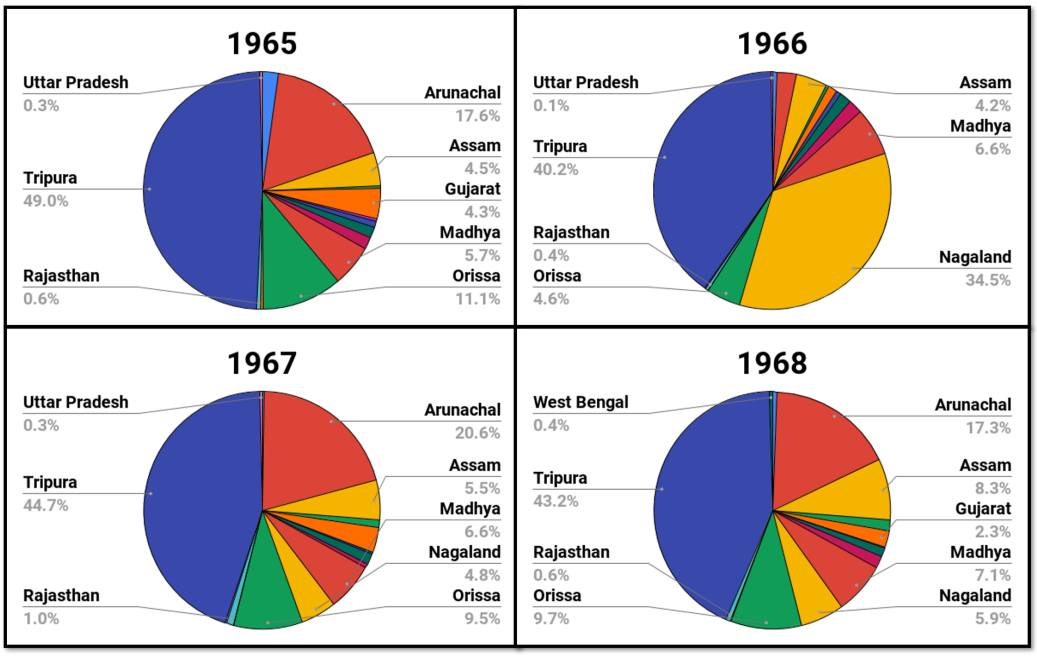

Figure 4.15: Relative contribution of high-prevalence states to S*f*R between 1965-68.

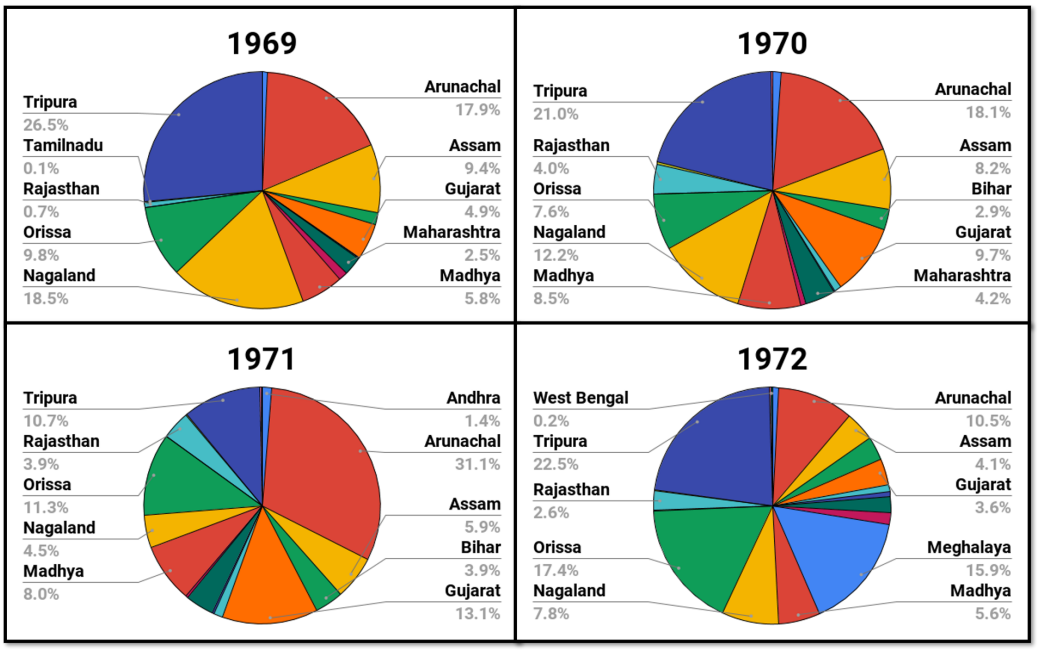

Figure 4.16: Relative contribution of high-prevalence states to S*f*R between 1969-72.

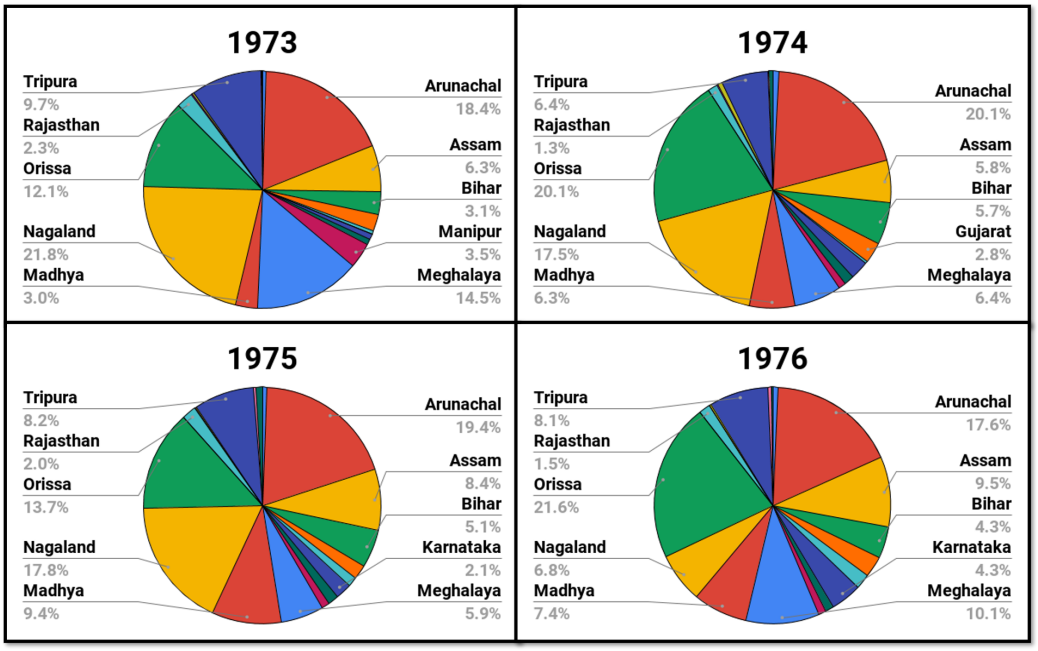

Figure 4.17: Relative contribution of high-prevalence states to S*f*R between 1973-76.

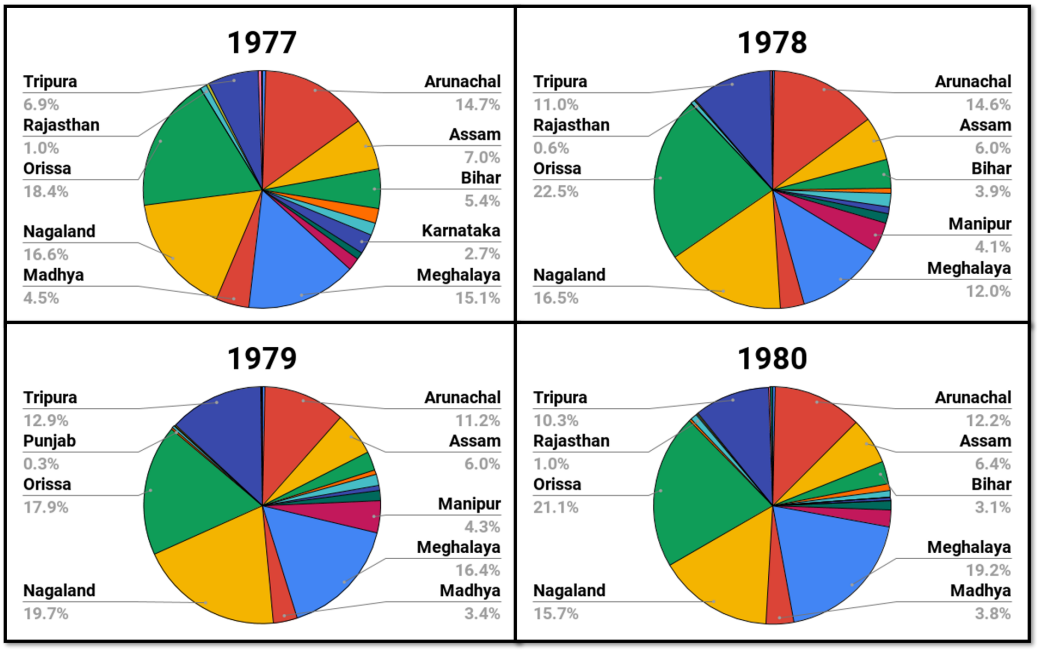

Figure 4.18: Relative contribution of high-prevalence states to S*f*R between 1977-80.

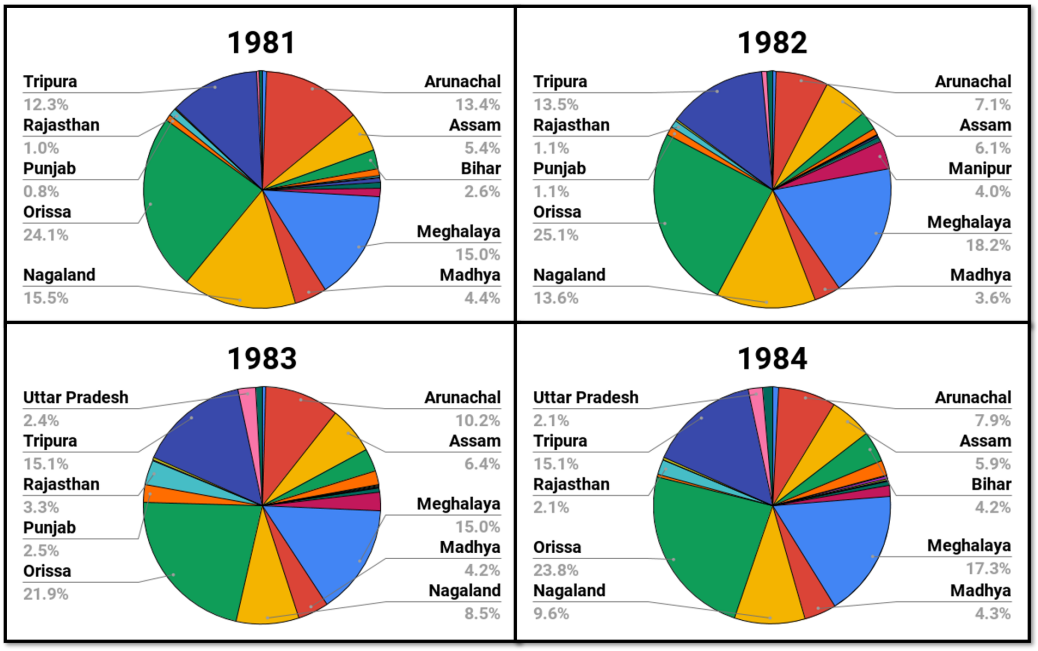

Figure 4.19: Relative contribution of high-prevalence states to S*f*R between 1981-84.

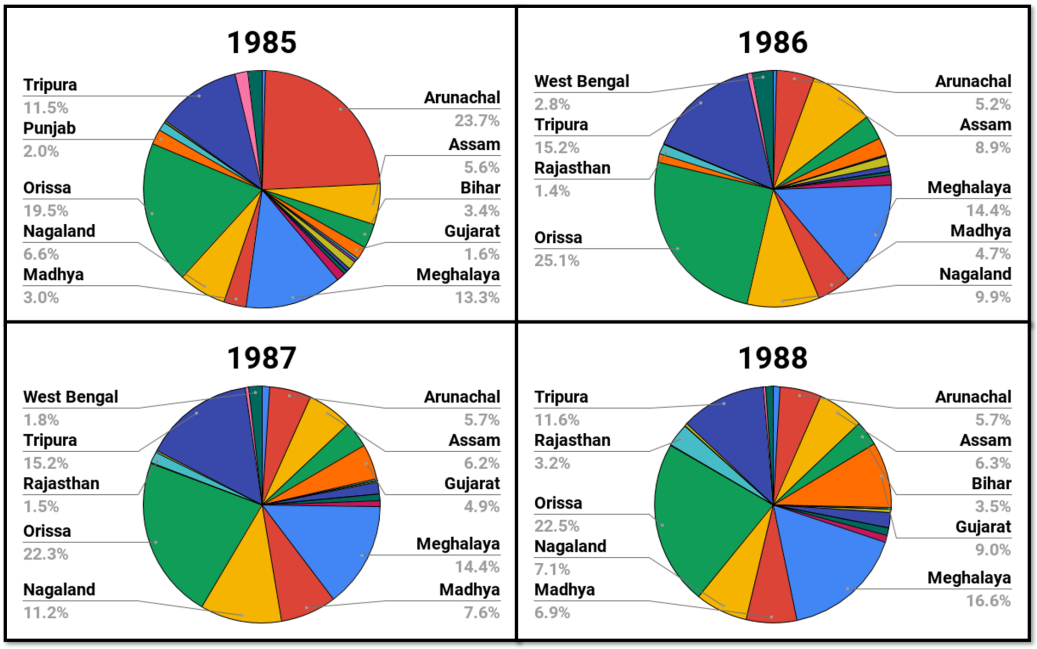

Figure 4.20: Relative contribution of high-prevalence states to S*f*R between 1985-88.

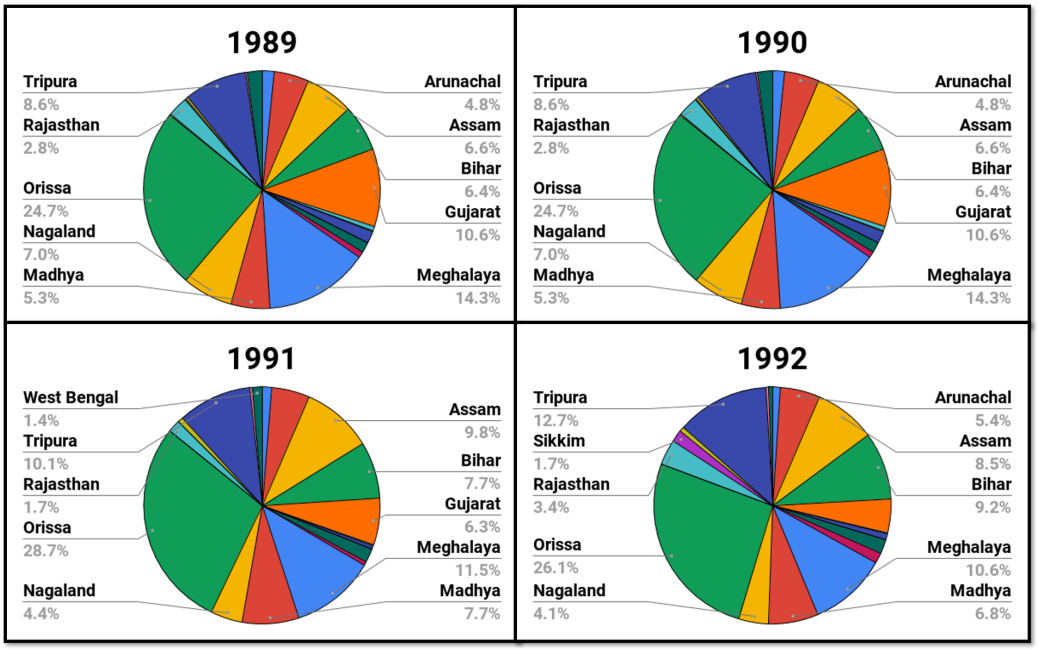

Figure 4.21: Relative contribution of high-prevalence states to S*f*R between 1989-92.

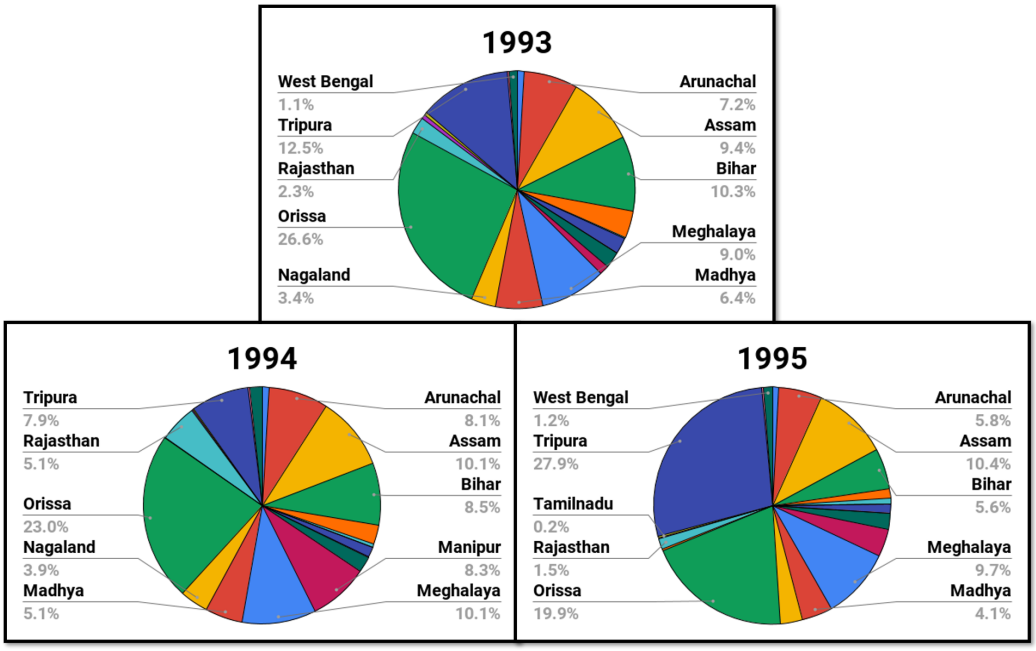

Figure 4.22: Relative contribution of high-prevalence states to S*f*R between 1992-95.

4.7 S*f*R distributions (1961-95) in states

It is clear from the S*f*R time series of all states that they have had different intensities of cases - some consistently high or low, and some having both high and low. The shape of the case distribution over 35 years can give important information on the severity of S*f*R malaria in them. Based on the shape of their distributions, states are classified in regions with low, intermediate and high *falciparum* prevalence. All plots have the same X-axis scale and bin size for easier comparison.

4.7.1 States with consistently low prevalence

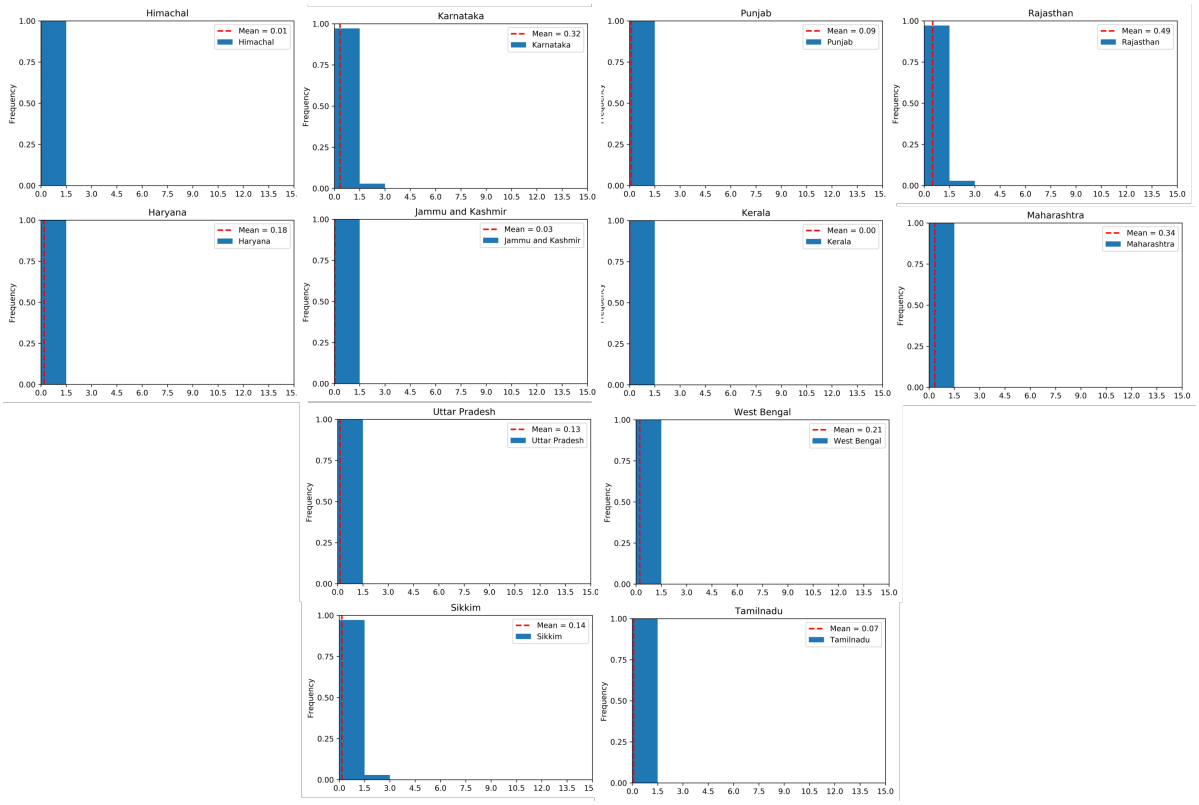

Figure 4.23: States with consistently low prevalence of S*f*R.

Certain states in India show consistently low prevalence of S*f*R between 1961-95 (Figure 4.23). It is however important to distinguish between states that have overall low malaria prevalence and specifically low S*f*R prevalence for accurate classification.

The states with intermediate but variable prevalence of S*f*R, and those with high and variable prevalence of S*f*R are shown in Figure 4.24 & 4.25.:

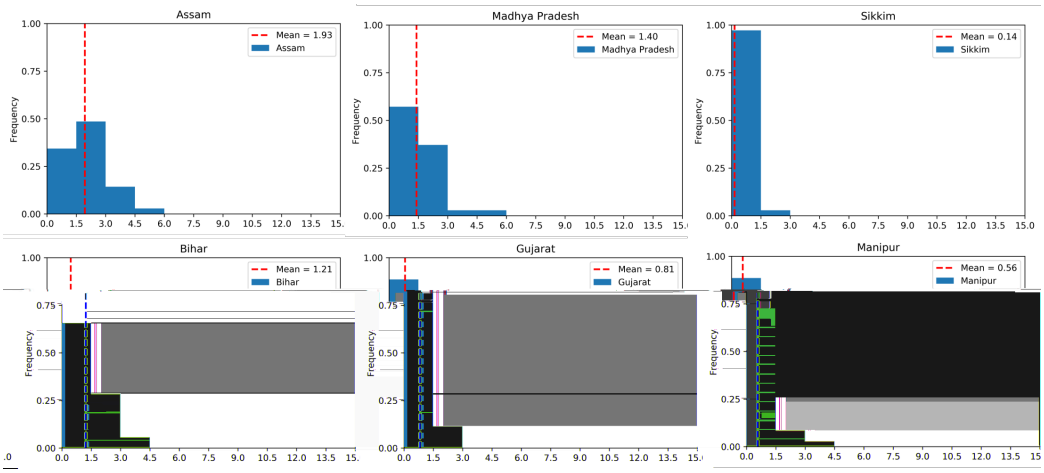

Figure 4.24: States with intermediate but variable prevalence of S*f*R.

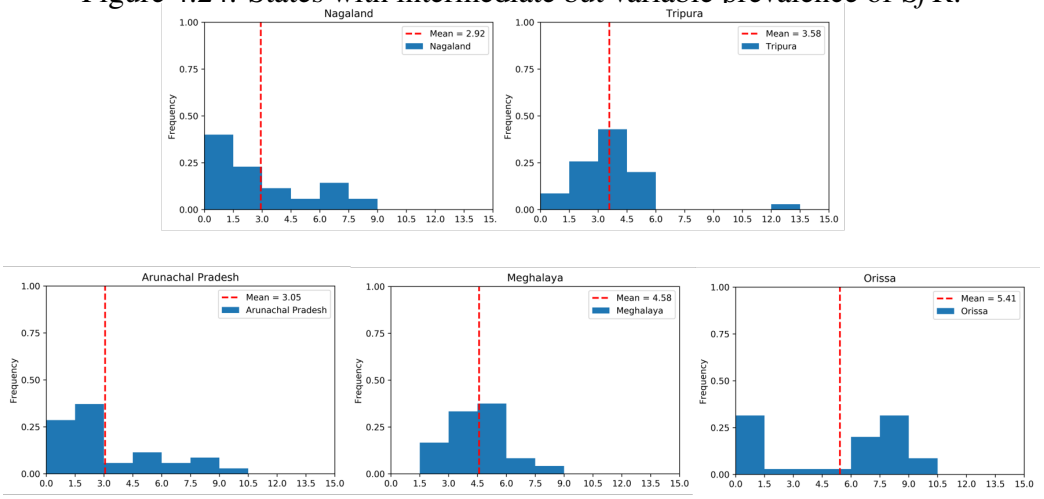

Figure 4.25: States with high and variable prevalence of S*f*R.

The hotspot states with high prevalence of S*f*R - Orissa, Tripura, and

Meghalaya - have an interesting characteristic. In majority of the years they show very high prevalence. Orissa has a unique bimodal distribution, and Nagaland and Arunachal Pradesh having long tails. More analysis with environmental, social and demographic variables needs to be done to understad these differences.

All the analyses shown above, through descriptive and statistical methods, clearly uncover some important information from the mass of tables for 35 years. Clearly more studies need to be done to understand the environmental, socio-economic variables that lead to state-wise differences in SfR prevalence and its future trajectory.

Chapter 5

Discussions and Future Directions

The work presented in this thesis is an attempt to theoretically study the myriad faces of evolution, spread and differential prevalence of the infectious disease malaria. Towards this two approaches - a mathematical modeling and a data curation and analysis - are employed. Both are commonly used methods in epidemiology research. For the first, we have used an existing realistic model of Malaria [57] in which, among other factors, the host immunity functions are included. I have done a thorough analysis of the dependence of these functions to several biologically realistic factors, such as age, immunity, mosquito density, mosquito biting rate etc. These are very important in epidemiology, as they influence the disease spread in a population with different age structure differently - a clear case being the recent COVID-19 pandemic in the world. Though the detailed mathematical analysis and simulations on the whole model and the immunity functions are for general cases, they can be applied and used for specific countries or regions after incorporating the region-specific data.

Plasmodium falciparum has gradually become the dominant malaria parasite in

India, which poses a significant challenge in endemic areas. High transmission rates entrenched with poor socio-economic conditions leading to low immunity and comorbidity induce significantly higher mortality rates due to *falciparum* infection that is the leading cause of cerebral malaria throughout the world. Differential equation based mathematical models for infectious disease have worked independently well in incorporating the biological factors at population levels; and can replicate, as well as predict, temporal dynamics of the disease spread for shorter duration. However compartmental differential equation models investigate system behavior of high-dimensional host-vector-pathogen interactions by studying simpler models that approximates the original by averaging over degrees of freedom. Heterogeneity, which is key driver of immunity and transmission dynamics, can often not be visualized in such systems. Similarly, spatial effects of the disease dynamics cannot be relayed through differential equation models. Agent-Based Models are extremely useful for decoding complex collective behavior using a ground-up approach. The realistic spatial dynamics of the system owing to heterogenous agents can be replicated in ABMs, which is often lost in mean-field models [63, 28, 47].

The intricacy of malaria transmission dynamics differs in space and time; hence it is necessary to isolate local and focal phenomenon for targeted policies to control and eradicate the infectious disease. Towards this analysis of malaria prevalence data in particular regions is very useful. We collected and curated a historical dataset of SfR prevalence in India between 1961-1995. Unfortunately this data set is highly coarse-grained - both spatially (states) and temporally (one data point for one year). This does not allow it to be useful for any mathematical modelling. In this work, the aim has been to extract as much information possible from the

mass of numbers using visualization and basic statistical methods. Each methodology used for classification of hot-spots for *falciparum* malaria reveals a unique aspect of the epidemiology of the parasite evolution in the country. Through the time series, spatial plots and pie-charts, we get an understanding of how *falciparum* malaria was introduced in the country- through the north-eastern states, and how the prevalence has gone up, and the contribution of individual states to the *falciparum*m disease burden. But it is through the distributions, classification methods and correlation techniques that we are able to trace the similarities, or the lack thereof within various regions of the country with respect to the parasite's endemicity. Initially, as the prevalence in the country is extremely low, it seems that the entire burden is borne by the states that first exhibit the *falciparum* malaria incidence. Over time, due to various biologically or demographically relevant factors, other states also emerge as areas of high prevalence, which is highlighted by spatial analysis of the data.

The challenges posed by malaria remain manifold- reduction of transmission rates by controlling vector population has been known to evoke evolutionary responses- DDT resistance, high biting rates and changed biting time, antigenic variation due to var gene recombination, gene introgression- to name a few. It has now become imperative to enhance our understanding of immune system interactions with the parasite to achieve the goal of worldwide elimination. Heterogeneity in immunity against the infectious disease- owing to a cumulative exposure to the parasite, the biology of the host, demography and socio-economic factors highlights fundamental gaps in our understanding of malarial epidemiology. Availability of high quality and high-resolution spatio-temporal epidemiological data is also an important corner stone in developing useful mathematical and statistical predictive

models for any disease. Hence, understanding the history of the emergence of the relatively newer parasite species not only helps in connecting the dots to the past, but its deeper understanding is panacea for eliminating the infectious disease.

Appendix A

Selected MATLAB Codes

```
%full model malaria
syms I f Ha wa m alpha h rho q mu_h Is0 b a0 amax dl dp dm ds Hs EIR
     a Pa lambda Is beta rho rhos R_s mu_m L_m psi C_Is C_Ia tau
index = 0;
for a = 0:0.05:60
index = index+1;
f=0.5; Ha = 500; wa = 30; h = 24.333; m =3; alpha = 0.67*365; rho0 =
     (1/180*365); mu_h = 0.0125; q = 3;
b = 0.2; a0 = 3; dl = 10; dp = 20; dm = 0.25; amax =80; ds = 5; Hs
    =40; EIR =104; Is0 =52; mu_m = 0.1*365; tau = 0.018; C_Is = 0.35;
     C_Ia = 0.03;
Pa = exp(-a/dl)*((EIR*b*dl*dp*exp(a/dl) - (EIR*a0*b*dl*dp*exp(a/dl -
     a/a0))/(a0 - dl))/(dl - dp) - (EIR*b*dl*dp)/(dl - dp) + (EIR*a0*
    b*dl*dp)/(a0*dl - a0*dp + dl*dp - dl^2)) - exp(-a/dp)*((EIR*b*dp
    ^2*exp(a/dp) - (EIR*a0*b*dp^2*exp(a/dp - a/a0))/(a0 - dp))/(dl -
    dp) - (EIR*b*dp^2 - (EIR*a0*b*dp^2)/(a0 - dp))/(dl - dp) + (EIR*b
    *dl*dp - (EIR*a0*b*dl*dp)/(a0 - dl))/(dl - dp) - (EIR*b*dl*dp)/(
    dl - dp) + (EIR*a0*b*dl*dp)/(a0*dl - a0*dp + dl*dp - dl^2));
lambda = EIR*b*(1 - exp(-amax/a0));
```

```
psi = exp(-tau*mu_m);
Is = lambda*ds*( 1 + (a0*exp(-a/a0) - ds*exp(-a/ds))/(ds-a0)) + Is0*
    exp(-a/dm);
beta = 1/(1 + ((Is/Is0)^2));
rho = q + (rho0*(1 + ((wa -1)*(Pa/Ha)^2/(1 + (Pa/Ha)^2))));
rhos = 17.38;
R_s= f*rhos + (1-f)*rho;
ode = @(T,I)[-m*alpha*I(7)*(1-exp((-1*a)/a0))*b*I(1) + beta*R_s*I(3)
     + rho*(I(4)) + mu_h - mu_h*I(1); m*alpha*I(7)*b*(1-exp((-1*a)/a0
    ))*I(1) - h*(I(2)) - mu_h*(I(2));
    beta*h*I(2) + beta*m*alpha*I(7)*(1-exp((-1*a)/a0))*b*I(4) - R_s*I
        (3) - mu_h*I(3);
    (1 -beta)*h* I(2) + (1 - beta)*R_s*I(3) - beta*m*alpha*I(7)*(1-
        exp((-1*a)/a0))*b*I(4) - (rho)*I(4) - mu_h*I(4);
     mu_m - alpha*(C_Is*I(3) + C_Ia*I(4))*I(5)- mu_m*I(5); alpha*(
         C_Is*I(3) + C_Ia*I(4))*I(5) - psi*alpha*(C_Is*I(3) + C_Ia*I
         (4))*I(5)-mu_m*I(6); psi*alpha*(C_Is*I(3) + C_Ia*I(4))*I(5)-
          mu_m*I(7)];
tspan = 0:0.0005:1;
options = odeset('RelTol',1e-8,'AbsTol',1e-10);
I0 = [0.99998; 0; 0.00002; 0; 0.999; 0.0; 0.001];
[T,I] = ode45(ode, tspan, I0, options);
% figure(1)

time = linspace(0,12,2001);

%plot(x, I(:,5),x, I(:,6), x, I(:,7));

%grid
y(index) = I(end,4);
age = linspace(0,60,1201);
% y

end
```

```
% p = plot(time, I(:,1),'--', time, I(:,2), '-',time, I(:,3), ':',
    time, I(:,4), '-.' )
p = plot(age, y, '--')
p(1).LineWidth = 2.5;
% p(2).LineWidth = 2.5;
% p(3).LineWidth = 2.5;
% p(4).LineWidth = 2.5;
% legend('parasite immunity half-life = 15 yrs')
 xlabel({'Age'})
ylabel({'Proportion of symptomatic human class'} )
ylim([0 1])
hold on
% %title('Recovery from sub-patent infections')
syms I f Ha wa m alpha h rho q mu_h Is0 b a0 amax dl dp dm ds Hs EIR
     a Pa lambda Is beta rho rhos R_s mu_m L_m psi C_Is C_Ia tau
index = 0;
for a = 0:0.05:60
index = index+1;
f=0.5; Ha = 500; wa = 30; h = 24.333; m =3; alpha = 0.67*365; rho0 =
     (1/180*365); mu_h = 0.0125; q = 3;
b = 0.2; a0 = 3; dl = 10; dp = 20; dm = 0.25; amax =80; ds = 10; Hs
    =40; EIR =100; Is0 =52; mu_m = 0.1*365; tau = 0.018; C_Is = 0.35;
     C_Ia = 0.03;
Pa = exp(-a/dl)*((EIR*b*dl*dp*exp(a/dl) - (EIR*a0*b*dl*dp*exp(a/dl -
     a/a0))/(a0 - dl))/(dl - dp) - (EIR*b*dl*dp)/(dl - dp) + (EIR*a0*
    b*dl*dp)/(a0*dl - a0*dp + dl*dp - dl^2)) - exp(-a/dp)*((EIR*b*dp
    ^2*exp(a/dp) - (EIR*a0*b*dp^2*exp(a/dp - a/a0))/(a0 - dp))/(dl -
    dp) - (EIR*b*dp^2 - (EIR*a0*b*dp^2)/(a0 - dp))/(dl - dp) + (EIR*b
    *dl*dp - (EIR*a0*b*dl*dp)/(a0 - dl))/(dl - dp) - (EIR*b*dl*dp)/(
    dl - dp) + (EIR*a0*b*dl*dp)/(a0*dl - a0*dp + dl*dp - dl^2));
lambda = EIR*b*(1 - exp(-amax/a0));
psi = exp(-tau*mu_m);
Is = lambda*ds*( 1 + (a0*exp(-a/a0) - ds*exp(-a/ds))/(ds-a0)) + Is0*
    exp(-a/dm);
beta = 1/(1 + ((Is/Is0)^2));
```

```
rho = q + (rho0*(1 + ((wa -1)*(Pa/Ha)^2/(1 + (Pa/Ha)^2))));
rhos = 17.38;
R_s= f*rhos + (1-f)*rho;
ode = @(T,I)[-m*alpha*I(7)*(1-exp((-1*a)/a0))*b*I(1) + beta*R_s*I(3)
     + rho*(I(4)) + mu_h - mu_h*I(1); m*alpha*I(7)*b*(1-exp((-1*a)/a0
    ))*I(1) - h*(I(2)) - mu_h*(I(2));
    beta*h*I(2) + beta*m*alpha*I(7)*(1-exp((-1*a)/a0))*b*I(4) - R_s*I
        (3) - mu_h*I(3);
    (1 -beta)*h* I(2) + (1 - beta)*R_s*I(3) - beta*m*alpha*I(7)*(1-
        exp((-1*a)/a0))*b*I(4) - (rho)*I(4) - mu_h*I(4);
     mu_m - alpha*(C_Is*I(3) + C_Ia*I(4))*I(5)- mu_m*I(5); alpha*(
         C_Is*I(3) + C_Ia*I(4))*I(5) - psi*alpha*(C_Is*I(3) + C_Ia*I
         (4))*I(5)-mu_m*I(6); psi*alpha*(C_Is*I(3) + C_Ia*I(4))*I(5)-
          mu_m*I(7)];
tspan = 0:0.0005:1;
options = odeset('RelTol',1e-8,'AbsTol',1e-10);
I0 = [0.99998; 0; 0.00002; 0; 0.999; 0.0; 0.001];
[T,I] = ode45(ode, tspan, I0, options);
% figure(1)

time = linspace(0,12,2001);

%plot(x, I(:,5),x, I(:,6), x, I(:,7));

%grid
y1(index) = I(end,4);
age = linspace(0,60,1201);
% y

end
% p = plot(time, I(:,1),'--', time, I(:,2), '-',time, I(:,3), ':',
    time, I(:,4), '-.' )
p = plot(age, y1, '--')
p(1).LineWidth = 2.5;
% p(2).LineWidth = 2.5;
```

```
% p(3).LineWidth = 2.5;
% p(4).LineWidth = 2.5;
legend('EIR = 50', 'EIR =100')
 xlabel({'Age'})
ylabel({'Proportion of symptomatic human class'} )
ylim([0 1])
% %title('Recovery from sub-patent infections')

% Symptomatic Prevalence
syms I f Ha wa m alpha h rho q mu_h Is0 b a0 amax dl dp dm ds Hs EIR
     a Pa lambda Is beta rho rhos R_s mu_m L_m psi C_Is C_Ia tau
index = 0;
for a = 0:0.05:80
index = index+1;
f=0.5; Ha = 500; wa = 30; h = 24.333; m =3; alpha = 0.67*365; rho0 =
     (1/180*365); mu_h = 0.0125; q = 3;
b = 0.2; a0 = 3; dl = 10; dp = 20; dm = 0.25; amax =80; ds = 5; Hs
    =40; EIR =25; Is0 =52; mu_m = 0.1*365; tau = 0.018; C_Is = 0.35;
    C_Ia = 0.03;
Pa = exp(-a/dl)*((EIR*b*dl*dp*exp(a/dl) - (EIR*a0*b*dl*dp*exp(a/dl -
     a/a0))/(a0 - dl))/(dl - dp) - (EIR*b*dl*dp)/(dl - dp) + (EIR*a0*
    b*dl*dp)/(a0*dl - a0*dp + dl*dp - dl^2)) - exp(-a/dp)*((EIR*b*dp
    ^2*exp(a/dp) - (EIR*a0*b*dp^2*exp(a/dp - a/a0))/(a0 - dp))/(dl -
    dp) - (EIR*b*dp^2 - (EIR*a0*b*dp^2)/(a0 - dp))/(dl - dp) + (EIR*b
    *dl*dp - (EIR*a0*b*dl*dp)/(a0 - dl))/(dl - dp) - (EIR*b*dl*dp)/(
    dl - dp) + (EIR*a0*b*dl*dp)/(a0*dl - a0*dp + dl*dp - dl^2));
lambda = EIR*b*(1 - exp(-amax/a0));
psi = exp(-tau*mu_m);
Is = lambda*ds*( 1 + (a0*exp(-a/a0) - ds*exp(-a/ds))/(ds-a0)) + Is0*
    exp(-a/dm);
beta = 1/(1 + ((Is/Is0)^2));
rho = q + (rho0*(1 + ((wa -1)*(Pa/Ha)^2/(1 + (Pa/Ha)^2))));
rhos = 17.38;
R_s= f*rhos + (1-f)*rho;
```

```
ode = @(T,I)[-m*alpha*I(7)*(1-exp((-1*a)/a0))*b*I(1) + beta*R_s*I(3)
     + rho*(I(4)) + mu_h - mu_h*I(1); m*alpha*I(7)*b*(1-exp((-1*a)/a0
    ))*I(1) - h*(I(2)) - mu_h*(I(2));
    beta*h*I(2) + beta*m*alpha*I(7)*(1-exp((-1*a)/a0))*b*I(4) - R_s*I
        (3) - mu_h*I(3);
    (1 -beta)*h* I(2) + (1 - beta)*R_s*I(3) - beta*m*alpha*I(7)*(1-
        exp((-1*a)/a0))*b*I(4) - (rho)*I(4) - mu_h*I(4);
     mu_m - alpha*(C_Is*I(3) + C_Ia*I(4))*I(5)- mu_m*I(5); alpha*(
         C_Is*I(3) + C_Ia*I(4))*I(5) - psi*alpha*(C_Is*I(3) + C_Ia*I
         (4))*I(5)-mu_m*I(6); psi*alpha*(C_Is*I(3) + C_Ia*I(4))*I(5)-
          mu_m*I(7)];
tspan = 0:0.0005:1;
options = odeset('RelTol',1e-8,'AbsTol',1e-10);
I0 = [0.99998; 0; 0.00002; 0; 0.999; 0.0; 0.001];
[T,I] = ode45(ode, tspan, I0, options);
% figure(1)

time = linspace(0,12,2001);

%plot(x, I(:,5),x, I(:,6), x, I(:,7));

%grid
y(index) = I(end,3);
age = linspace(0,60,2001);
% y

end
% p = plot(time, I(:,1),'--', time, I(:,2), '-',time, I(:,3), ':',
    time, I(:,4), '-.' )
p = plot(age, y, '--')
p(1).LineWidth = 2.5;
% p(2).LineWidth = 2.5;
% p(3).LineWidth = 2.5;
% p(4).LineWidth = 2.5;
% legend('parasite immunity half-life = 15 yrs')
```

```
 xlabel({'Age'})
ylabel({'Proportion of symptomatic human class'} )
ylim([0 1])
hold on
for a = 0:0.05:80
index = index+1;
f=0.5; Ha = 500; wa = 30; h = 24.333; m =3; alpha = 0.67*365; rho0 =
     (1/180*365); mu_h = 0.0125; q = 3;
b = 0.2; a0 = 3; dl = 10; dp = 20; dm = 0.25; amax =80; ds = 5; Hs
    =40; EIR =50; Is0 =52; mu_m = 0.1*365; tau = 0.018; C_Is = 0.35;
    C_Ia = 0.03;
Pa = exp(-a/dl)*((EIR*b*dl*dp*exp(a/dl) - (EIR*a0*b*dl*dp*exp(a/dl -
     a/a0))/(a0 - dl))/(dl - dp) - (EIR*b*dl*dp)/(dl - dp) + (EIR*a0*
    b*dl*dp)/(a0*dl - a0*dp + dl*dp - dl^2)) - exp(-a/dp)*((EIR*b*dp
    ^2*exp(a/dp) - (EIR*a0*b*dp^2*exp(a/dp - a/a0))/(a0 - dp))/(dl -
    dp) - (EIR*b*dp^2 - (EIR*a0*b*dp^2)/(a0 - dp))/(dl - dp) + (EIR*b
    *dl*dp - (EIR*a0*b*dl*dp)/(a0 - dl))/(dl - dp) - (EIR*b*dl*dp)/(
    dl - dp) + (EIR*a0*b*dl*dp)/(a0*dl - a0*dp + dl*dp - dl^2));
lambda = EIR*b*(1 - exp(-amax/a0));
psi = exp(-tau*mu_m);
Is = lambda*ds*( 1 + (a0*exp(-a/a0) - ds*exp(-a/ds))/(ds-a0)) + Is0*
    exp(-a/dm);
beta = 1/(1 + ((Is/Is0)^2));
rho = q + (rho0*(1 + ((wa -1)*(Pa/Ha)^2/(1 + (Pa/Ha)^2))));
rhos = 17.38;
R_s= f*rhos + (1-f)*rho;
ode = @(T,I)[-m*alpha*I(7)*(1-exp((-1*a)/a0))*b*I(1) + beta*R_s*I(3)
     + rho*(I(4)) + mu_h - mu_h*I(1); m*alpha*I(7)*b*(1-exp((-1*a)/a0
    ))*I(1) - h*(I(2)) - mu_h*(I(2));
    beta*h*I(2) + beta*m*alpha*I(7)*(1-exp((-1*a)/a0))*b*I(4) - R_s*I
        (3) - mu_h*I(3);
    (1 -beta)*h* I(2) + (1 - beta)*R_s*I(3) - beta*m*alpha*I(7)*(1-
        exp((-1*a)/a0))*b*I(4) - (rho)*I(4) - mu_h*I(4);
     mu_m - alpha*(C_Is*I(3) + C_Ia*I(4))*I(5)- mu_m*I(5); alpha*(
         C_Is*I(3) + C_Ia*I(4))*I(5) - psi*alpha*(C_Is*I(3) + C_Ia*I
```

```
        (4))*I(5)-mu_m*I(6); psi*alpha*(C_Is*I(3) + C_Ia*I(4))*I(5)-
         mu_m*I(7)];
tspan = 0:0.0005:1;
options = odeset('RelTol',1e-8,'AbsTol',1e-10);
I0 = [0.99998; 0; 0.00002; 0; 0.999; 0.0; 0.001];
[T,I] = ode45(ode, tspan, I0, options);
% figure(1)

time = linspace(0,12,2001);

%plot(x, I(:,5),x, I(:,6), x, I(:,7));

%grid
y(index) = I(end,3);
age = linspace(0,60,1601);
% y

end
% p = plot(time, I(:,1),'--', time, I(:,2), '-',time, I(:,3), ':',
    time, I(:,4), '-.' )
p = plot(age, y, '--')
p(1).LineWidth = 2.5;
% %title('Recovery from sub-patent infections')
hold on
syms I f Ha wa m alpha h rho q mu_h Is0 b a0 amax dl dp dm ds Hs EIR
     a Pa lambda Is beta rho rhos R_s mu_m L_m psi C_Is C_Ia tau
index = 0;
for a = 0:0.05:80
index = index+1;
f=0.5; Ha = 500; wa = 30; h = 24.333; m =3; alpha = 0.67*365; rho0 =
     (1/180*365); mu_h = 0.0125; q = 3;
b = 0.2; a0 = 3; dl = 10; dp = 20; dm = 0.25; amax =80; ds = 10; Hs
    =40; EIR =104; Is0 =52; mu_m = 0.1*365; tau = 0.018; C_Is = 0.35;
     C_Ia = 0.03;
```

```
Pa = exp(-a/dl)*((EIR*b*dl*dp*exp(a/dl) - (EIR*a0*b*dl*dp*exp(a/dl -
     a/a0))/(a0 - dl))/(dl - dp) - (EIR*b*dl*dp)/(dl - dp) + (EIR*a0*
    b*dl*dp)/(a0*dl - a0*dp + dl*dp - dl^2)) - exp(-a/dp)*((EIR*b*dp
    ^2*exp(a/dp) - (EIR*a0*b*dp^2*exp(a/dp - a/a0))/(a0 - dp))/(dl -
    dp) - (EIR*b*dp^2 - (EIR*a0*b*dp^2)/(a0 - dp))/(dl - dp) + (EIR*b
    *dl*dp - (EIR*a0*b*dl*dp)/(a0 - dl))/(dl - dp) - (EIR*b*dl*dp)/(
    dl - dp) + (EIR*a0*b*dl*dp)/(a0*dl - a0*dp + dl*dp - dl^2));
lambda = EIR*b*(1 - exp(-amax/a0));
psi = exp(-tau*mu_m);
Is = lambda*ds*( 1 + (a0*exp(-a/a0) - ds*exp(-a/ds))/(ds-a0)) + Is0*
    exp(-a/dm);
beta = 1/(1 + ((Is/Is0)^2));
rho = q + (rho0*(1 + ((wa -1)*(Pa/Ha)^2/(1 + (Pa/Ha)^2))));
rhos = 17.38;
R_s= f*rhos + (1-f)*rho;
ode = @(T,I)[-m*alpha*I(7)*(1-exp((-1*a)/a0))*b*I(1) + beta*R_s*I(3)
     + rho*(I(4)) + mu_h - mu_h*I(1); m*alpha*I(7)*b*(1-exp((-1*a)/a0
    ))*I(1) - h*(I(2)) - mu_h*(I(2));
    beta*h*I(2) + beta*m*alpha*I(7)*(1-exp((-1*a)/a0))*b*I(4) - R_s*I
        (3) - mu_h*I(3);
    (1 -beta)*h* I(2) + (1 - beta)*R_s*I(3) - beta*m*alpha*I(7)*(1-
        exp((-1*a)/a0))*b*I(4) - (rho)*I(4) - mu_h*I(4);
     mu_m - alpha*(C_Is*I(3) + C_Ia*I(4))*I(5)- mu_m*I(5); alpha*(
         C_Is*I(3) + C_Ia*I(4))*I(5) - psi*alpha*(C_Is*I(3) + C_Ia*I
         (4))*I(5)-mu_m*I(6); psi*alpha*(C_Is*I(3) + C_Ia*I(4))*I(5)-
          mu_m*I(7)];
tspan = 0:0.0005:1;
options = odeset('RelTol',1e-8,'AbsTol',1e-10);
I0 = [0.99998; 0; 0.00002; 0; 0.999; 0.0; 0.001];
[T,I] = ode45(ode, tspan, I0, options);
% figure(1)

time = linspace(0,12,2001);

%plot(x, I(:,5),x, I(:,6), x, I(:,7));
```

```
%grid
y(index) = I(end,3);
age = linspace(0,60,1601);
% y

end
% p = plot(time, I(:,1),'--', time, I(:,2), '-',time, I(:,3), ':',
    time, I(:,4), '-.' )
p = plot(age, y2, '--')
p(1).LineWidth = 2.5;
% p(2).LineWidth = 2.5;
% p(3).LineWidth = 2.5;
% p(4).LineWidth = 2.5;
legend('EIR=25','EIR = 50', 'EIR =100')
 xlabel({'Age'})
ylabel({'Proportion of symptomatic human class'} )
ylim([0 1])
% %title('Recovery from sub-patent infections')

%Clinical Immunity prevalence
syms I f Ha wa m alpha h rho q mu_h Is0 b a0 amax dl dp dm ds Hs EIR
     a Pa lambda Is beta rho rhos R_s mu_m L_m psi C_Is C_Ia tau
index = 0;
for a = 0:0.05:80
index = index+1;
f=0.5; Ha = 500; wa = 30; h = 24.333; m =3; alpha = 0.67*365; rho0 =
     (1/180*365); mu_h = 0.0125; q = 3;
b = 0.2; a0 = 3; dl = 10; dp = 20; dm = 0.25; amax =80; ds = 5; Hs
    =40; EIR =50; Is0 =52; mu_m = 0.1*365; tau = 0.018; C_Is = 0.35;
    C_Ia = 0.03;
Pa = exp(-a/dl)*((EIR*b*dl*dp*exp(a/dl) - (EIR*a0*b*dl*dp*exp(a/dl -
     a/a0))/(a0 - dl))/(dl - dp) - (EIR*b*dl*dp)/(dl - dp) + (EIR*a0*
    b*dl*dp)/(a0*dl - a0*dp + dl*dp - dl^2)) - exp(-a/dp)*((EIR*b*dp
    ^2*exp(a/dp) - (EIR*a0*b*dp^2*exp(a/dp - a/a0))/(a0 - dp))/(dl -
```

```
    dp) - (EIR*b*dp^2 - (EIR*a0*b*dp^2)/(a0 - dp))/(dl - dp) + (EIR*b
    *dl*dp - (EIR*a0*b*dl*dp)/(a0 - dl))/(dl - dp) - (EIR*b*dl*dp)/(
    dl - dp) + (EIR*a0*b*dl*dp)/(a0*dl - a0*dp + dl*dp - dl^2));
lambda = EIR*b*(1 - exp(-amax/a0));
psi = exp(-tau*mu_m);
Is = lambda*ds*( 1 + (a0*exp(-a/a0) - ds*exp(-a/ds))/(ds-a0)) + Is0*
    exp(-a/dm);
beta = 1/(1 + ((Is/Is0)^2));
rho = q + (rho0*(1 + ((wa -1)*(Pa/Ha)^2/(1 + (Pa/Ha)^2))));
rhos = 17.38;
R_s= f*rhos + (1-f)*rho;
ode = @(T,I)[-m*alpha*I(7)*(1-exp((-1*a)/a0))*b*I(1) + beta*R_s*I(3)
     + rho*(I(4)) + mu_h - mu_h*I(1); m*alpha*I(7)*b*(1-exp((-1*a)/a0
    ))*I(1) - h*(I(2)) - mu_h*(I(2));
    beta*h*I(2) + beta*m*alpha*I(7)*(1-exp((-1*a)/a0))*b*I(4) - R_s*I
        (3) - mu_h*I(3);
    (1 -beta)*h* I(2) + (1 - beta)*R_s*I(3) - beta*m*alpha*I(7)*(1-
        exp((-1*a)/a0))*b*I(4) - (rho)*I(4) - mu_h*I(4);
     mu_m - alpha*(C_Is*I(3) + C_Ia*I(4))*I(5)- mu_m*I(5); alpha*(
         C_Is*I(3) + C_Ia*I(4))*I(5) - psi*alpha*(C_Is*I(3) + C_Ia*I
         (4))*I(5)-mu_m*I(6); psi*alpha*(C_Is*I(3) + C_Ia*I(4))*I(5)-
          mu_m*I(7)];
tspan = 0:0.0005:1;
options = odeset('RelTol',1e-8,'AbsTol',1e-10);
I0 = [0.99998; 0; 0.00002; 0; 0.999; 0.0; 0.001];
[T,I] = ode45(ode, tspan, I0, options);
% figure(1)

time = linspace(0,12,2001);

%plot(x, I(:,5),x, I(:,6), x, I(:,7));

%grid
y(index) = I(end,4);
age = linspace(0,80,1601);
```

```
% y

end
hold on
p = plot(age, y, '--')
p(1).LineWidth = 2.5;

syms I f Ha wa m alpha h rho q mu_h Is0 b a0 amax dl dp dm ds Hs EIR
    a Pa lambda Is beta rho rhos R_s mu_m L_m psi C_Is C_Ia tau
index = 0;
for a = 0:0.05:80
index = index+1;
f=0.5; Ha = 500; wa = 30; h = 24.333; m =3; alpha = 0.67*365; rho0 =
    (1/180*365); mu_h = 0.0125; q = 3;
b = 0.2; a0 = 3; dl = 10; dp = 20; dm = 0.25; amax =80; ds = 5; Hs
   =40; EIR =75; Is0 =52; mu_m = 0.1*365; tau = 0.018; C_Is = 0.35;
   C_Ia = 0.03;
Pa = exp(-a/dl)*((EIR*b*dl*dp*exp(a/dl) - (EIR*a0*b*dl*dp*exp(a/dl -
    a/a0))/(a0 - dl))/(dl - dp) - (EIR*b*dl*dp)/(dl - dp) + (EIR*a0*
   b*dl*dp)/(a0*dl - a0*dp + dl*dp - dl^2)) - exp(-a/dp)*((EIR*b*dp
   ^2*exp(a/dp) - (EIR*a0*b*dp^2*exp(a/dp - a/a0))/(a0 - dp))/(dl -
   dp) - (EIR*b*dp^2 - (EIR*a0*b*dp^2)/(a0 - dp))/(dl - dp) + (EIR*b
   *dl*dp - (EIR*a0*b*dl*dp)/(a0 - dl))/(dl - dp) - (EIR*b*dl*dp)/(
   dl - dp) + (EIR*a0*b*dl*dp)/(a0*dl - a0*dp + dl*dp - dl^2));
lambda = EIR*b*(1 - exp(-amax/a0));
psi = exp(-tau*mu_m);
Is = lambda*ds*( 1 + (a0*exp(-a/a0) - ds*exp(-a/ds))/(ds-a0)) + Is0*
   exp(-a/dm);
beta = 1/(1 + ((Is/Is0)^2));
rho = q + (rho0*(1 + ((wa -1)*(Pa/Ha)^2/(1 + (Pa/Ha)^2))));
rhos = 17.38;
R_s= f*rhos + (1-f)*rho;
ode = @(T,I)[-m*alpha*I(7)*(1-exp((-1*a)/a0))*b*I(1) + beta*R_s*I(3)
    + rho*(I(4)) + mu_h - mu_h*I(1); m*alpha*I(7)*b*(1-exp((-1*a)/a0
   ))*I(1) - h*(I(2)) - mu_h*(I(2));
```

```
    beta*h*I(2) + beta*m*alpha*I(7)*(1-exp((-1*a)/a0))*b*I(4) - R_s*I
        (3) - mu_h*I(3);
    (1 -beta)*h* I(2) + (1 - beta)*R_s*I(3) - beta*m*alpha*I(7)*(1-
        exp((-1*a)/a0))*b*I(4) - (rho)*I(4) - mu_h*I(4);
     mu_m - alpha*(C_Is*I(3) + C_Ia*I(4))*I(5)- mu_m*I(5); alpha*(
         C_Is*I(3) + C_Ia*I(4))*I(5) - psi*alpha*(C_Is*I(3) + C_Ia*I
         (4))*I(5)-mu_m*I(6); psi*alpha*(C_Is*I(3) + C_Ia*I(4))*I(5)-
          mu_m*I(7)];
tspan = 0:0.0005:1;
options = odeset('RelTol',1e-8,'AbsTol',1e-10);
I0 = [0.99998; 0; 0.00002; 0; 0.999; 0.0; 0.001];
[T,I] = ode45(ode, tspan, I0, options);
% figure(1)

time = linspace(0,12,2001);

%plot(x, I(:,5),x, I(:,6), x, I(:,7));

%grid
y2(index) = I(end,4);
age = linspace(0,80,1601);
% y

end
% p = plot(time, I(:,1),'--', time, I(:,2), '-',time, I(:,3), ':',
    time, I(:,4), '-.' )
p = plot(age, y2, '--')
p(1).LineWidth = 2.5;
% p(2).LineWidth = 2.5;
% p(3).LineWidth = 2.5;
% p(4).LineWidth = 2.5;
% legend('parasite immunity half-life = 15 yrs')
 xlabel({'Age'})
ylabel({'Proportion of symptomatic human class'} )
ylim([0 1])
```

```
% % %title('Recovery from sub-patent infections')
hold on
syms I f Ha wa m alpha h rho q mu_h Is0 b a0 amax dl dp dm ds Hs EIR
    a Pa lambda Is beta rho rhos R_s mu_m L_m psi C_Is C_Ia tau
index = 0;
for a = 0:0.05:80
index = index+1;
f=0.5; Ha = 500; wa = 30; h = 24.333; m =3; alpha = 0.67*365; rho0 =
    (1/180*365); mu_h = 0.0125; q = 3;
b = 0.2; a0 = 3; dl = 10; dp = 20; dm = 0.25; amax =80; ds = 5; Hs
   =40; EIR =110; Is0 =52; mu_m = 0.1*365; tau = 0.018; C_Is = 0.35;
    C_Ia = 0.03;
Pa = exp(-a/dl)*((EIR*b*dl*dp*exp(a/dl) - (EIR*a0*b*dl*dp*exp(a/dl -
    a/a0))/(a0 - dl))/(dl - dp) - (EIR*b*dl*dp)/(dl - dp) + (EIR*a0*
   b*dl*dp)/(a0*dl - a0*dp + dl*dp - dl^2)) - exp(-a/dp)*((EIR*b*dp
   ^2*exp(a/dp) - (EIR*a0*b*dp^2*exp(a/dp - a/a0))/(a0 - dp))/(dl -
   dp) - (EIR*b*dp^2 - (EIR*a0*b*dp^2)/(a0 - dp))/(dl - dp) + (EIR*b
   *dl*dp - (EIR*a0*b*dl*dp)/(a0 - dl))/(dl - dp) - (EIR*b*dl*dp)/(
   dl - dp) + (EIR*a0*b*dl*dp)/(a0*dl - a0*dp + dl*dp - dl^2));
lambda = EIR*b*(1 - exp(-amax/a0));
psi = exp(-tau*mu_m);
Is = lambda*ds*( 1 + (a0*exp(-a/a0) - ds*exp(-a/ds))/(ds-a0)) + Is0*
   exp(-a/dm);
beta = 1/(1 + ((Is/Is0)^2));
rho = q + (rho0*(1 + ((wa -1)*(Pa/Ha)^2/(1 + (Pa/Ha)^2))));
rhos = 17.38;
R_s= f*rhos + (1-f)*rho;
ode = @(T,I)[-m*alpha*I(7)*(1-exp((-1*a)/a0))*b*I(1) + beta*R_s*I(3)
    + rho*(I(4)) + mu_h - mu_h*I(1); m*alpha*I(7)*b*(1-exp((-1*a)/a0
   ))*I(1) - h*(I(2)) - mu_h*(I(2));
   beta*h*I(2) + beta*m*alpha*I(7)*(1-exp((-1*a)/a0))*b*I(4) - R_s*I
       (3) - mu_h*I(3);
   (1 -beta)*h* I(2) + (1 - beta)*R_s*I(3) - beta*m*alpha*I(7)*(1-
       exp((-1*a)/a0))*b*I(4) - (rho)*I(4) - mu_h*I(4);
```

```
    mu_m - alpha*(C_Is*I(3) + C_Ia*I(4))*I(5)- mu_m*I(5); alpha*(
        C_Is*I(3) + C_Ia*I(4))*I(5) - psi*alpha*(C_Is*I(3) + C_Ia*I
        (4))*I(5)-mu_m*I(6); psi*alpha*(C_Is*I(3) + C_Ia*I(4))*I(5)-
         mu_m*I(7)];
tspan = 0:0.0005:1;
options = odeset('RelTol',1e-8,'AbsTol',1e-10);
I0 = [0.99998; 0; 0.00002; 0; 0.999; 0.0; 0.001];
[T,I] = ode45(ode, tspan, I0, options);
% figure(1)

time = linspace(0,12,2001);

%plot(x, I(:,5),x, I(:,6), x, I(:,7));

%grid
y3(index) = I(end,4);
age = linspace(0,80,1601);
% y

end
% p = plot(time, I(:,1),'--', time, I(:,2), '-',time, I(:,3), ':',
    time, I(:,4), '-.' )
p = plot(age, y3, '--')
p(1).LineWidth = 2.5;
% p(2).LineWidth = 2.5;
% p(3).LineWidth = 2.5;
% p(4).LineWidth = 2.5;
legend('EIR =50','EIR=75','EIR=100', 'fontweight', 'bold')
xlabel({'Age'}, 'fontweight', 'bold')
ylabel({'Proportion of asymptomatic human class'},'fontweight', '
    bold' )
ylim([0 1])


%comparisons of parasite immunity prevalence
```

```
clearvars; clc; close all;
 b = 0.2; Im = 0.146; a0 =3; dp = 20; dl = 10; wa = 30; Ha = 500;
     rho0 = 1/180;
 ds =5; dm = 0.25; a0 =3; Is0 = 52; EIR = 50;
 amax =60; index = 0;
for a = 0:0.5:80
index = index+1;
Is(index) = EIR*b*(1 - exp(-amax/a0))*ds*( 1 + (a0*exp(-a/a0) - ds*
    exp(-a/ds))/(ds-a0)) + Is0*exp(-a/dm);
Pa(index) = exp(-a/dl)*((EIR*b*dl*dp*exp(a/dl) - (EIR*a0*b*dl*dp*exp
    (a/dl - a/a0))/(a0 - dl))/(dl - dp) - (EIR*b*dl*dp)/(dl - dp) + (
    EIR*a0*b*dl*dp)/(a0*dl - a0*dp + dl*dp - dl^2)) - exp(-a/dp)*((
    EIR*b*dp^2*exp(a/dp) - (EIR*a0*b*dp^2*exp(a/dp - a/a0))/(a0 - dp)
    )/(dl - dp) - (EIR*b*dp^2 - (EIR*a0*b*dp^2)/(a0 - dp))/(dl - dp)
    + (EIR*b*dl*dp - (EIR*a0*b*dl*dp)/(a0 - dl))/(dl - dp) - (EIR*b*
    dl*dp)/(dl - dp) + (EIR*a0*b*dl*dp)/(a0*dl - a0*dp + dl*dp - dl
    ^2));
age = linspace(0,80,161);

 end

p = plot(age, Is, age,Pa, '-')
p(1).LineWidth = 2.5;
p(2).LineWidth = 2.5;

legend('clinical immunity', 'parasite immunity')
xlabel({'Age', 'in years'}, 'fontweight', 'bold')
ylabel('immunity equilibria','fontweight', 'bold' )

%Force of infection
syms Im alpha b m a a0 lambda
Im = 0.146; alpha = 0.67; b = 0.2; a0 =3; m =3 ;


index=0;
```

```
for a = 0:0.5:60
    index=index+1;
   m  = [0,0.1,0.5,1,1.5,3,6,12,15];
for i =1:numel(m)
lambda(index,i) = m(i)*alpha*Im*b*(1-exp((-a)/(a0)));
y = lambda;
age = linspace(0,60,121);
end
end
plot(age, y)
p = plot(age, y, '-');
p(1).LineWidth = 2.5;

legend('mosquito to human ratio = 0.00', 'mosquito to human ratio =
    0.1', 'mosquito to human ratio = 0.5', 'mosquito to human ratio =
     1', 'mosquito to human ratio = 1.5', 'mosquito to human ratio =
    3', 'mosquito to human ratio = 6', 'mosquito to human ratio = 12'
    , 'mosquito to human ratio = 15')
xlabel({'Age'})
ylabel({'Force of infection','1/yr'} )
% %title('Recovery from sub-patent infections')
%parameter dependence clinical immunity
b=0.2; A= 0.67*365; a= 20; m = 3; a0=3; I = 0.0106; d = 0.25; l = 5;
ys = zeros(6,6);
count_a = 1;

for A = 0:0.2*365:1*365
    count_m = 1;
    for I = 0:0.2:01
ode = @(T,Y)[-Y(1)/d;
    m*A*b*(1-exp((-1*a)/a0))*I - Y(2)/l;
    -Y(1)/d + m*A*b*(1-exp((-1*a)/a0))*I - Y(2)/l];
tspan = linspace(0, 60, 600);
Y0 = [0.01;0;0.01;];
[T,Y] = ode45(ode ,tspan, Y0);
```

```
ys(count_m,count_a) = Y(end);
count_m = count_m +1;
    end

count_a = count_a +1;
end
%for i = 1:7
%hold on
%plot (0:0.2:1,ys(i,:))
%xlabel('Probability of Incoulation')
%ylabel(' Final Clinical Immunity');
%legend ( 'm = 0', 'm = 2', 'm = 4', 'm =6', 'm = 8', 'm = 10')
%end
hold on

b=0.2; A= 0.67*365; a= 2; m = 3; a0=3; I = 0.0106; d = 0.25; l = 5;
yb = zeros(6,6);
count_b = 1;

for b = 0:0.2:1
    count_m1 = 1;
    for I = 0:0.2:1
ode = @(T,Y)[-Y(1)/d;
    m*A*b*(1-exp((-1*a)/a0))*I - Y(2)/l;
    -Y(1)/d + m*A*b*(1-exp((-1*a)/a0))*I - Y(2)/l];
tspan = linspace(0, 60, 600);
Y0 = [52;0;52;];
[T,Y] = ode45(ode ,tspan, Y0);
yb(count_m1,count_b) = Y(end);
count_m1 = count_m1 +1;
    end

count_b = count_b +1;

end
```

```
S1 = surf ( [0:0.2:1], [0:0.2:01], yb)
S1.FaceColor = 'interp';
S1.EdgeColor = 'none';
colormap 'cool'
xlabel('biting rate')
ylabel('Infected mosquito proportion')
zlabel('Clinical Immunity')
hold on
S2 = surf ( [0:0.2:1], [0:0.2:01], ys)
rotate3d on
S2.FaceColor = 'interp';
S2.EdgeColor = 'none';
xlabel('Probability of incolution')
ylabel('Infected mosquito proportion')
zlabel('Clinical Immunity')


%aron model
h = 0.5:0.1:4.5;
tau = 2:1:4
for i = 1:numel(h)
    for j = 1:numel(tau)
        gamma(i,j) = (h(i)*(exp(-h(i)*tau(j))))/(1-(exp(-h(i)*tau(j))
            ));

    end
end
gamma
plot(h, gamma,'linewidth',2.5)
legend('tau = 2yr','tau = 3yr', 'tau=4 yr')
xlabel({'Rate of Infection','(1/yr)'})
ylabel({'Loss of Immunity'})
title('Rate loss of immunity')
clc; clearvars; close all
```

```
%Mathematical modelling of immunity to malaria- Aron
syms S h gamma R r q I tau
r = 0.8; q = 0.2; tau = 5;
for h = [0.05, 0.5, 5]
    gamma = (h*(exp(-h*tau)))/(1-(exp(-h*tau)));
    ode = @(a,I)[-I(1)*h + r*I(2) + gamma*I(3); h*I(1) - r*I(2) - q*I
        (2);
        q*I(2) - gamma*I(3)];
    tspan = linspace(0, 40, 10000);
    I0 = [1;0;0;];
    [a,I] = ode45(ode ,tspan, I0 );
    hold on
    plot(a, I(:,2), 'linewidth',2.5 ) %percentage infected vs age
        plot
    legend('h = 0.05','h = 0.5', 'h = 5 ')
xlabel({'Age','(yr.)'})
ylabel({'Percentage Infected Population'})
title('Prevalence of Infected Population Aron Model')
```

References

[1] Acevedo, M.A., Prosper, O., Lopiano, K., Ruktanonchai, N., Caughlin, T.T., Martcheva, M., Osenberg, C.W., Smith, D.L., 2015. Spatial heterogeneity, host movement and mosquito-borne disease transmission. PloS one 10.

[2] Acharya, P., Garg, M., Kumar, P., Munjal, A., Raja, K., 2017. Host–parasite interactions in human malaria: Clinical implications of basic research. Frontiers in microbiology 8, 889.

[3] Alves, F.P., Durlacher, R.R., Menezes, M.J., Krieger, H., Silva, L.H.P., Camargo, E.P., 2002. High prevalence of asymptomatic plasmodium vivax and plasmodium falciparum infections in native amazonian populations. The American journal of tropical medicine and hygiene 66, 641–648.

[4] Aly, A.S., Vaughan, A.M., Kappe, S.H., 2009. Malaria parasite development in the mosquito and infection of the mammalian host. Annual review of microbiology 63, 195–221.

[5] Aron, J.L., 1983. Dynamics of acquired immunity boosted by exposure to infection. Mathematical Biosciences 64, 249–259.

[6] Aron, J.L., 1988. Mathematical modeling of immunity to malaria. Mathe-

matical Biosciences 90, 385–396.

[7] Aron, J.L., May, R.M., 1982. The population dynamics of malaria, in: The population dynamics of infectious diseases: theory and applications. Springer, pp. 139–179.

[8] Bacaër, N., et al., 2012. On the biological interpretation of a definition for the parameter r 0 in periodic population models. Journal of mathematical biology 65, 601–621.

[9] Battle, K.E., Lucas, T.C., Nguyen, M., Howes, R.E., Nandi, A.K., Twohig, K.A., Pfeffer, D.A., Cameron, E., Rao, P.C., Casey, D., et al., 2019. Mapping the global endemicity and clinical burden of plasmodium vivax, 2000–17: a spatial and temporal modelling study. The Lancet 394, 332–343.

[10] Bouwman, H., Van den Berg, H., Kylin, H., 2011. Ddt and malaria prevention: addressing the paradox. Environmental health perspectives 119, 744–747.

[11] Brauer, F., 2008. Compartmental models in epidemiology, in: Mathematical epidemiology. Springer, pp. 19–79.

[12] Carneiro, I., Roca-Feltrer, A., Griffin, J.T., Smith, L., Tanner, M., Schellenberg, J.A., Greenwood, B., Schellenberg, D., 2010. Age-patterns of malaria vary with severity, transmission intensity and seasonality in sub-saharan africa: a systematic review and pooled analysis. PloS one 5.

[13] Carter, R., Mendis, K.N., 2002. Evolutionary and historical aspects of the burden of malaria. Clinical microbiology reviews 15, 564–594.

[14] CCfDCa, P., . Malaria-biology: Cdc centers for disease control and prevention;[updated 14.11. 18; cited 2019 15.01.].

[15] Chiyaka, C., Garira, W., Dube, S., 2009. Effects of treatment and drug resistance on the transmission dynamics of malaria in endemic areas. Theoretical population biology 75, 14–29.

[16] Cowman, A.F., Crabb, B.S., 2006. Invasion of red blood cells by malaria parasites. Cell 124, 755–766.

[17] Cox, F.E., 2010. History of the discovery of the malaria parasites and their vectors. Parasites & vectors 3, 5.

[18] Das, A., Anvikar, A.R., Cator, L.J., Dhiman, R.C., Eapen, A., Mishra, N., Nagpal, B.N., Nanda, N., Raghavendra, K., Read, A.F., et al., 2012. Malaria in india: the center for the study of complex malaria in india. Acta tropica 121, 267–273.

[19] DeAngelis, D.L., 2018. Individual-based models and approaches in ecology: populations, communities and ecosystems. CRC Press.

[20] Dent, A., Malhotra, I., Mungai, P., Muchiri, E., Crabb, B.S., Kazura, J.W., King, C.L., 2006. Prenatal malaria immune experience affects acquisition of plasmodium falciparum merozoite surface protein-1 invasion inhibitory antibodies during infancy. The Journal of Immunology 177, 7139–7145.

[21] Dent, A.E., Malhotra, I., Wang, X., Babineau, D., Yeo, K.T., Anderson, T., Kimmel, R.J., Angov, E., Lanar, D.E., Narum, D., et al., 2016. Contrasting patterns of serologic and functional antibody dynamics to plasmodium

falciparum antigens in a kenyan birth cohort. Clin. Vaccine Immunol. 23, 104–116.

[22] Dhingra, N., Jha, P., Sharma, V.P., Cohen, A.A., Jotkar, R.M., Rodriguez, P.S., Bassani, D.G., Suraweera, W., Laxminarayan, R., Peto, R., et al., 2010. Adult and child malaria mortality in india: a nationally representative mortality survey. The Lancet 376, 1768–1774.

[23] Diamond-Smith, N., Singh, N., Gupta, R.D., Dash, A., Thimasarn, K., Campbell, O.M., Chandramohan, D., 2009. Estimating the burden of malaria in pregnancy: a case study from rural madhya pradesh, india. Malaria journal 8, 24.

[24] Diekmann, O., Heesterbeek, J.A.P., Metz, J.A., 1990. On the definition and the computation of the basic reproduction ratio r 0 in models for infectious diseases in heterogeneous populations. Journal of mathematical biology 28, 365–382.

[25] Dietz, K., 1993. The estimation of the basic reproduction number for infectious diseases. Statistical methods in medical research 2, 23–41.

[26] Doolan, D.L., Dobaño, C., Baird, J.K., 2009. Acquired immunity to malaria. Clinical microbiology reviews 22, 13–36.

[27] Drakeley, C., Sutherland, C., Bousema, J.T., Sauerwein, R.W., Targett, G.A., 2006. The epidemiology of plasmodium falciparum gametocytes: weapons of mass dispersion. Trends in parasitology 22, 424–430.

[28] Van den Driessche, P., Watmough, J., 2002. Reproduction numbers and sub-

threshold endemic equilibria for compartmental models of disease transmission. Mathematical biosciences 180, 29–48.

[29] Eckhoff, P., 2013. Mathematical models of within-host and transmission dynamics to determine effects of malaria interventions in a variety of transmission settings. The American journal of tropical medicine and hygiene 88, 817–827.

[30] Eckhoff, P.A., 2012. Malaria parasite diversity and transmission intensity affect development of parasitological immunity in a mathematical model. Malaria journal 11, 419.

[31] EMOD, 2019. Compartmental models and emod. URL: https://idmod.org/docs/malaria/model-compartments.html.

[32] Enderle, J.D., 2012. Compartmental modeling, in: Introduction to Biomedical Engineering. Elsevier, pp. 359–445.

[33] Eradication, N.M., 19. Malaria and Its Control in India. volume 1. Government of India.

[34] Filipe, J.A., Riley, E.M., Drakeley, C.J., Sutherland, C.J., Ghani, A.C., 2007. Determination of the processes driving the acquisition of immunity to malaria using a mathematical transmission model. PLoS computational biology 3.

[35] Galarnyk, M., 2018. Understanding boxplots. URL: https://towardsdatascience.com/understanding-boxplots-5e2df7bcbd51.

[36] Gatton, M.L., Cheng, Q., 2004. Modeling the development of acquired clin-

ical immunity to plasmodium falciparum malaria. Infection and immunity 72, 6538–6545.

[37] Ghani, A.C., Sutherland, C.J., Riley, E.M., Drakeley, C.J., Griffin, J.T., Gosling, R.D., Filipe, J.A., 2009. Loss of population levels of immunity to malaria as a result of exposure-reducing interventions: consequences for interpretation of disease trends. PLoS One 4.

[38] Grimm, V., 1999. Ten years of individual-based modelling in ecology: what have we learned and what could we learn in the future? Ecological modelling 115, 129–148.

[39] Gu, W., Novak, R.J., 2005. Habitat-based modeling of impacts of mosquito larval interventions on entomological inoculation rates, incidence, and prevalence of malaria. The American journal of tropical medicine and hygiene 73, 546–552.

[40] Gupta, S., Hill, A.V., 1995. Dynamic interactions in malaria: host heterogeneity meets parasite polymorphism. Proceedings of the Royal Society of London. Series B: Biological Sciences 261, 271–277.

[41] Gupta, S., Snow, R.W., Donnelly, C.A., Marsh, K., Newbold, C., 1999. Immunity to non-cerebral severe malaria is acquired after one or two infections. Nature medicine 5, 340–343.

[42] Hassett, M.R., Roepe, P.D., 2019. Origin and spread of evolving artemisinin-resistant plasmodium falciparum malarial parasites in southeast asia. The American journal of tropical medicine and hygiene 101, 1204–1211.

[43] Hay, S.I., Gething, P.W., Snow, R.W., 2010. India's invisible malaria burden. Lancet 376, 1716.

[44] Hviid, L., 2005. Naturally acquired immunity to plasmodium falciparum malaria in africa. Acta tropica 95, 270–275.

[45] Hviid, L., Staalsoe, T., 2004. Malaria immunity in infants: a special case of a general phenomenon? Trends in parasitology 20, 66–72.

[46] Jolliffe, I.T., Cadima, J., 2016. Principal component analysis: a review and recent developments. Philosophical Transactions of the Royal Society A: Mathematical, Physical and Engineering Sciences 374, 20150202.

[47] Judson, O.P., 1994. The rise of the individual-based model in ecology. Trends in Ecology & Evolution 9, 9–14.

[48] Keegan, L.T., Dushoff, J., 2013. Population-level effects of clinical immunity to malaria. BMC infectious diseases 13, 428.

[49] Kumar, A., Valecha, N., Jain, T., Dash, A.P., 2007. Burden of malaria in india: retrospective and prospective view. The American journal of tropical medicine and hygiene 77, 69–78.

[50] Kumar, H., Somanathan, R., 2015. State and district boundary changes in india: 1961-2001. Available at SSRN 2687484 .

[51] Langhi, D.M., Orlando Bordin, J., 2006. Duffy blood group and malaria. Hematology 11, 389–398.

[52] Loy, D.E., Liu, W., Li, Y., Learn, G.H., Plenderleith, L.J., Sundararaman, S.A., Sharp, P.M., Hahn, B.H., 2017. Out of africa: origins and evolution of

the human malaria parasites plasmodium falciparum and plasmodium vivax. International journal for parasitology 47, 87–97.

[53] MacDonald, G., 1953. The analysis of malaria epidemics. Tropical diseases bulletin 50, 871–889.

[54] Macdonald, G., et al., 1957. The epidemiology and control of malaria. The Epidemiology and Control of Malaria. .

[55] Malhotra, I., Dent, A., Mungai, P., Wamachi, A., Ouma, J.H., Narum, D.L., Muchiri, E., Tisch, D.J., King, C.L., 2009. Can prenatal malaria exposure produce an immune tolerant phenotype?: A prospective birth cohort study in kenya. PLoS medicine 6.

[56] Mandal, S., Sarkar, R.R., Sinha, S., 2011. Mathematical models of malaria-a review. Malaria journal 10, 202.

[57] Mandal, S., Sinha, S., Sarkar, R.R., 2013. A realistic host-vector transmission model for describing malaria prevalence pattern. Bulletin of mathematical biology 75, 2499–2528.

[58] MATLAB, Release, S.T., 2016. The mathworks, inc .

[59] Mendis, K.N., Naotunne, T.d.S., Karunaweera, N.D., Del Giudice, G., Grau, G.E., Carter, R., 1990. Anti-parasite effects of cytokines in malaria. Immunology letters 25, 217–220.

[60] Murungi, L.M., Sondén, K., Odera, D., Oduor, L.B., Guleid, F., Nkumama, I.N., Otiende, M., Kangoye, D.T., Fegan, G., Färnert, A., et al., 2017. Cord

blood igg and the risk of severe plasmodium falciparum malaria in the first year of life. International journal for parasitology 47, 153–162.

[61] NAG-ASE, M., VAILLANCOURT, R., 2000. Behind and beyond the l\/[atlab one suite .

[62] Organization, W.H., et al., 1979. Environmental health criteria 9: Ddt and its derivatives .

[63] Parunak, H.V.D., Savit, R., Riolo, R.L., 1998. Agent-based modeling vs. equation-based modeling: A case study and users' guide, in: International Workshop on Multi-Agent Systems and Agent-Based Simulation, Springer. pp. 10–25.

[64] Pattanayak, S., Sharma, V., Kalra, N., Orlov, V., Sharma, R., 1994. Malaria paradigms in india and control strategies. Indian journal of malariology 31, 141–199.

[65] Paul, A.S., Egan, E.S., Duraisingh, M.T., 2015. Host-parasite interactions that guide red blood cell invasion by malaria parasites. Current opinion in hematology 22, 220.

[66] Pradhan, S., Pradhan, M.M., Dutta, A., Shah, N.K., Joshi, P.L., Pradhan, K., Sharma, S., Daumerie, P.G., Banerji, J., Duparc, S., et al., 2019. Improved access to early diagnosis and complete treatment of malaria in odisha, india. PloS one 14.

[67] Rodriguez-Barraquer, I., Arinaitwe, E., Jagannathan, P., Kamya, M.R., Rosenthal, P.J., Rek, J., Dorsey, G., Nankabirwa, J., Staedke, S.G., Kilama,

M., et al., 2018. Quantification of anti-parasite and anti-disease immunity to malaria as a function of age and exposure. Elife 7, e35832.

[68] Ross, R., 1911. Some quantitative studies in epidemiology.

[69] Ross, R., 1915. Some a priori pathometric equations. British medical journal 1, 546.

[70] Sarma, D.K., Mohapatra, P.K., Bhattacharyya, D.R., Chellappan, S., Karuppusamy, B., Barman, K., Senthil Kumar, N., Dash, A.P., Prakash, A., Balabaskaran Nina, P., 2019. Malaria in north-east india: Importance and implications in the era of elimination. Microorganisms 7, 673.

[71] Sattenspiel, L., 1990. Modeling the spread of infectious disease in human populations. American Journal of Physical Anthropology 33, 245–276.

[72] Sattenspiel, L., Lloyd, A., 2009. The geographic spread of infectious diseases: models and applications. volume 5. Princeton University Press.

[73] Schofield, L., Mueller, I., 2006. Clinical immunity to malaria. Current molecular medicine 6, 205–221.

[74] Sharma, V.P., 2009. Hidden burden of malaria in indian women. Malaria Journal 8, 281.

[75] Smith, D.L., Battle, K.E., Hay, S.I., Barker, C.M., Scott, T.W., McKenzie, F.E., 2012. Ross, macdonald, and a theory for the dynamics and control of mosquito-transmitted pathogens. PLoS pathogens 8.

[76] Smith, T., Maire, N., Ross, A., Penny, M., Chitnis, N., Schapira, A., Studer, A., Genton, B., Lengeler, C., Tediosi, F., et al., 2008. Towards a compre-

hensive simulation model of malaria epidemiology and control. Parasitology 135, 1507–1516.

[77] Stevenson, M.M., Riley, E.M., 2004. Innate immunity to malaria. Nature Reviews Immunology 4, 169–180.

[78] Team, Q.D., et al., 2016. Qgis geographic information system. Open source geospatial foundation project .

[79] Udomsangpetch, R., Wåhlin, B., Carlson, J., Berzins, K., Torii, M., Aikawa, M., Perlmann, P., Wahlgren, M., 1989. Plasmodium falciparum-infected erythrocytes form spontaneous erythrocyte rosettes. Journal of Experimental Medicine 169, 1835–1840.

[80] VanderPlas, J., 2016. Python data science handbook: Essential tools for working with data. " O'Reilly Media, Inc.".

[81] Victoria, . Ocr. URL: https://www.scan2cad.com/tips/how-does-ocr-work/.

[82] Weiss, D.J., Lucas, T.C., Nguyen, M., Nandi, A.K., Bisanzio, D., Battle, K.E., Cameron, E., Twohig, K.A., Pfeffer, D.A., Rozier, J.A., et al., 2019. Mapping the global prevalence, incidence, and mortality of plasmodium falciparum, 2000–17: a spatial and temporal modelling study. The Lancet 394, 322–331.

[83] WHO, 2019. World malaria report 2019 .

[84] Wilson, P.T., Malhotra, I., Mungai, P., King, C.L., Dent, A.E., 2013.

Transplacentally transferred functional antibodies against plasmodium falciparum decrease with age. Acta tropica 128, 149–153.